NASA TECHNICAL NOTE

NASA TN D-5661

c. 1

NASA TN D-5661

DESIGN CHARTS OF STATIC AND ROTARY STABILITY DERIVATIVES FOR CROPPED DOUBLE-DELTA WINGS IN SUBSONIC COMPRESSIBLE FLOW

by John E. Lamar

Langley Research Center
Langley Station, Hampton, Va.

NATIONAL AERONAUTICS AND SPACE ADMINISTRATION • WASHINGTON, D. C. • FEBRUARY 1970

1. Report No. NASA TN D-5661	2. Government Accession No.	3. Recipient's Catalog No.

4. Title and Subtitle

DESIGN CHARTS OF STATIC AND ROTARY STABILITY DERIVATIVES FOR CROPPED DOUBLE-DELTA WINGS IN SUBSONIC COMPRESSIBLE FLOW

5. Report Date: February 1970

6. Performing Organization Code

7. Author(s): John E. Lamar

8. Performing Organization Report No. L-6716

10. Work Unit No. 126-13-10-01-23

9. Performing Organization Name and Address
NASA Langley Research Center
Hampton, Va. 23365

11. Contract or Grant No.

13. Type of Report and Period Covered: Technical Note

12. Sponsoring Agency Name and Address
National Aeronautics and Space Administration
Washington, D.C. 20546

14. Sponsoring Agency Code

15. Supplementary Notes

16. Abstract

An evaluation of a modified version of the Multhopp subsonic lifting-surface theory was made by comparing the theoretical values with experimental data. Near zero lift, the theory was found to predict reasonably adequately the lift-curve slope, aerodynamic center, damping in roll, damping in pitch, and lift coefficient due to pitch rate for delta and cropped delta planforms and also the lift-curve slope for double-delta planforms. Based on this theory, a series of design charts has been prepared for cropped double-delta planforms in subsonic compressible flow.

17. Key Words Suggested by Author(s)
Design charts
Cropped double-delta wings
Static and rotary derivatives

18. Distribution Statement
Unclassified – Unlimited

19. Security Classif. (of this report)	20. Security Classif. (of this page)	21. No. of Pages	22. Price*
Unclassified	Unclassified	79	$3.00

*For sale by the Clearinghouse for Federal Scientific and Technical Information
Springfield, Virginia 22151

DESIGN CHARTS OF STATIC AND ROTARY STABILITY DERIVATIVES FOR CROPPED DOUBLE-DELTA WINGS IN SUBSONIC COMPRESSIBLE FLOW

By John E. Lamar
Langley Research Center

SUMMARY

An evaluation of a modified version of the Multhopp subsonic lifting-surface theory was made by comparing the theoretical values with experimental data. Near zero lift, the theory was found to predict reasonably adequately the lift-curve slope, aerodynamic center, damping in roll, damping in pitch, and lift coefficient due to pitch rate for delta and cropped delta planforms and also the lift-curve slope for double-delta planforms. Based on this theory, a series of design charts has been prepared for cropped double-delta planforms in subsonic compressible flow.

INTRODUCTION

The National Aeronautics and Space Administration has programs underway to provide aerodynamic design information on aircraft configurations and components for speeds ranging from low subsonic to hypersonic. Information has already been published that indicates the consideration which has been given to both fixed and variable geometry wings for use in the design of supersonic transport and military aircraft. (See, for example, refs. 1 and 2.)

A class of fixed wings, the cropped double-delta wings, has found recent application in the design of these aircraft. Examples of proposed and actual aircraft using the concept of cropped double-delta wings are the latest Boeing supersonic transport (ref. 3), the Swedish SAAB 35 Draken and SAAB 37 Viggen (ref. 4), and the Lockheed A-11, also designated YF-12A and SR-71 (ref. 4). A search of the literature has indicated the existence of some design data, but only a few systematic investigations have been performed on cropped double-delta planforms in the subsonic and supersonic speed regimes. (See, for example, refs. 5 and 6.)

In order that a part of this void might be filled, a systematic investigation using the modified Multhopp subsonic compressible lifting-surface approach of reference 7 (after it was shown to be applicable) with the appropriate boundary conditions was undertaken

to determine the lift-curve slope, aerodynamic center, damping in roll, damping in pitch, and lift coefficient due to pitch rate for nine families of cropped double-delta planforms. The purpose of the present paper is to present the results of this investigation in design-chart form. The design charts presented are for the attached-flow condition only and do not include the effects of leading-edge separation, which are discussed in reference 8.

SYMBOLS

A aspect ratio, $\frac{b^2}{S}$

b wing span, feet (meters)

C_L lift coefficient, $\frac{\text{Lift}}{q_\infty S}$

C_{L_α} lift-curve slope, $\frac{\partial C_L}{\partial \alpha}$, per degree

C_{L_q} lift coefficient due to pitch rate, $\frac{\partial C_L}{\partial \frac{q\bar{c}}{2V}}$, per radian

C_l rolling-moment coefficient, $\frac{\text{Rolling moment}}{q_\infty Sb}$

C_{l_p} damping-in-roll parameter, $\frac{\partial C_l}{\partial \frac{pb}{2V}}$, per radian

C_m pitching-moment coefficient about $\bar{c}/4$ point, $\frac{\text{Pitching moment}}{q_\infty S\bar{c}}$

C_{m_q} damping-in-pitch parameter, $\frac{\partial C_m}{\partial \frac{q\bar{c}}{2V}}$, per radian

c_r root chord

$c_r' = \frac{c_r}{\beta}$

$\bar{c} = \frac{\text{Mean geometric chord of the total wing}}{b/2}$

$\bar{c}' = \frac{\bar{c}}{\beta}$

M_∞ subsonic free-stream Mach number

m number of span stations where pressure modes are defined

N number of chordal control points at each of m span stations

p roll rate, radians/second

q pitch rate about $\bar{c}/4$, radians/second

q_∞ free-stream dynamic pressure, pounds/foot^2 (newtons/meter^2)

S total wing area, feet^2 (meters^2)

V free-stream velocity, feet/second (meters/second)

x,y rectangular Cartesian coordinates nondimensionalized with respect to $b/2$, where origin is in plane of symmetry at half root chord (positive x, aft; positive y, along right wing panel)

x_{ac} aerodynamic center, in fractions of $\bar{c}'$, measured from leading edge of $\bar{c}'$ (positive aft), $\frac{-\partial C_m}{\partial C_L} + \frac{1}{4}$

y_b spanwise location of leading-edge break, feet (meters)

α angle of attack, degrees

$\beta = \sqrt{1 - M_\infty^2}$

Λ outboard leading-edge sweep angle, degrees

$\Lambda' = \tan^{-1}(\tan \Lambda/\beta)$, degrees

λ overall taper ratio, $\frac{\text{Tip chord}}{\text{Root chord}}$

χ inboard leading-edge sweep angle, degrees

$\chi' = \tan^{-1}(\tan \chi/\beta)$, degrees

METHOD OF ANALYSIS

The method used in this paper for predicting lifting pressures, hereafter called the present method, employs the modified Multhopp approach. (See ref. 7.) Briefly, this method employs an acceleration potential (developed from a sheet of pressure doublets) in conjunction with the linearized Euler equations to relate the pressure difference across the wing to the downward velocity over the wing surface. The effects of compressibility are accounted for by using the Prandtl-Glauert rule.

Formulation of the problem of determining the pressure difference across the wing leads to an integral equation to which the solution in closed form is difficult, except for certain classes of wings, because the answers sought (surface loadings) are a part of the integrand. Also adding to the difficulty of solution is the presence of a second-order singularity which is in the integrand. For these reasons it has been necessary to resort to an approximate solution which makes use of a finite, rather than unlimited, number of boundary points over the wing at which the flow is constrained to be tangent. Coupled with this finite number of boundary points is a series representation of the lifting pressures which have the same number of unknowns as there are boundary points and whose values are determined by a process of matrix algebra.

In reference 7 the accuracy of the numerical results of the modified Multhopp method was shown to be dependent on the combination of the number of spanwise stations m where each of N chordwise control (boundary) points was located. Two methods of estimating the appropriate combinations of N and m were studied in reference 7; one was concerned with computing the correct leading-edge thrust from the chord loadings and the other with seeking the aerodynamic center for which convergence had occurred.

The converged-aerodynamic-center method was selected to determine the appropriate pair of N and m to be used in this report because it involved less computational labor. Upon examining the results of reference 7 and making use of the method described therein, a pattern of $N = 8$ and $m = 23$ was postulated to be sufficient for the kinds of planforms to be studied herein. In order to verify that this pattern would give results which lay in a converged-aerodynamic-center region, the aerodynamic center was calculated for several different sets of N and m and is plotted as a function of m in figure 1 for one of the families of cropped double-delta planforms for which design charts were prepared. A ± 2-percent $\bar{c}'$ error band is plotted about the $N = 8$ and $m = 23$ results, and for $m > 11$ the aerodynamic-center values appear to lie within this band. However, the predicted results obtained with the $N = 8$ and $m = 23$ pattern are not necessarily the same as would be found for an infinite number of points, but the two answers should compare closely. (The $N = 8$ and $m = 23$ control-point pair was also used in predicting the rotary aerodynamic characteristics.)

Although the present method was developed for steady, longitudinal, lifting problems, it can be used to compute rotary stability derivatives because of the relationship developed in the lifting-surface theory between tangential-flow boundary conditions and the downwash produced by a sheet of pressure doublets. The manner in which computation for rotary stability derivatives is made is based on recognizing, as pointed out in reference 9, that the steady-state rolling and pitching maneuvers are equivalent to linear twist and parabolic camber, respectively. This equivalence can be seen by realizing that the upwash on the upgoing wing in steady, rolling flight is just py and the tangent of the angle that the section makes with the free stream is just py/V. (The tangent of an angle is approximately equal to the angle in radians for small angles.) Integrating this expression along the chord gives a straight mean camber line, but one that is twisted along the span. A similar procedure can be used to obtain the mean camber line for the pitching motion about the reference point. The upwash is just qx for the upgoing part of the wing. The tangent of the angle that it makes (small angles of attack) with the free stream is just qx/V. Integrating this along the chord results in a parabolic camber.

VERIFICATION

In order to verify the applicability of the present method for predicting the static and rotary aerodynamic characteristics of the cropped double-delta planforms, a comparison of the results from this method with experimental data (refs. 10 to 18) and with results from other theories (refs. 19 and 20) is presented in table I for delta, cropped delta, and double-delta wings. It should be noted that in this table no comparisons are presented for cropped double-delta wings because experimental data were lacking. However, comparisons of data for the other wings with results from the present method indicate that this method was applicable to wings with breaks in the leading edge and cropped tips and, hence, to cropped double-delta wings. Results from the present method are also compared with experimental data in figure 2. The theoretical methods selected for comparison are those which predict only the rotary stability derivatives since the theoretical methods which predict the static stability derivatives were compared with results from the present method in reference 7. In examining table I, it should be remembered that the theoretical method of reference 19 has an inherent restriction associated with it because its derivation was based on wings with vanishing aspect ratios.

Static Stability Derivatives

Generally good agreement is found between the theoretical and experimental values for C_{L_α}, where the theoretical values have variations of about ± 10 percent from the experimental values. (See fig. 2.) Also, the predicted x_{ac} values generally agree well with the experimental values and have variations of about ± 10 percent from the

experimental values or ±5 percent of $\bar{c}$. No comparison between the theoretical and experimental location of x_{ac} could be made for the double-delta wings of $A = 1.60$ because reference 18 reports that the pitching-moment data were questionable, and hence not presented, for small angles of attack.

Rotary Stability Derivatives

Comparison of results from the present method with experimental data and results from the other theories for the rotary stability derivatives is restricted to the delta and cropped delta planforms since (1) no experimental rotary derivatives were found for the double-delta wings and (2) the theoretical methods of references 19 and 20 were not readily (if at all) applicable to the double-delta wings.

Damping in roll $\left(C_{l_p}\right)$.- The present method generally predicts values of C_{l_p} about 20 percent more negative than those measured experimentally for a wing of $A \geqq 1.0$. A large part of this loss in theoretical damping may be due to the wing tips of the experimental model experiencing a stall condition for which the present method does not account. The actual individual differences between the experimental data and values from the present method are smaller for all configurations than those resulting from use of the method of reference 19, which was developed for slender wings only. However, when experimental data and values from the present method are compared with values from the method of reference 20, it is found that the predicted values of reference 20 agree almost as well with experimental data as values from the present method for the delta wings and agree slightly better with experimental data for the cropped delta wings. Hence, either the method of reference 20 or the present method could be applied with almost equal accuracy for delta or cropped delta wings but the present method is more easily applied to cropped double-delta wings.

Damping in pitch $\left(C_{m_q}\right)$.- The present method generally predicts values of C_{m_q} which are about 30 percent less stable than the experimental values; however, the results obtained by this method agree better with experimental data than those obtained by the method of reference 19, which predicts results that are consistently more stable than experimental data and results from the present method. The method of reference 19 is based on slender-wing theory and is obviously outside of its range of applicability.

Lift coefficient due to pitch rate $\left(C_{L_q}\right)$.- The present method generally predicts values of C_{L_q} about 25 percent larger than the experimental values; however, the results from this method agree better with experimental data than the results predicted from the method of reference 19. The method of reference 19 is again obviously outside its range of applicability.

General observation.- If a consistent set of experimental data and the corresponding predicted values from the present method, as given in table I, were plotted against aspect ratio, it would be found that the correct trends are predicted by the present method for all three rotary stability derivatives.

DATA PRESENTATION

Because of the multiplicity of planforms that can be encountered in connection with composite wings, such as the cropped double-delta planform studied here, design charts cannot be expected to eliminate the need for computer calculations to determine accurately the aerodynamic characteristics of any particular planform. However, design charts which broadly cover the range of planform parameters of general interest for aircraft which must fly at both subsonic and supersonic speeds are felt to be useful in selecting the general type of planform which might best satisfy the various aerodynamic requirements for the preliminary design thereby reducing the computer study requirements. Design charts, which illustrate the degree to which some of the more important aerodynamic parameters are affected by the various geometric variables, are presented herein.

In considering composite planforms, a variety of geometry controlling parameters are available for selection as the independent variables. However, since all of the configurations studied have straight unswept trailing edges, the following variables are the ones selected for use herein:

(1) Inboard leading-edge sweep angle (χ)

(2) Outboard leading-edge sweep angle (Λ)

(3) Spanwise location of the leading-edge break y_b

(4) Overall taper ratio (λ)

These variables, and in particular χ and Λ, were used to develop design charts at $M_\infty = 0$. However, the charts can be used for any subsonic Mach number if the wing geometric properties are corrected in accordance with the Prandtl-Glauert rule. Hence, the design charts are presented in terms of these corrected variables χ' and Λ' and also in terms of y_b and λ.

Wing geometric characteristics.- Unfortunately, the design charts based on the four variables just discussed do not allow convenient identification of other dependent parameters of interest, such as aspect ratio and mean geometric chord. Therefore, charts of wing geometric characteristics have been prepared which show the variation of inboard sweep angles and mean geometric chord with aspect ratio; these are presented as figures 3 and 4, respectively. Since the wing trailing edge is straight, a knowledge of the

mean geometric chord allows a ready determination of the moment reference point $\bar{c}'/4$ with respect to the trailing or leading edge of the root chord.

Wing aerodynamic characteristics.- The static aerodynamic characteristics for the cropped double-delta planforms are presented in figures 5 and 6. Figure 5 shows the lift-curve slope and figure 6 the aerodynamic center. The rotary aerodynamic characteristics for the cropped double-delta planforms are shown in figures 7, 8, and 9. Damping in roll and damping in pitch are shown in figures 7 and 8, respectively, and lift coefficient due to pitch rate is presented in figure 9.

Figure 10 is a summary of data which presents the aerodynamic-center locations for cropped delta wings as a function of λ. This figure is included herein because it shows an interesting occurrence; that is, regardless of the leading-edge sweep angle, a cropped delta wing has its aerodynamic center at approximately 25 percent of the planform mean geometric chord when the taper ratio is 0.32. Reference 21 reports a similar finding except that the taper ratio required was slightly different.

The reasoning used in reference 21 was that if planforms with limiting aspect ratios of zero and infinity both had their aerodynamic centers at the 25-percent mean-geometric-chord location, then perhaps, by suitable planform variation, the aerodynamic center could be kept at the 25-percent mean-geometric-chord point within these two aspect ratio limits. By using this basic reasoning, which does not hold for a delta wing (see ref. 22), the taper ratio required for a cropped delta wing was determined to be ≈ 0.303.

CONCLUDING REMARKS

An evaluation of a modified version of the Multhopp subsonic lifting-surface theory was made by comparing the theoretical values with experimental data. Near zero lift, the theory was found to predict reasonably adequately the lift-curve slope, aerodynamic center, damping in roll, damping in pitch, and lift coefficient due to pitch rate for delta and cropped delta planforms and also the lift-curve slope for double-delta planforms. Based on this theory, a series of design charts has been prepared for cropped double-delta planforms in subsonic compressible flow.

Langley Research Center,
National Aeronautics and Space Administration,
Langley Station, Hampton, November 21, 1969.

REFERENCES

1. Ray, Edward J.: NASA Supersonic Commercial Air Transport (SCAT) Configurations: A Summary and Index of Experimental Characteristics. NASA TM X-1329, 1967.

2. Spearman, M. Leroy; and Foster, Gerald V.: A Summary of Research on Variable-Sweep Fighter Airplanes. NASA TM X-1185, 1965.

3. O'Lone, Richard G.: SST Redesign Permits Titanium Gains. Aviat. Week Space Technol., vol. 89, no. 25, Dec. 16, 1968, pp. 41-43.

4. Taylor, John W. R., ed.: Jane's All the World's Aircraft, 1968-1969. McGraw-Hill Book Co., Inc.

5. Tumilowicz, Robert A.: Characteristics of a Family of Double-Delta Wings Designed to Reduce Aerodynamic Center Shift With Mach Number. M.S. Thesis, Polytech. Inst. Brooklyn, 1965.

6. Benepe, David B.; Kouri, Bobby G.; Webb, J. Bert; et al.: Aerodynamic Characteristics of Non-Straight-Taper Wings. AFFDL-TR-66-73, U.S. Air Force, Oct. 1966. (Available from DDC as AD 809409.)

7. Lamar, John E.: A Modified Multhopp Approach for Predicting Lifting Pressures and Camber Shape for Composite Planforms in Subsonic Flow. NASA TN D-4427, 1968.

8. Polhamus, Edward C.: A Concept of the Vortex Lift of Sharp-Edge Delta Wings Based on a Leading-Edge-Suction Analogy. NASA TN D-3767, 1966.

9. Etkin, Bernard: Dynamics of Flight – Stability and Control. John Wiley & Sons, Inc., c.1959.

10. Tosti, Louis P.: Low-Speed Static Stability and Damping-in-Roll Characteristics of Some Swept and Unswept Low-Aspect-Ratio Wings. NACA TN 1468, 1947.

11. Lange and Wacke: Test Report on Three- and Six-Component Measurements on a Series of Tapered Wings of Small Aspect Ratio (Partial Report: Triangular Wing). NACA TM 1176, 1948.

12. Jaquet, Byron M.; and Brewer, Jack D.: Low-Speed Static-Stability and Rolling Characteristics of Low-Aspect-Ratio Wings of Triangular and Modified Triangular Plan Forms. NACA RM L8L29, 1949.

13. Lange and Wacke: Test Report on Three- and Six-Component Measurements on a Series of Tapered Wings of Small Aspect Ratio (Partial Report: Trapezoidal Wings). NACA TM 1225, 1949.

14. Goodman, Alex; and Jaquet, Byron M.: Low-Speed Pitching Derivatives of Low-Aspect-Ratio Wings of Triangular and Modified Triangular Plan Forms. NACA RM L50C02, 1950.

15. Berndt, Sune B.: Three Component Measurement and Flow Investigation of Plane Delta Wings at Low Speed and Zero Yaw. KTH-Aero TN 4, Div. Aeronaut., Roy. Inst. Technol. (Stockholm), 1949.

16. Goodman, Alex; and Adair, Glenn H.: Estimation of the Damping in Roll of Wings Through the Normal Flight Range of Lift Coefficient. NACA TN 1924, 1949.

17. Hopkins, Edward J.; Hicks, Raymond M.; and Carmichael, Ralph L.: Aerodynamic Characteristics of Several Cranked Leading-Edge Wing-Body Combination at Mach Numbers From 0.4 to 2.94. NASA TN D-4211, 1967.

18. Wentz, William H., Jr.; and Kohlman, David L.: Wind Tunnel Investigations of Vortex Breakdown on Slender Sharp-Edged Wings. Rep. FRL 68-013 (Grant NGR-17-002-043), Univ. of Kansas Center for Res., Inc., Nov. 27, 1968.

19. Ribner, Herbert S.: The Stability Derivatives of Low-Aspect-Ratio Triangular Wings at Subsonic and Supersonic Speeds. NACA TN 1423, 1947.

20. Queijo, M. J.: Theory for Computing Span Loads and Stability Derivatives Due to Sideslip, Yawing, and Rolling for Wings in Subsonic Compressible Flow. NASA TN D-4929, 1968.

21. Berndt, Sune B.: Note on the Position of the Aerodynamic Center of Pointed Wings at Subsonic Speeds. KTH-Aero TN 5, Div. Aeronaut., Roy. Inst. Technol. (Stockholm), 1949.

22. Jones, Robert T.: Properties of Low-Aspect-Ratio Pointed Wings at Speeds Below and Above the Speed of Sound. NACA Rep. 835, 1946. (Supersedes NACA TN 1032.)

TABLE I.- WINGS AND REFERENCES USED IN THE VERIFYING PROCEDURE AT LOW SUBSONIC MACH NUMBERS

Geometric parameters					Static stability derivatives		Rotary stability derivatives			References
A	χ, deg	Λ, deg	$\frac{y_b}{b/2}$	λ	C_{L_α}	x_{ac}	C_{l_p}	C_{m_q}	C_{L_q}	
Delta wing										
0.25	0	86.4	0	0	0.006	0.466	-----	-----	----	Unpublished experiment
					.0065	.459	-----	-----	----	Present method
.50	0	82.9	0	0	.0125	.464	-0.01	-----	----	10
					.0125	.443	-.046	-----	----	Present method
					-----	----	-.049	-----	----	Method of 19
1.00	0	76	0	0	.024	.400	-.035	-----	----	10
					.022	.402	-----	-----	----	11
					.023	.421	-----	-----	----	15
					.023	.414	-.087	-----	----	Present method
					-----	----	-.098	-----	----	Method of 19
1.07	0	75	0	0	.024	.450	-.075	-0.72	1.39	12, 14
					.024	.410	-.093	-.720	1.766	Present method
					-----	----	-.105	-1.261	2.521	Method of 19
1.67	0	67.4	0	0	.034	.391	-----	-----	----	15
					.034	.386	-----	-----	----	Present method
2.00	0	63.4	0	0	.0425	.346	-.117	-----	----	10
					.037	.375	-----	-----	----	11
					.0385	.375	-.153	-----	----	Present method
					-----	----	-.196	-----	----	Method of 19
					-----	----	-.161	-----	----	Method of 20
2.31	0	60	0	0	.042	.400	-.17	-1.00	2.05	12, 14, 16
					.042	.368	-.171	-.995	2.842	Present method
					-----	----	-.227	-2.721	5.443	Method of 19
					-----	----	-.180	-----	----	Method of 20
2.5	0	58	0	0	.045	.374	-----	-----	----	15
					.045	.363	-----	-----	----	Present method
3.00	0	53	0	0	.050	.320	-.168	-----	----	10
					.048	.355	-----	-----	----	11
					.050	.352	-.204	-----	----	Present method
					-----	----	-.295	-----	----	Method of 19
					-----	----	-.221	-----	----	Method of 20
4.00	0	45	0	0	.057	.362	-.22	-1.50	2.85	12, 14, 16
					.058	.338	-.241	-1.106	3.634	Present method
					-----	----	-.393	-4.712	9.425	Method of 19
					-----	----	-.278	-----	----	Method of 20
Cropped delta wings										
0.54	0	75.9	0	0.303	0.016	0.289	-----	-----	----	15
					.014	.256	-----	-----	----	Present method
.89	0	67.4	0	.303	.025	.282	-----	-----	----	15
					.023	.257	-----	-----	----	Present method
.99	0	45	0	.58	.0175	.220	-0.085	-0.800	1.18	12, 14
					.0255	.174	-.098	-.491	1.727	Present method
					-----	----	-.095	-----	----	Method of 20
1.33	0	66.8	0	.125	.030	.367	-----	-----	----	13
					.031	.338	-----	-----	----	Present method
1.33	0	61	0	.250	.032	.322	-----	-----	----	13
					.032	.279	-----	-----	----	Present method
1.33	0	45	0	.500	.033	.267	-----	-----	----	13
					.032	.203	-----	-----	----	Present method
1.34	0	58	0	.303	.034	.264	-----	-----	----	15
					.032	.258	-----	-----	----	Present method
1.99	0	45	0	.36	.036	.250	-.16	-1.09	2.15	12, 14
					.043	.246	-.185	-.708	2.709	Present method
					-----	----	-.179	-----	----	Method of 20
3.00	0	45	0	.15	.050	.340	-.22	-1.25	2.60	12, 14
					.053	.305	-.241	-.949	3.352	Present method
					-----	----	-.239	-----	----	Method of 20
Double-delta wing										
1.30	82	60	0.500	0	0.024	0.647	-----	-----	----	17
					.025	.583	-----	-----	----	Present method
1.60	75	65	.474	0	.0365	----	-----	-----	----	18
					.032	.455	-----	-----	----	Present method
1.60	80	65	.320	0	.036	----	-----	-----	----	18
					.032	.488	-----	-----	----	Present method

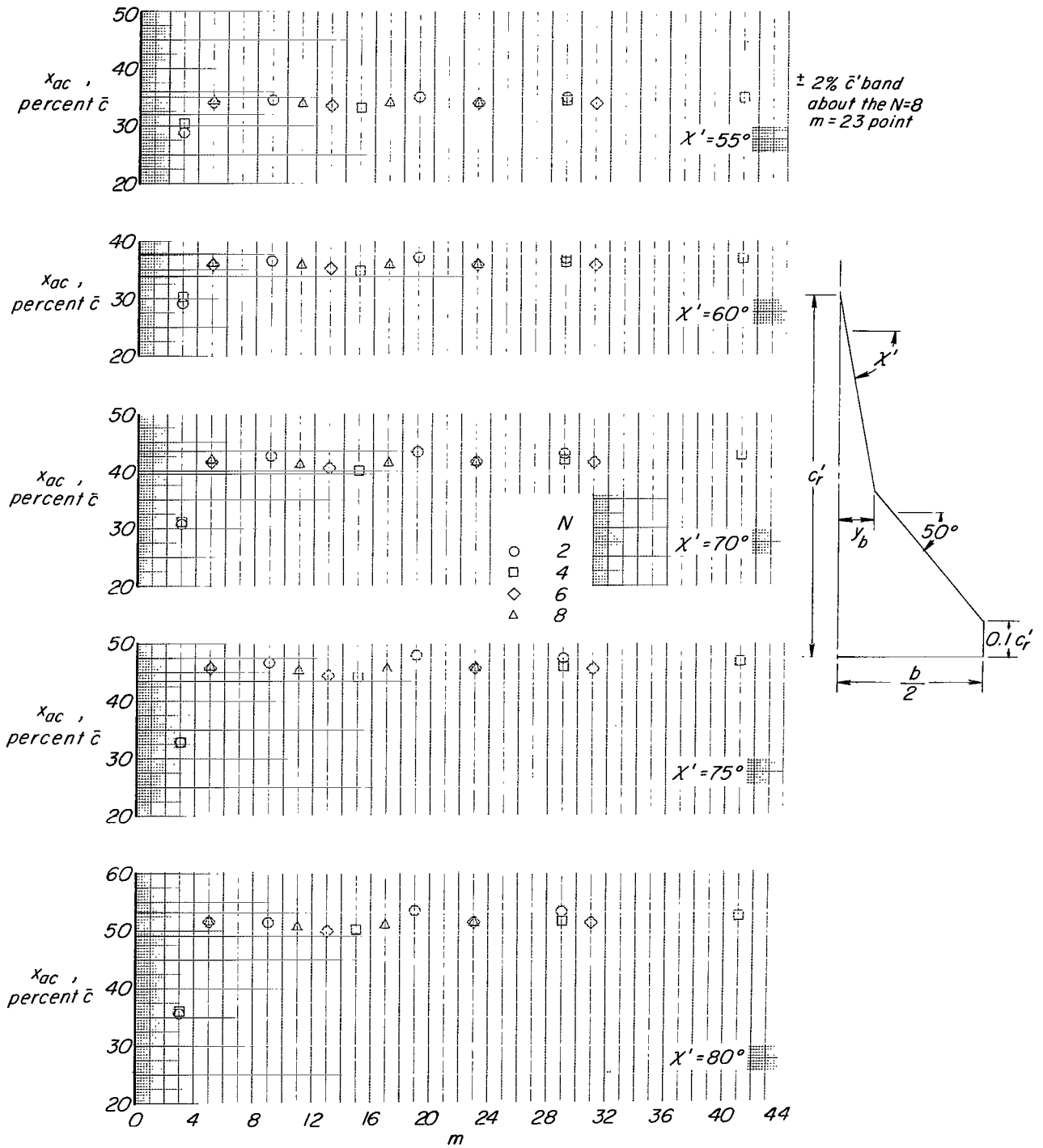

(a) Different transformed leading-edge inboard sweep angles are used. $\Lambda' = 50°$; $\lambda = 0.10$; $\frac{y_b}{b/2} = 0.50$.

Figure 1.- Effect of number of chordwise and spanwise stations on the aerodynamic center for typical cropped double-delta planforms.

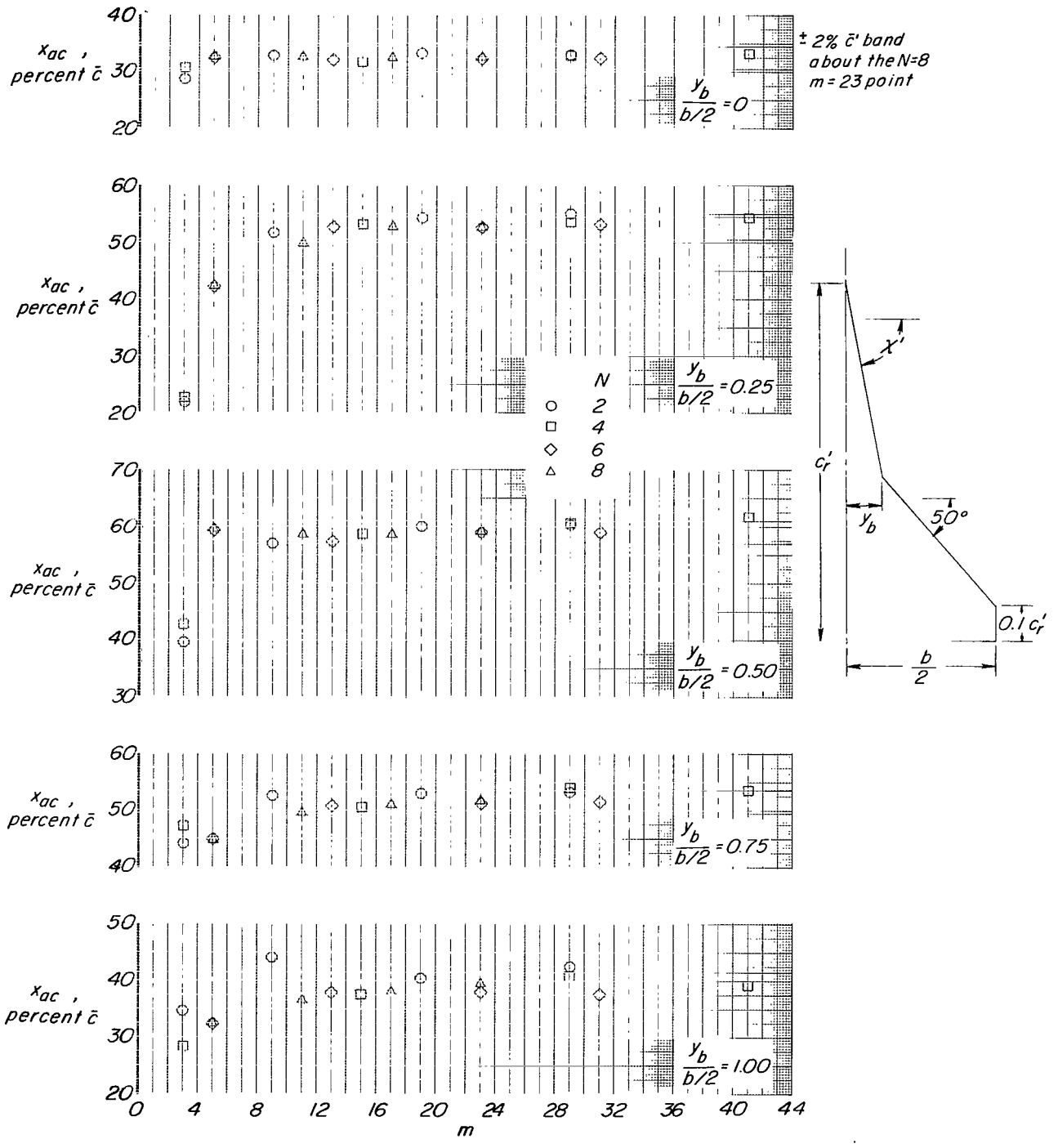

(b) Different leading-edge break ratios are used. $\chi' = 85^0$; $\Lambda' = 50^0$; $\lambda = 0.10$.

Figure 1.- Concluded.

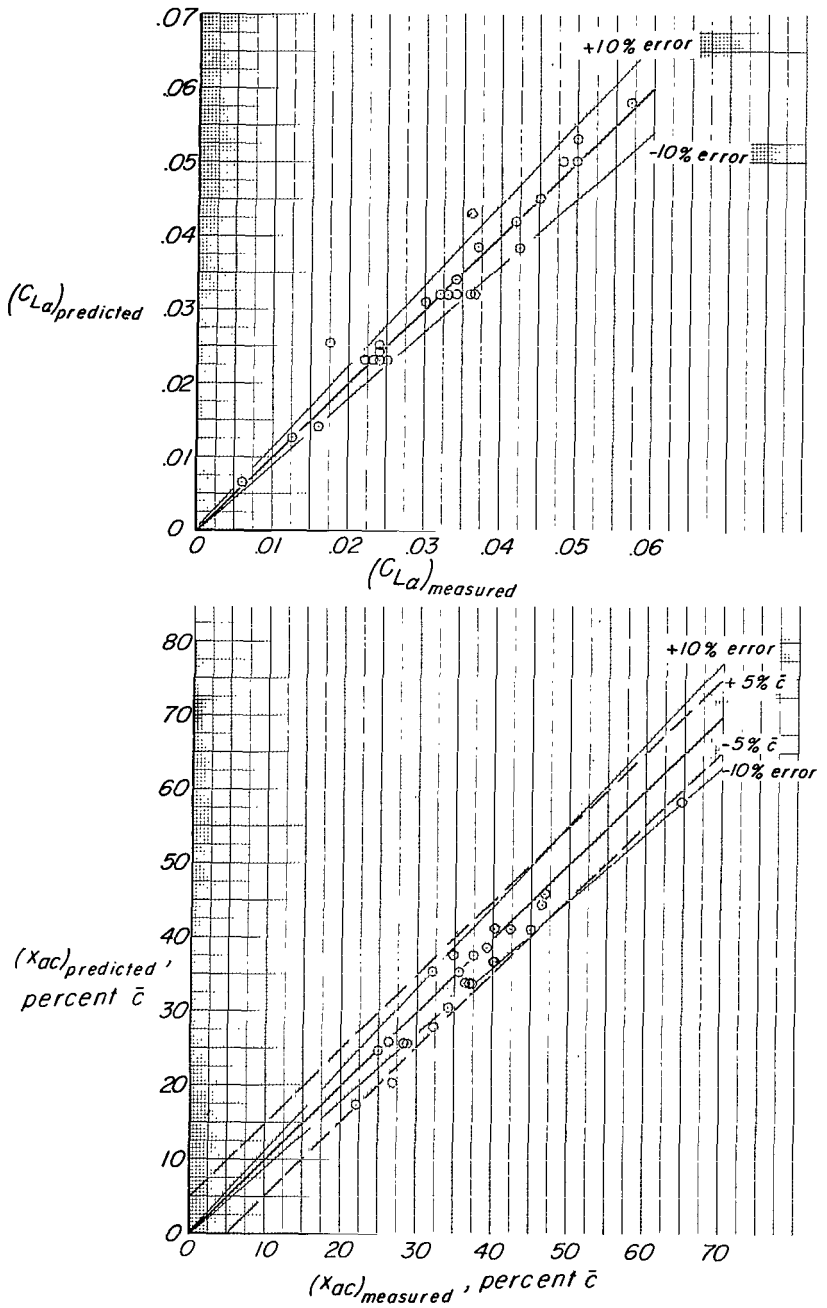

(a) Static derivatives.

Figure 2.- Prediction accuracy of modified Multhopp method at N = 8 and m = 23 for some aerodynamic characteristics of delta and delta-like wings.

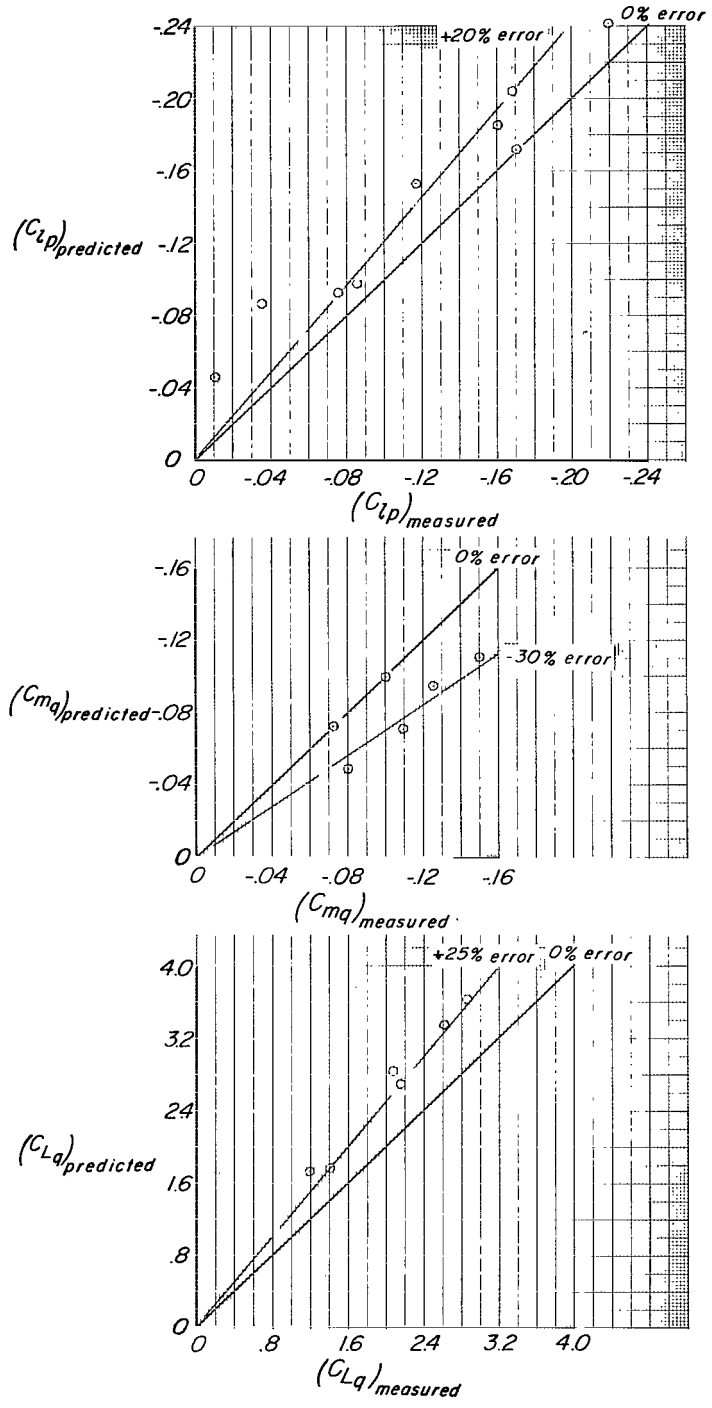

(b) Rotary derivatives.

Figure 2.- Concluded.

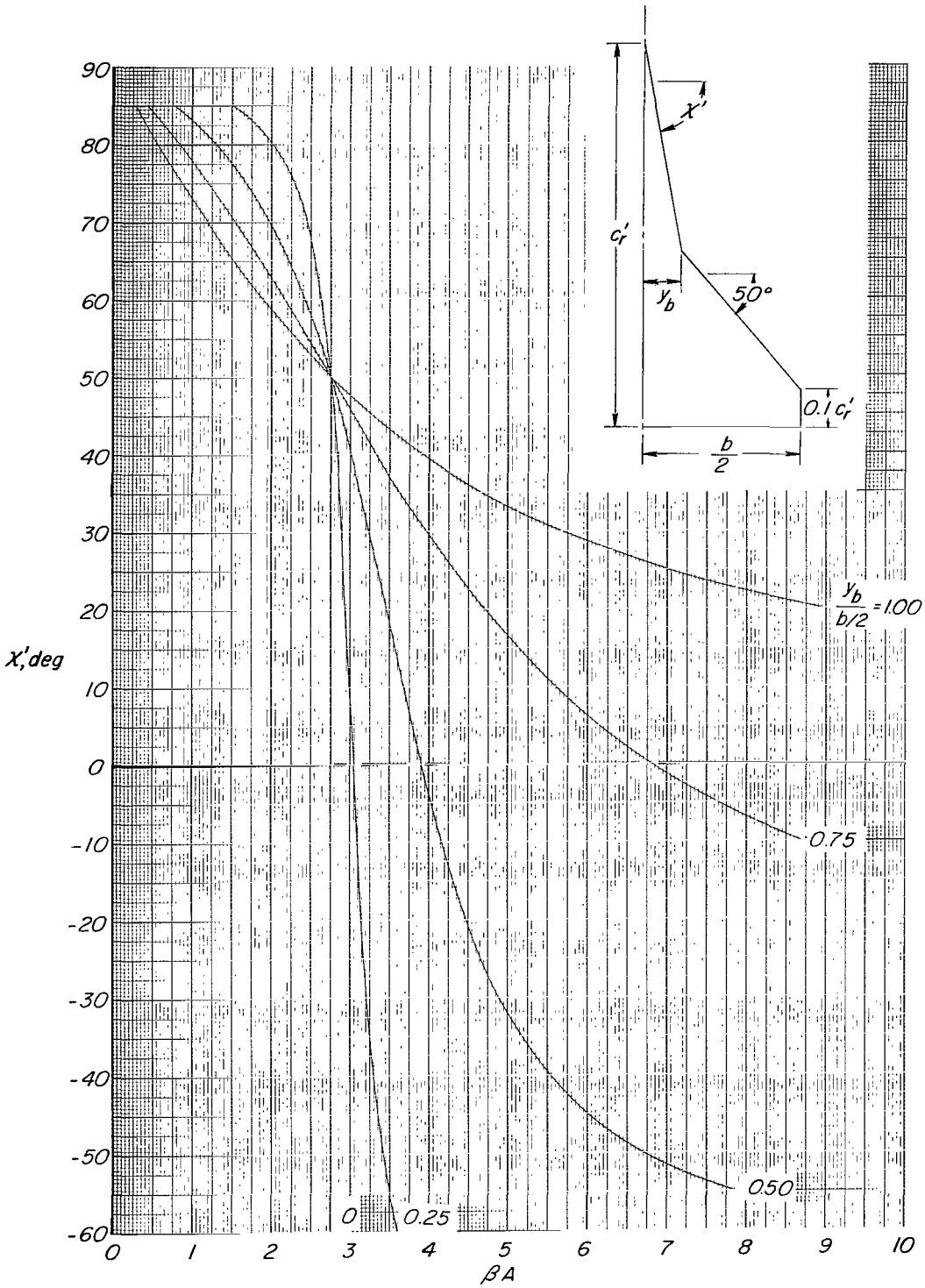

(a) $\Lambda' = 50^0$; $\lambda = 0.1$.

Figure 3.- Geometric characteristics of cropped double-delta planforms – relationship of parameters.

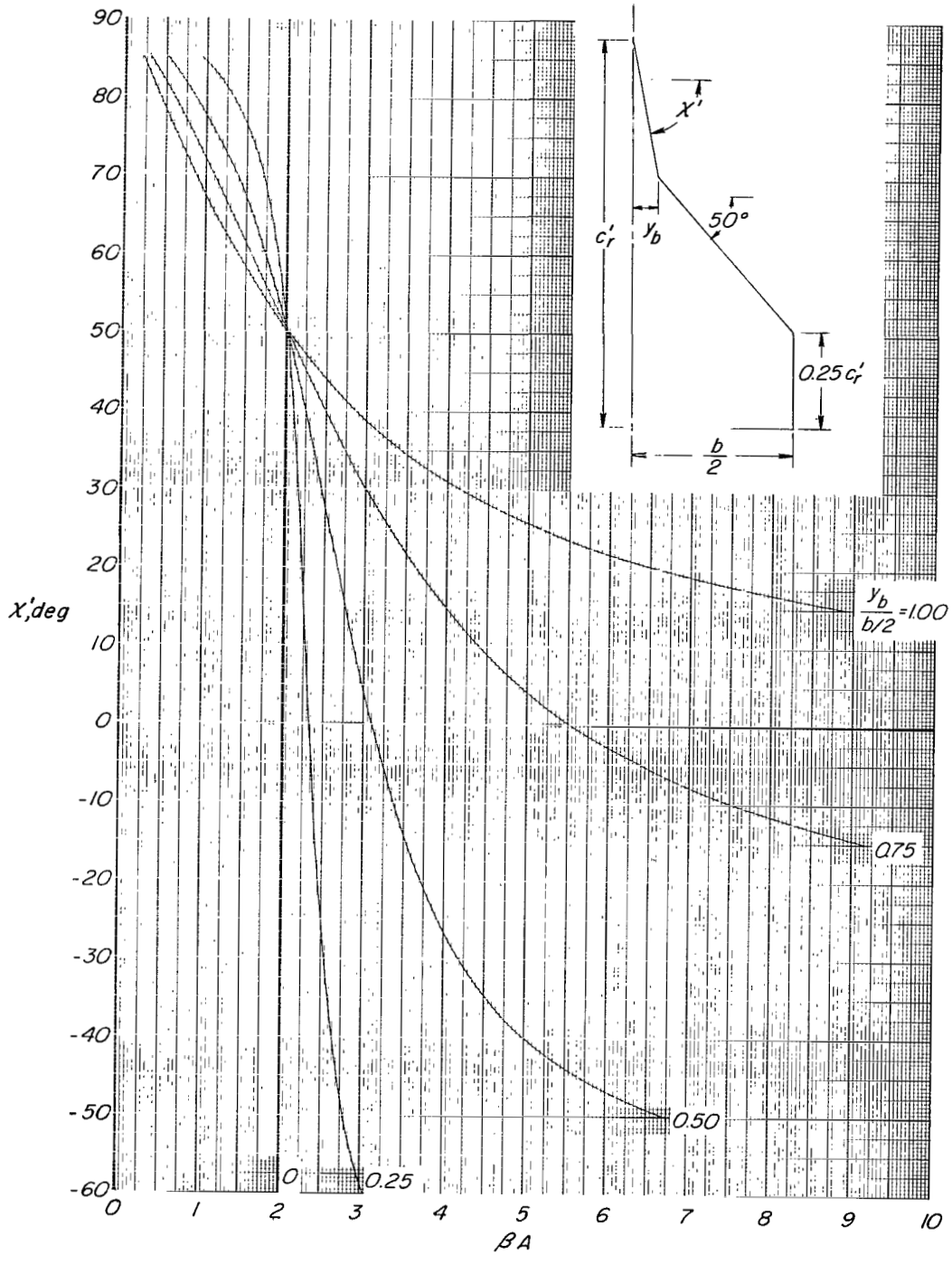

(b) $\Lambda' = 50^0$; $\lambda = 0.25$.

Figure 3.- Continued.

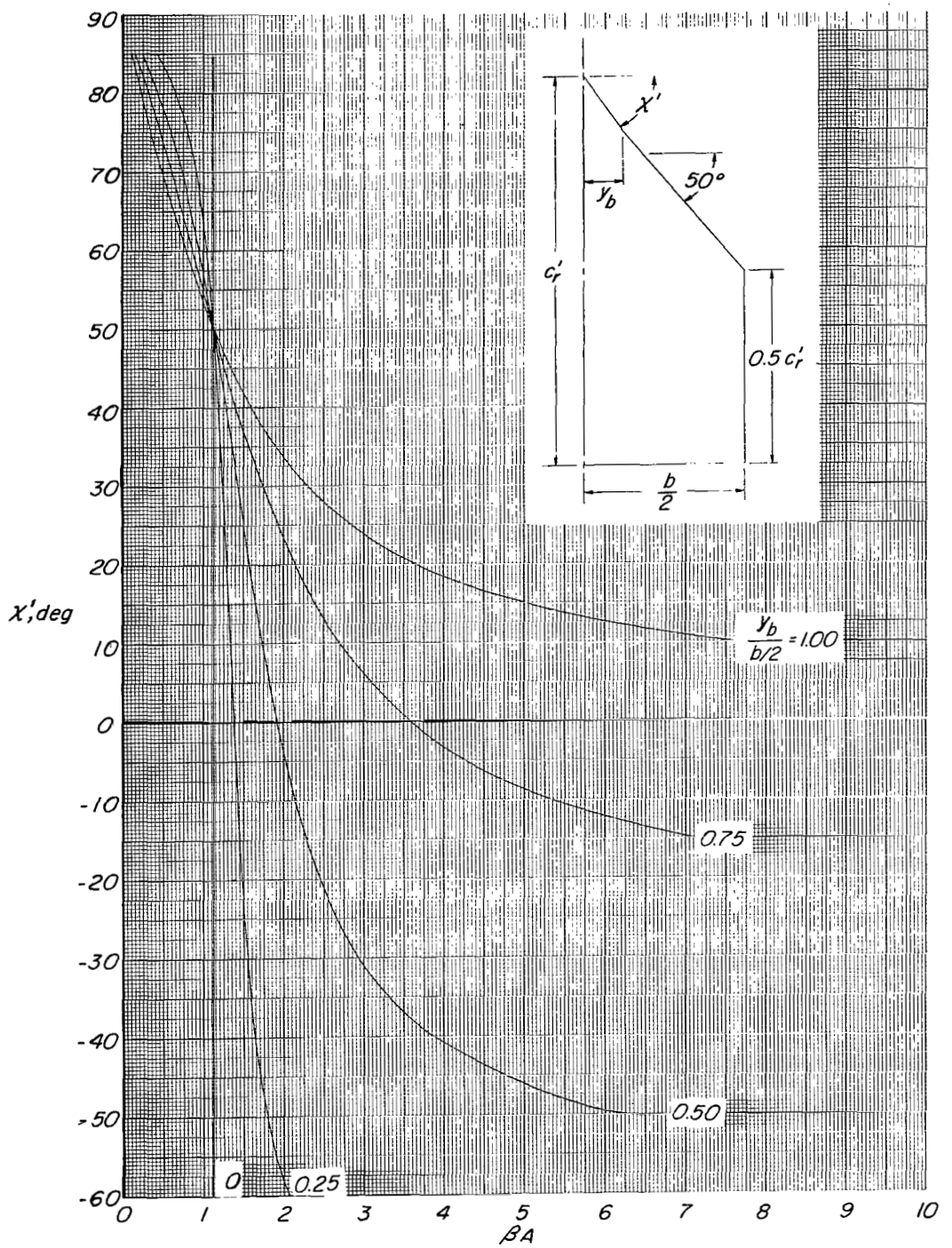

(c) $\Lambda' = 50^0$; $\lambda = 0.50$.

Figure 3.- Continued.

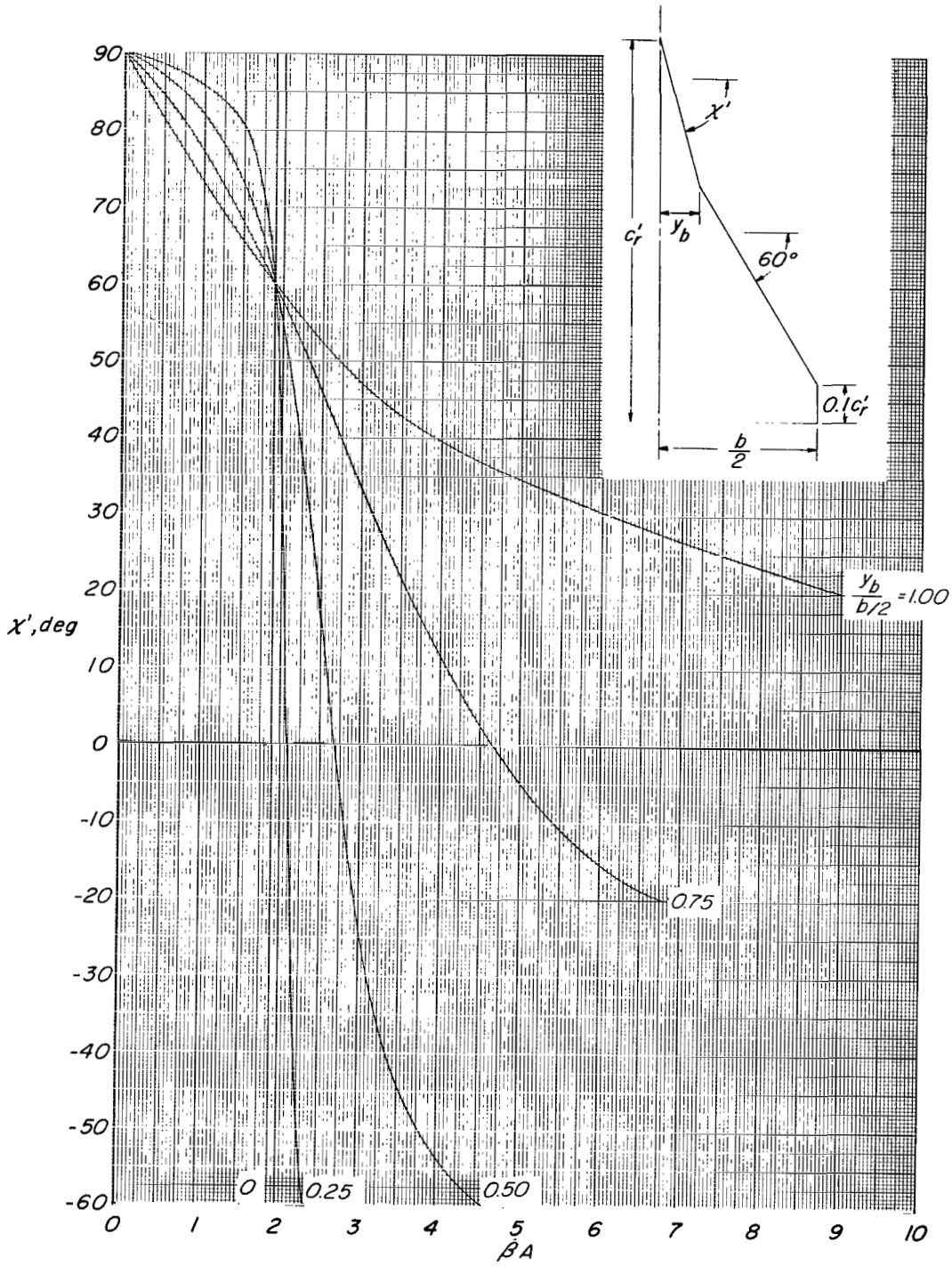

(d) $\Lambda' = 60^0$; $\lambda = 0.1$.

Figure 3.- Continued.

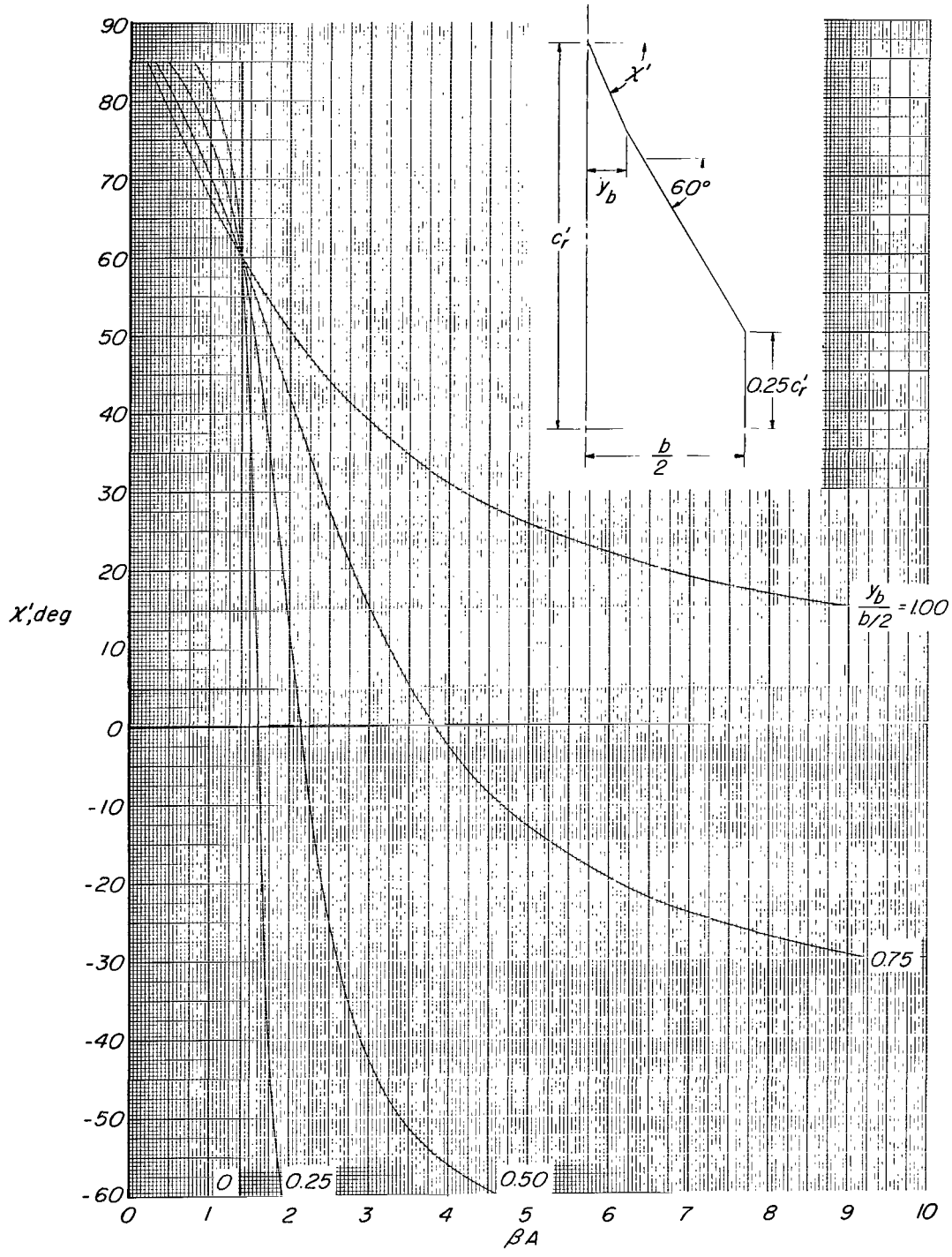

(e) $\Lambda' = 60^0$; $\lambda = 0.25$.

Figure 3.- Continued.

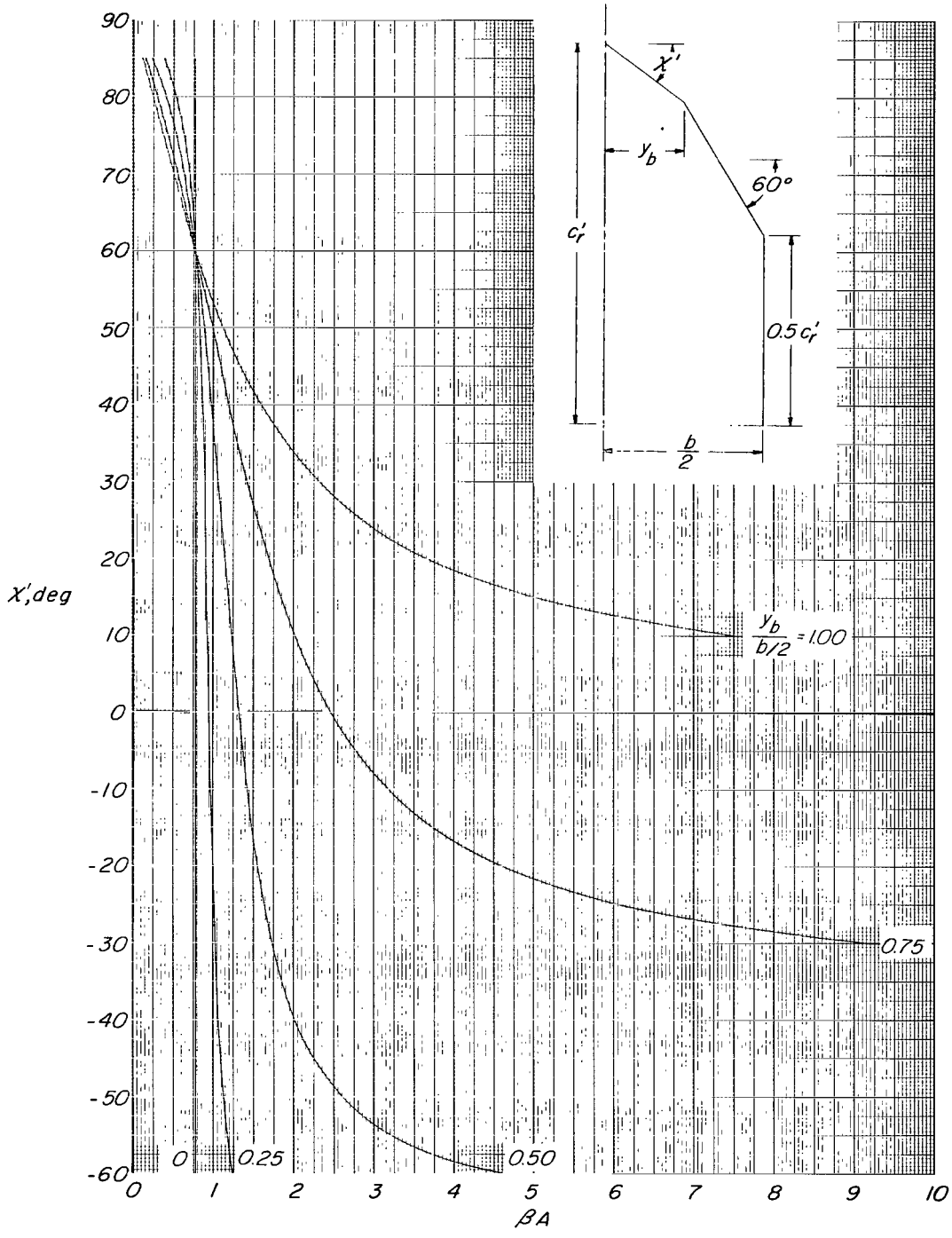

(f) $\Lambda' = 60^0$; $\lambda = 0.50$.

Figure 3.- Continued.

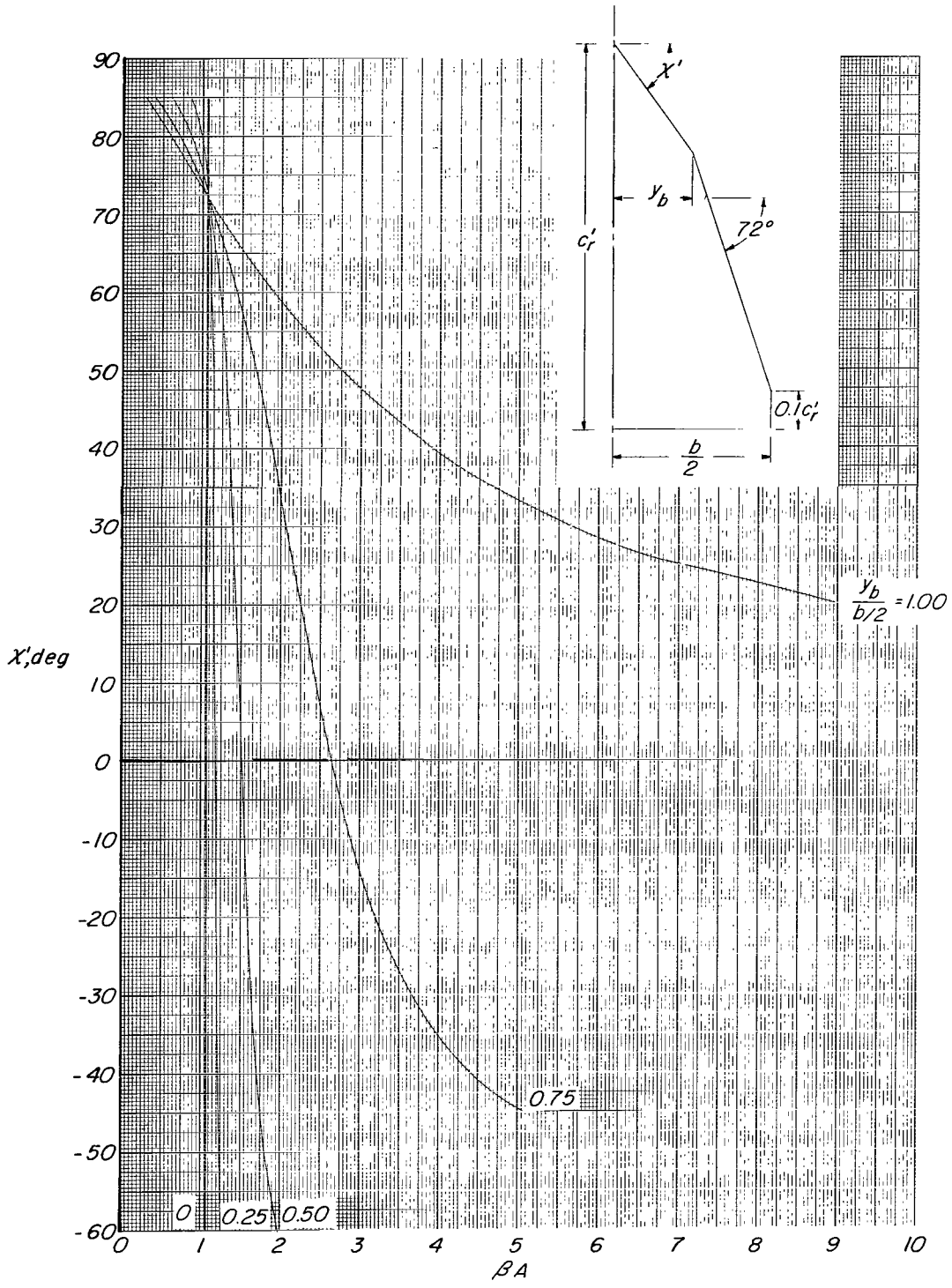

(g) $\Lambda' = 72^0$; $\lambda = 0.10$.

Figure 3.- Continued.

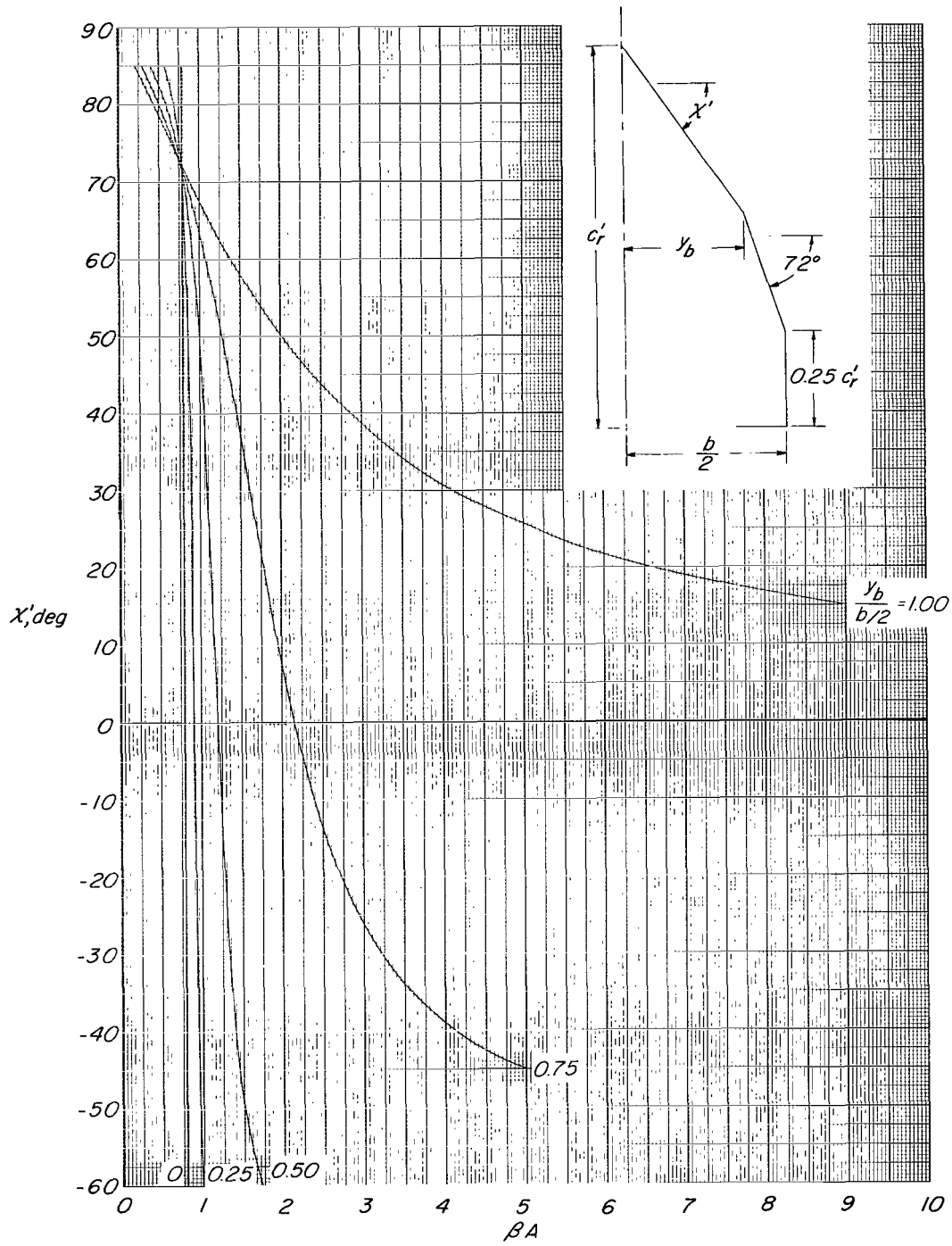

(h) $\Lambda' = 72^0$; $\lambda = 0.25$.

Figure 3.- Continued.

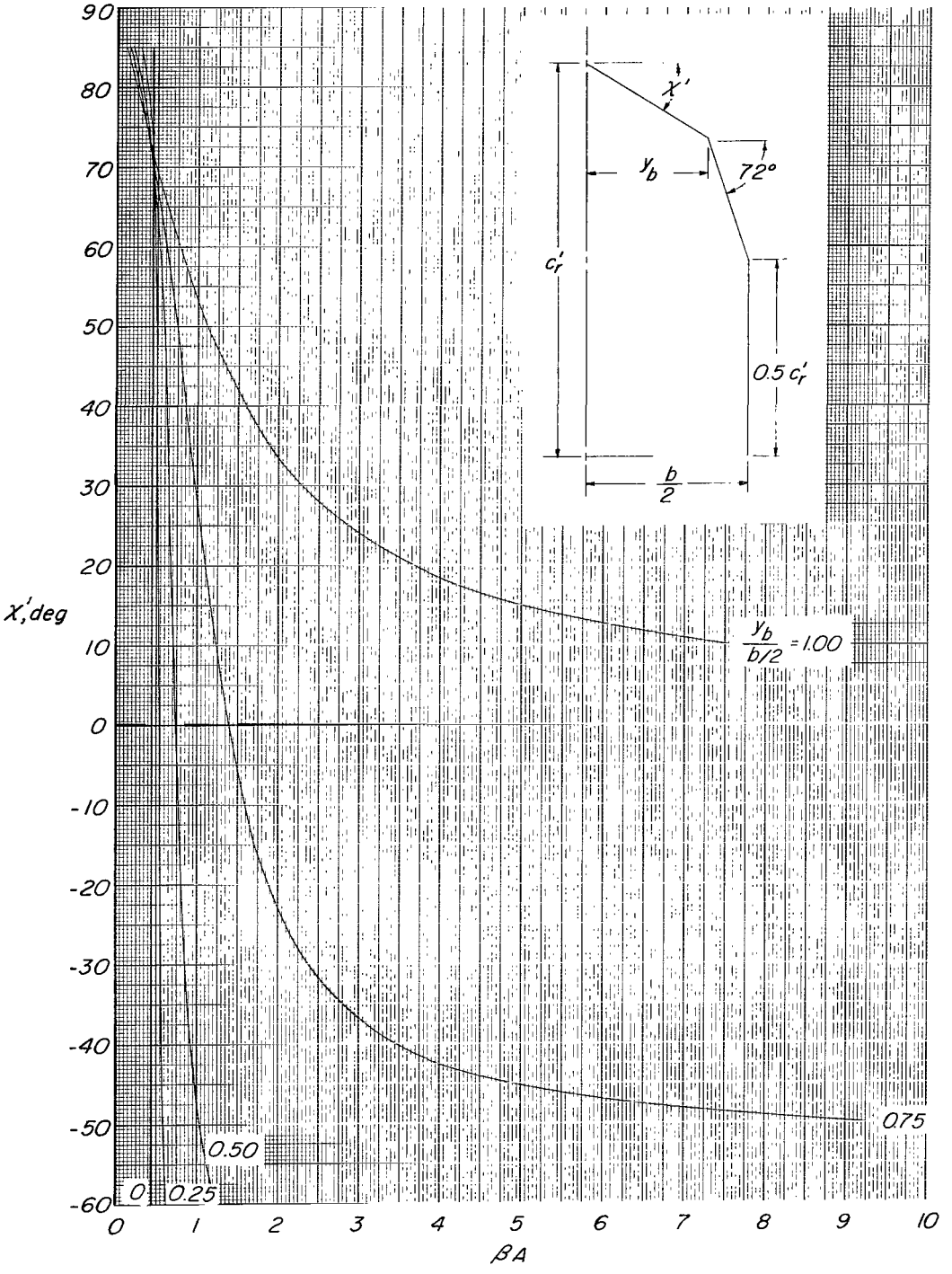

(i) $\Lambda' = 72^0$; $\lambda = 0.50$.

Figure 3.- Concluded.

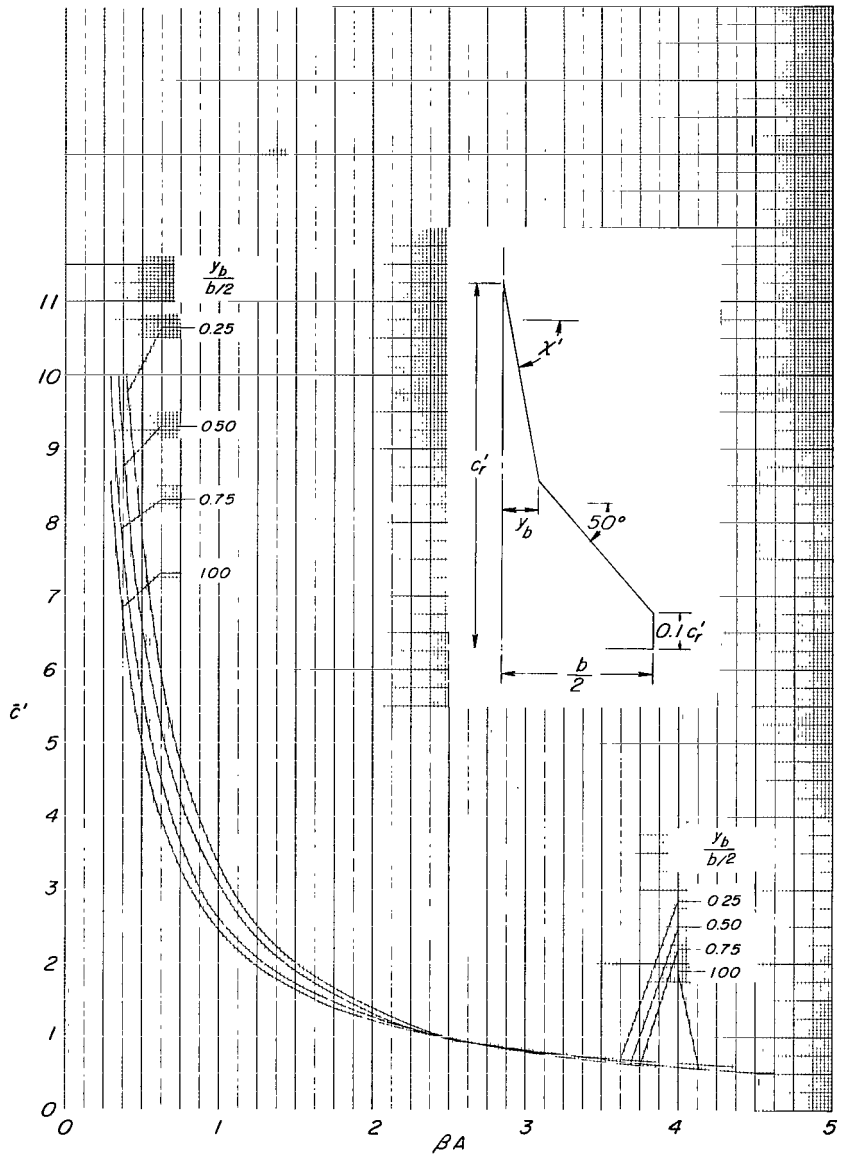

(a) $\Lambda' = 50^0$; $\lambda = 0.10$.

Figure 4.- Geometric characteristics of cropped double-delta planforms – mean geometric chords.

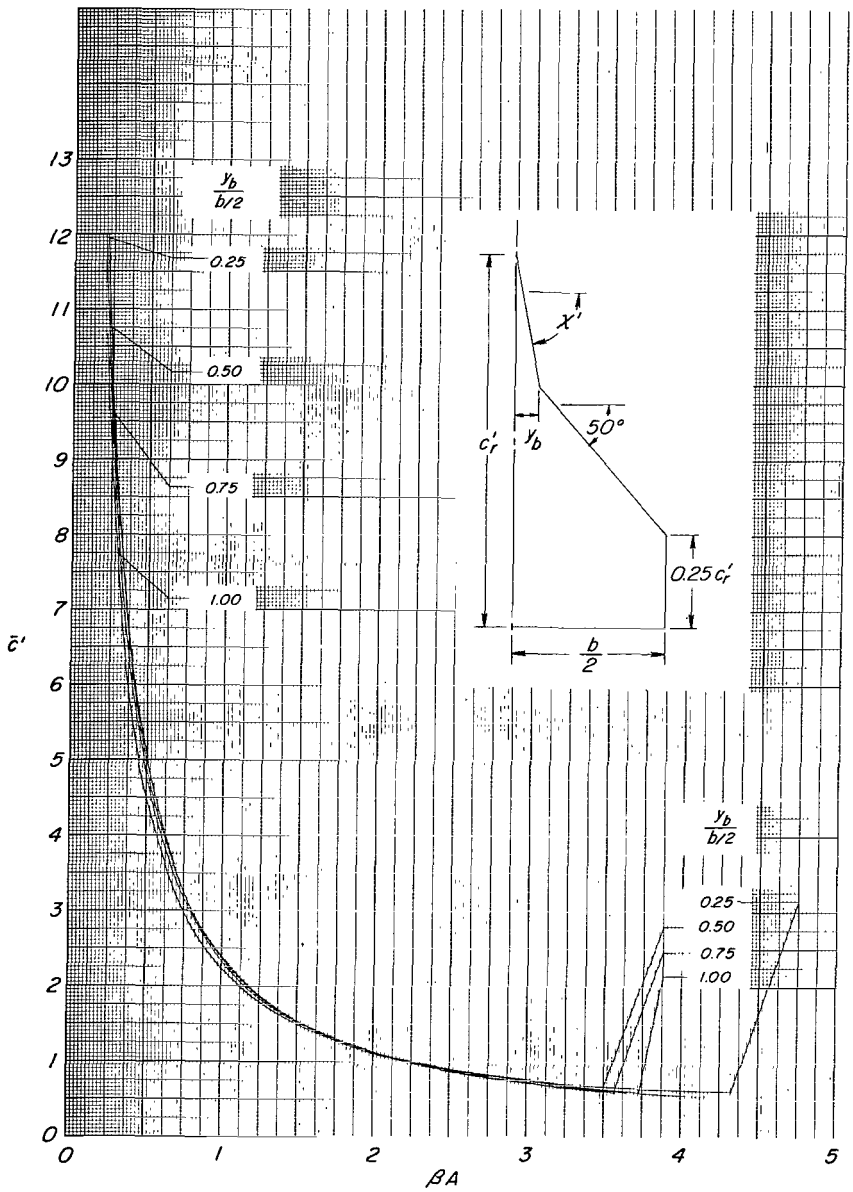

(b) $\Lambda' = 50^0$; $\lambda = 0.25$.

Figure 4.- Continued.

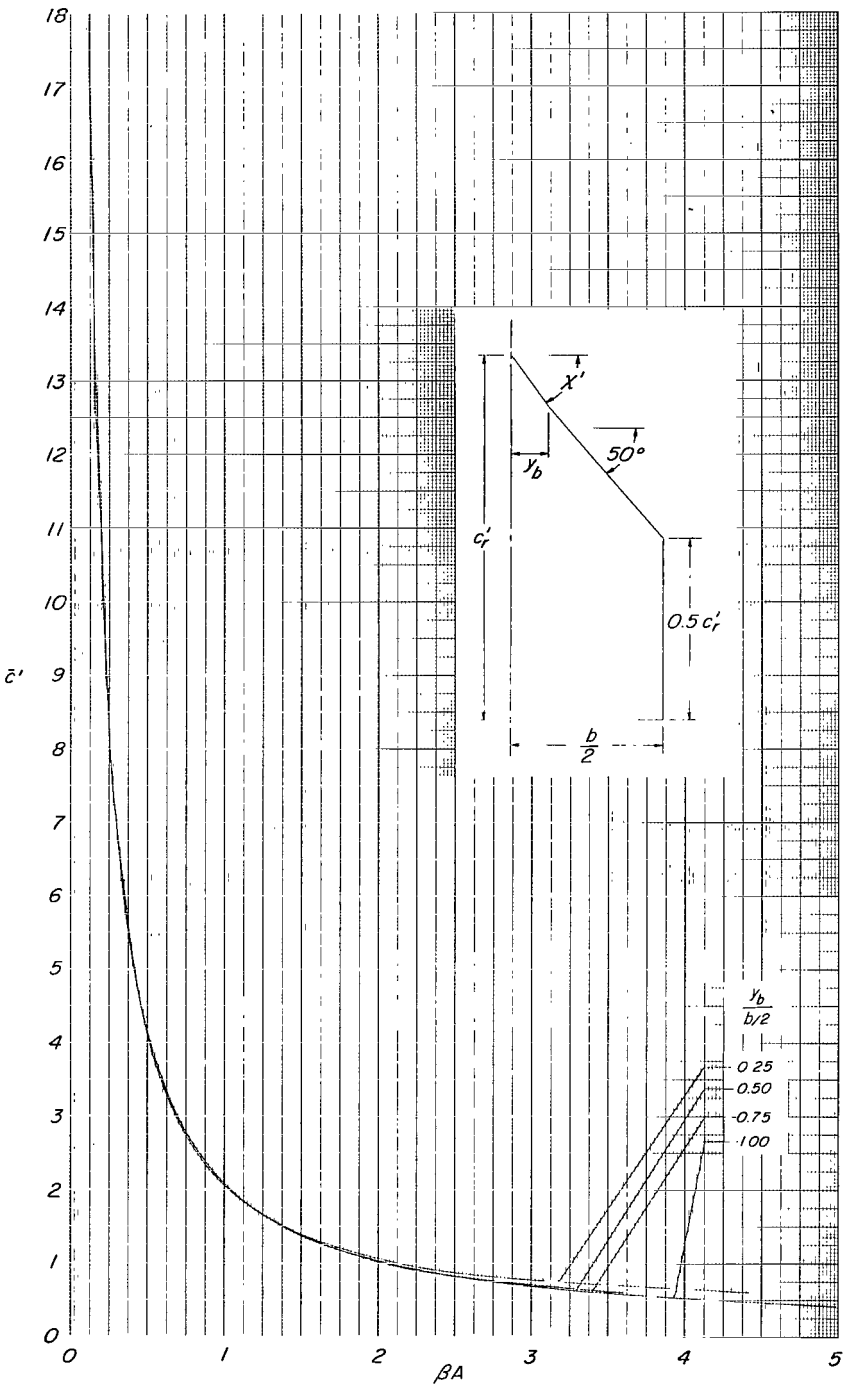

(c) $\Lambda' = 50^0$; $\lambda = 0.50$.

Figure 4.- Continued.

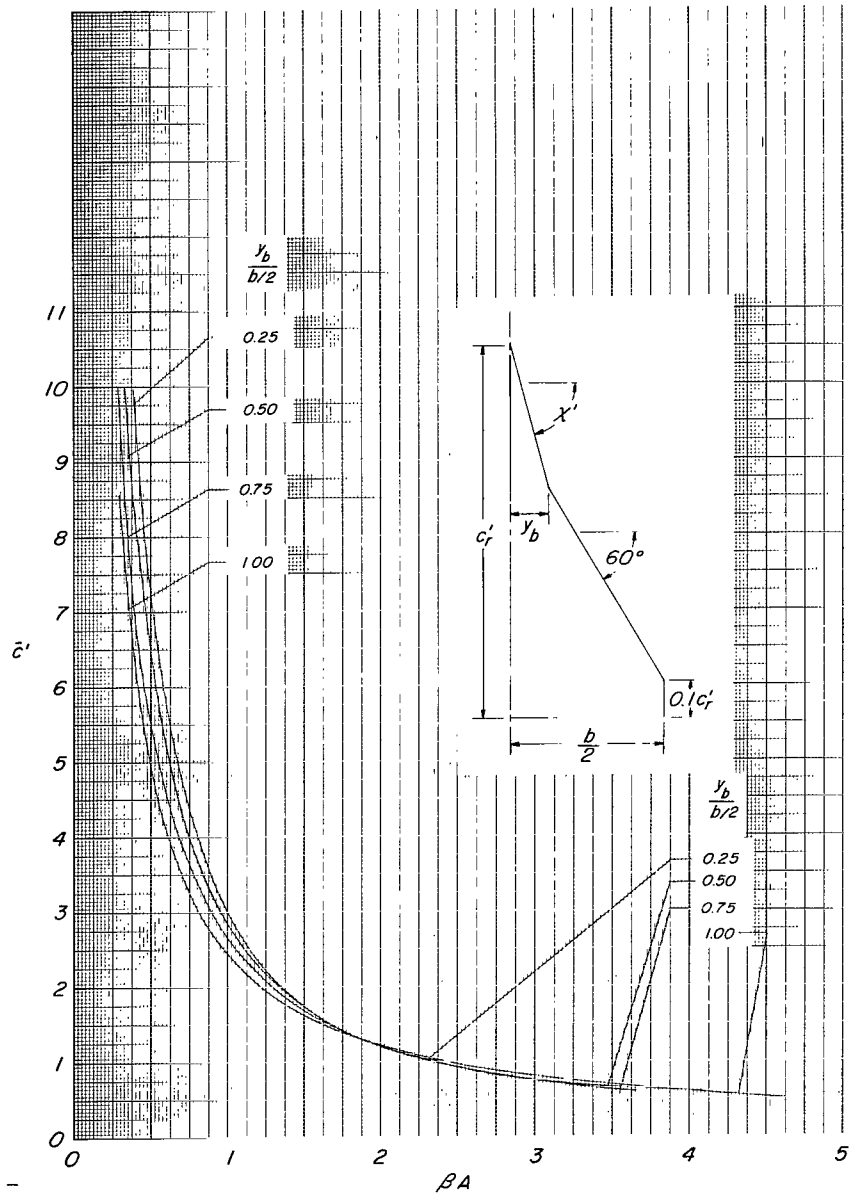

(d) $\Lambda' = 60^0$; $\lambda = 0.10$.

Figure 4.- Continued.

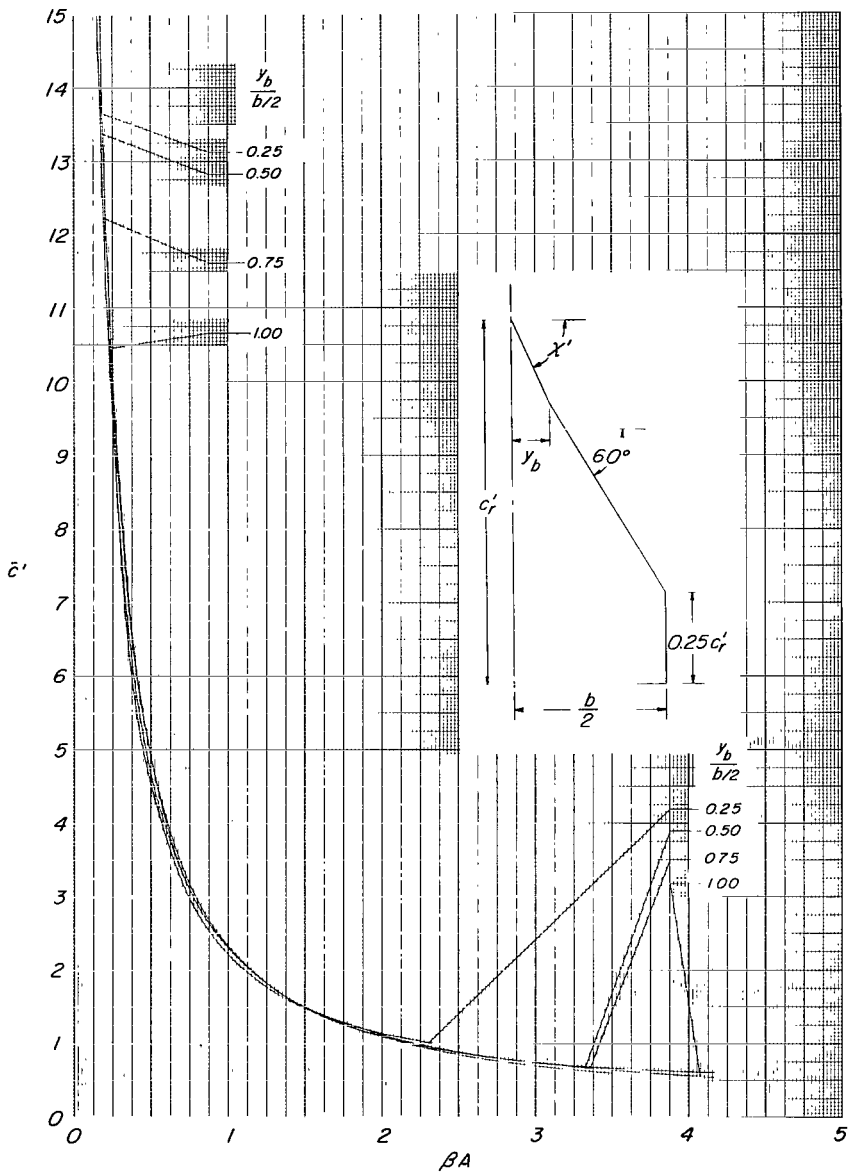

(e) $\Lambda' = 60^0$; $\lambda = 0.25$.

Figure 4.- Continued.

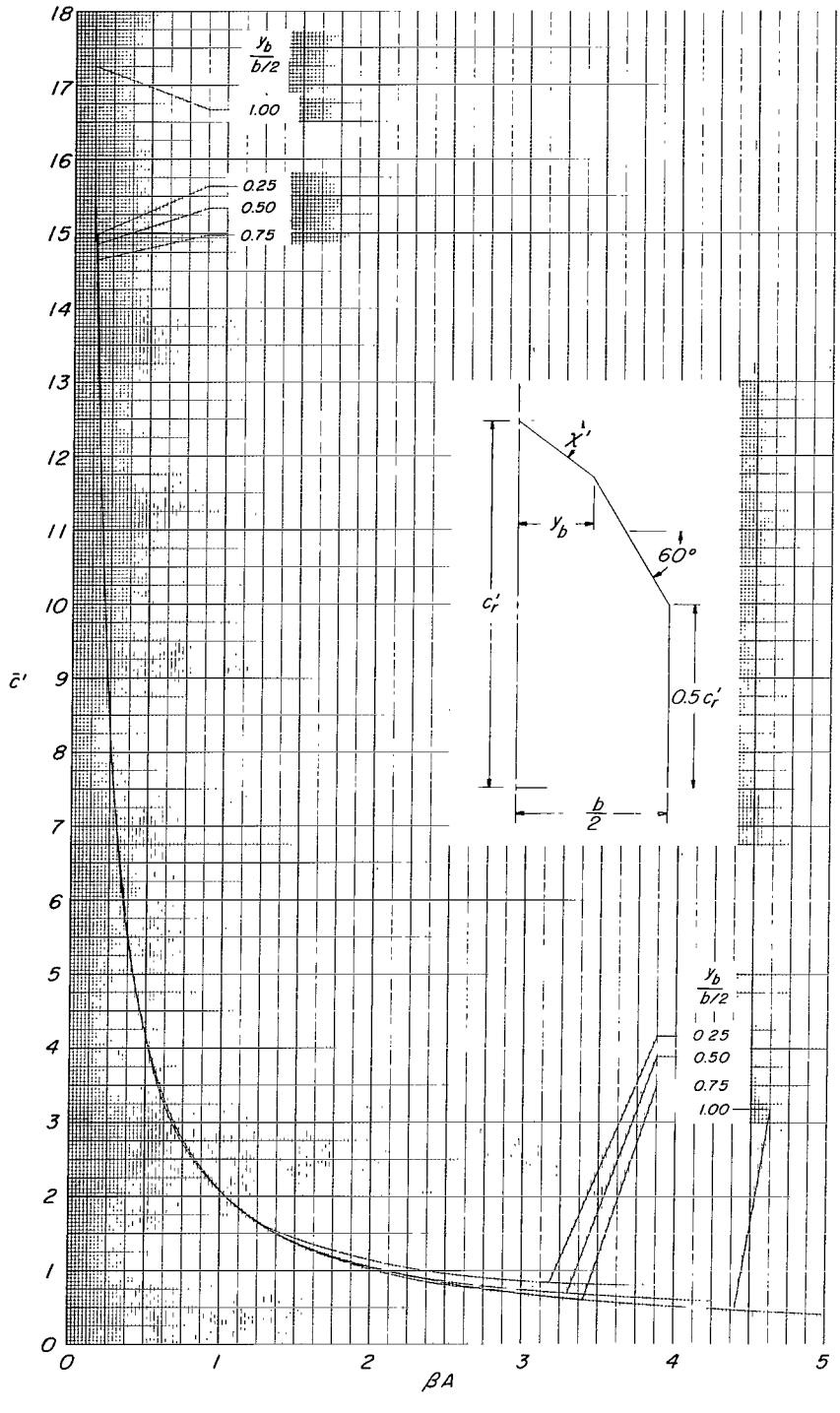

(f) $\Lambda' = 60^0$; $\lambda = 0.50$.

Figure 4.- Continued.

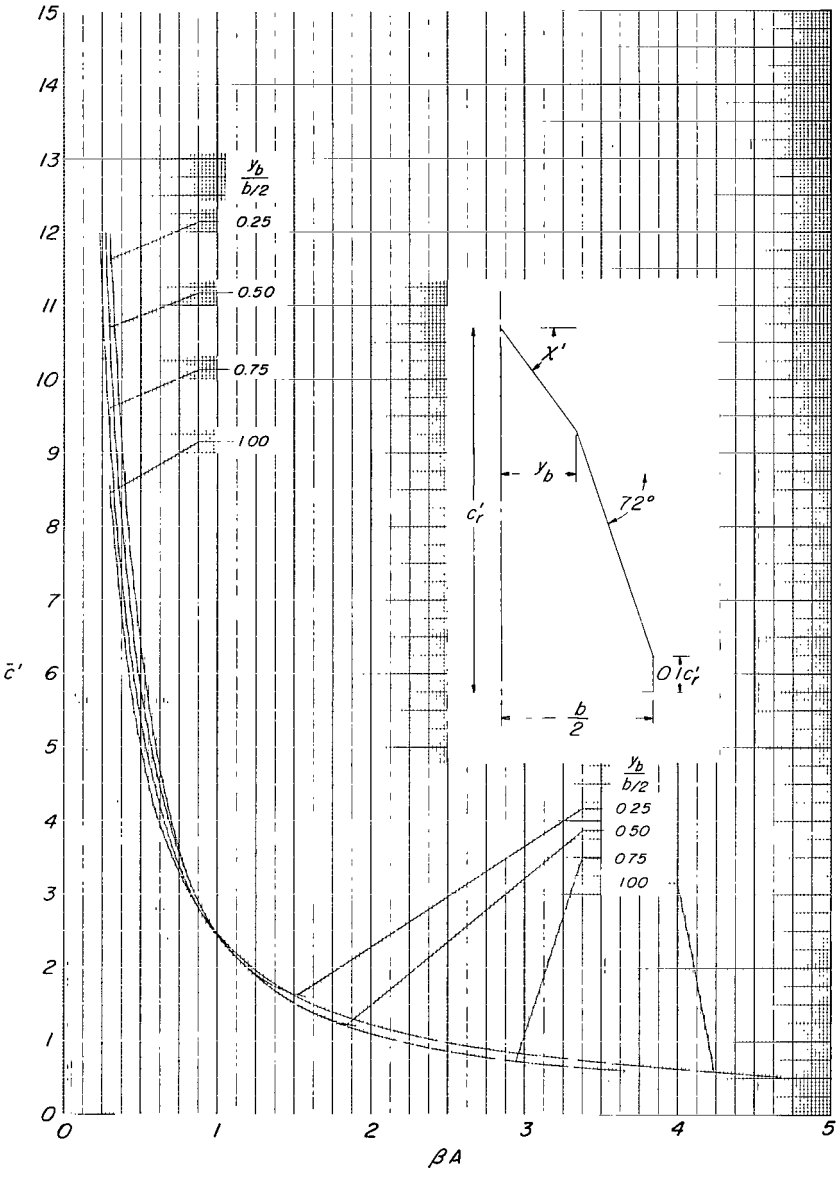

(g) $\Lambda' = 72^0$; $\lambda = 0.10$.

Figure 4.- Continued.

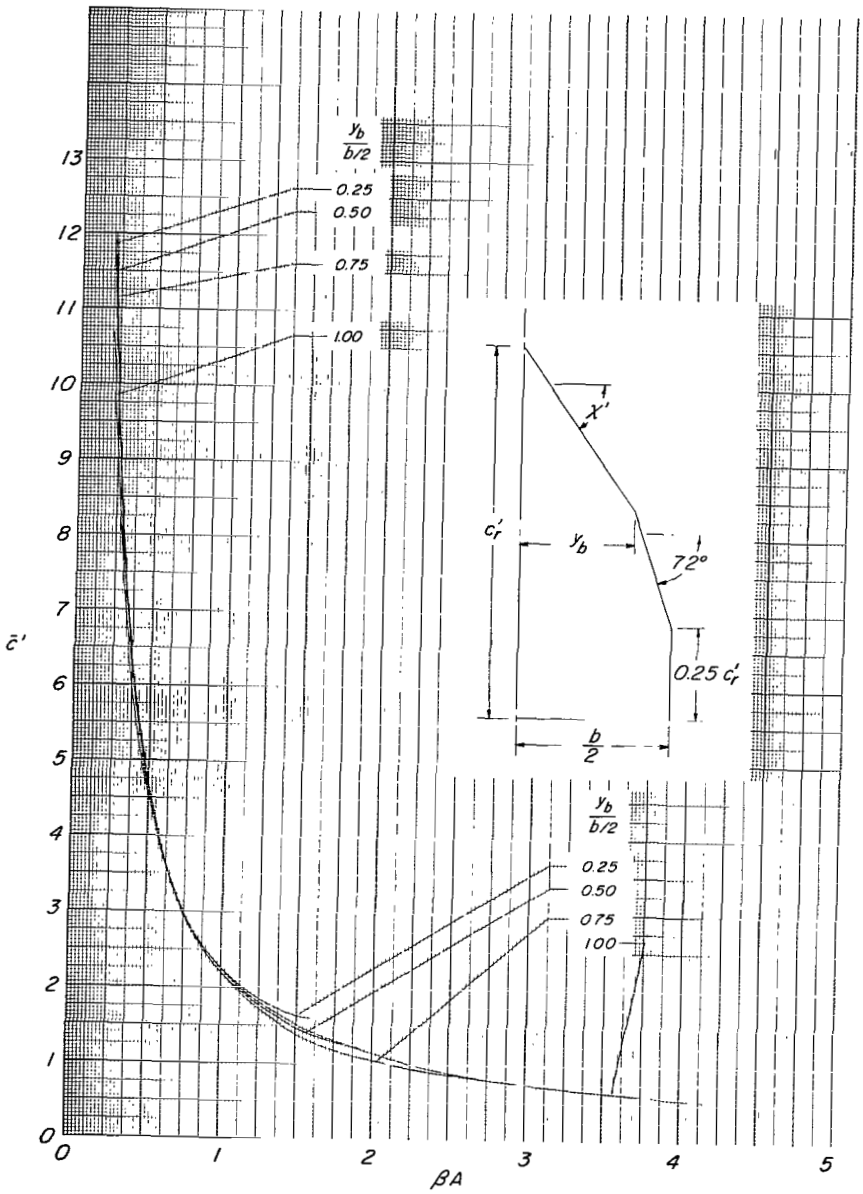

(h) $\Lambda' = 72^0$; $\lambda = 0.25$.

Figure 4.- Continued.

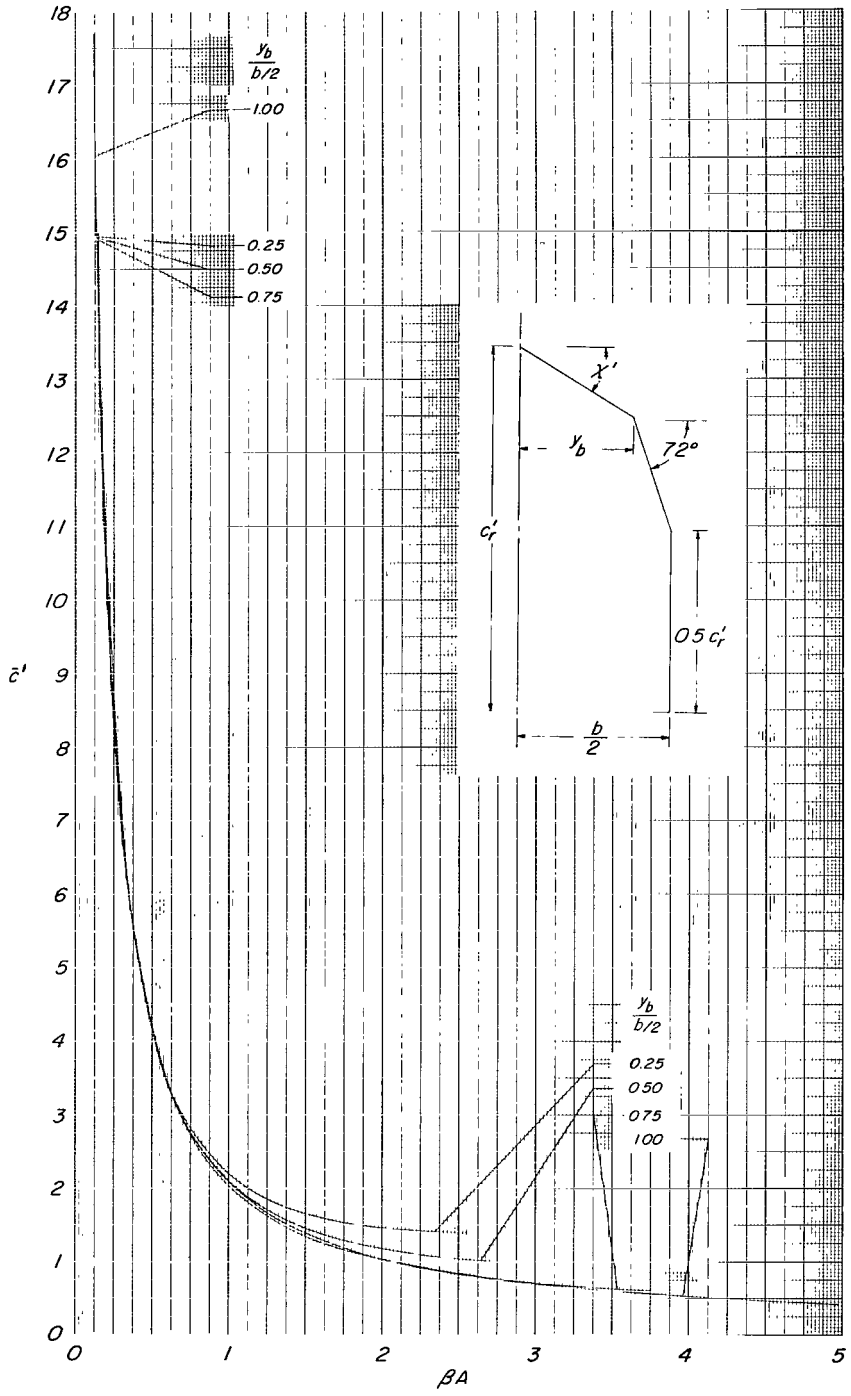

(i) $\Lambda' = 72^0$; $\lambda = 0.50$.

Figure 4.- Concluded.

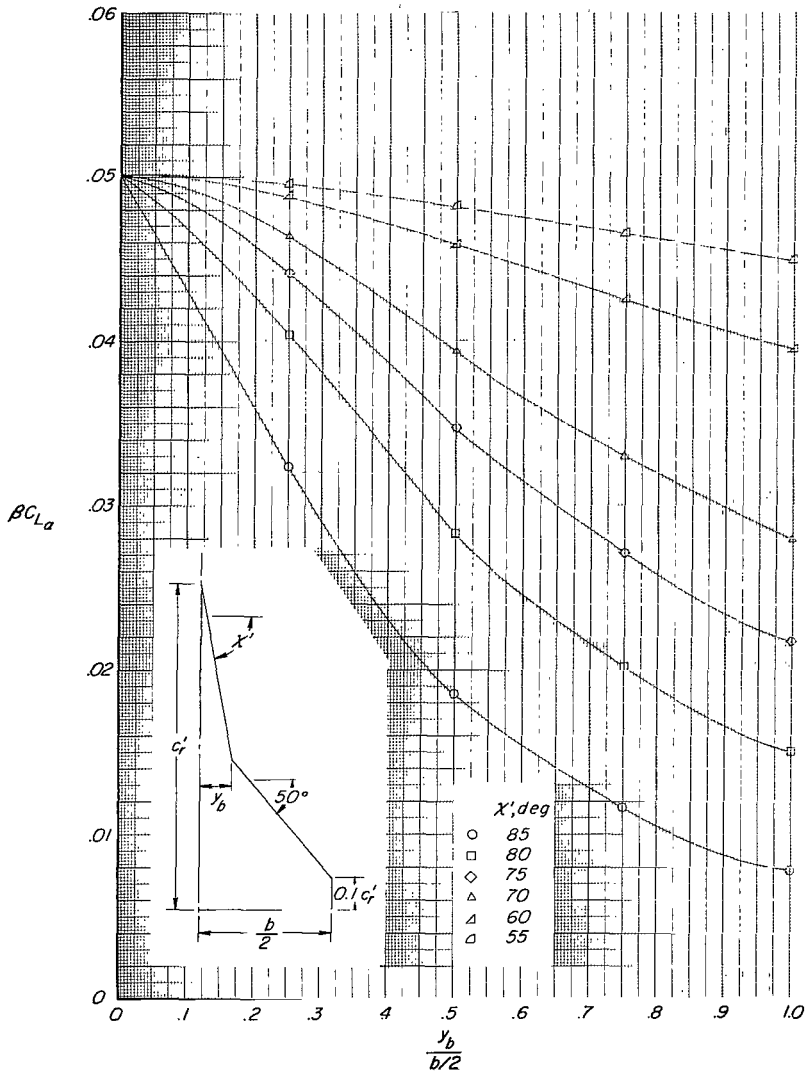

(a) $\Lambda' = 50^0$; $\lambda = 0.10$.

Figure 5.- Lift-curve slope for cropped double-delta planforms.

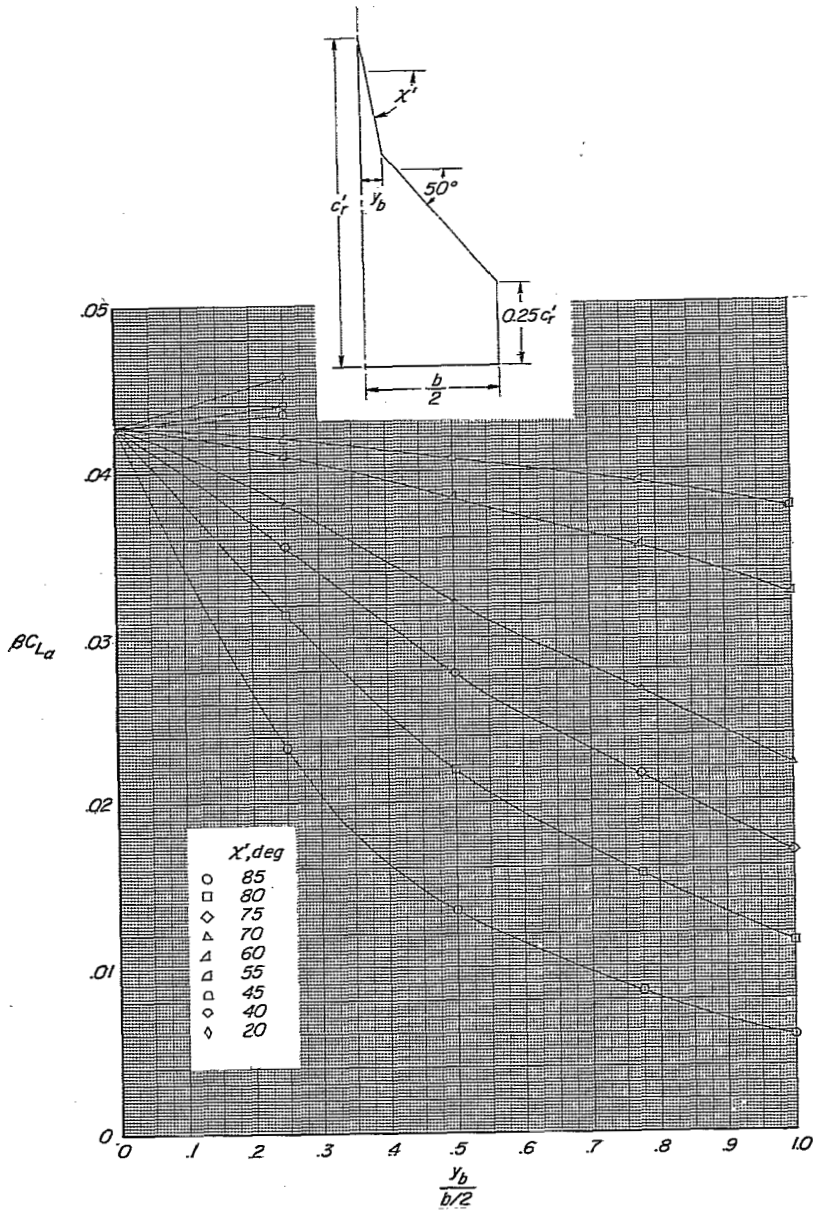

(b) $\Lambda' = 50^0$; $\lambda = 0.25$.

Figure 5.- Continued.

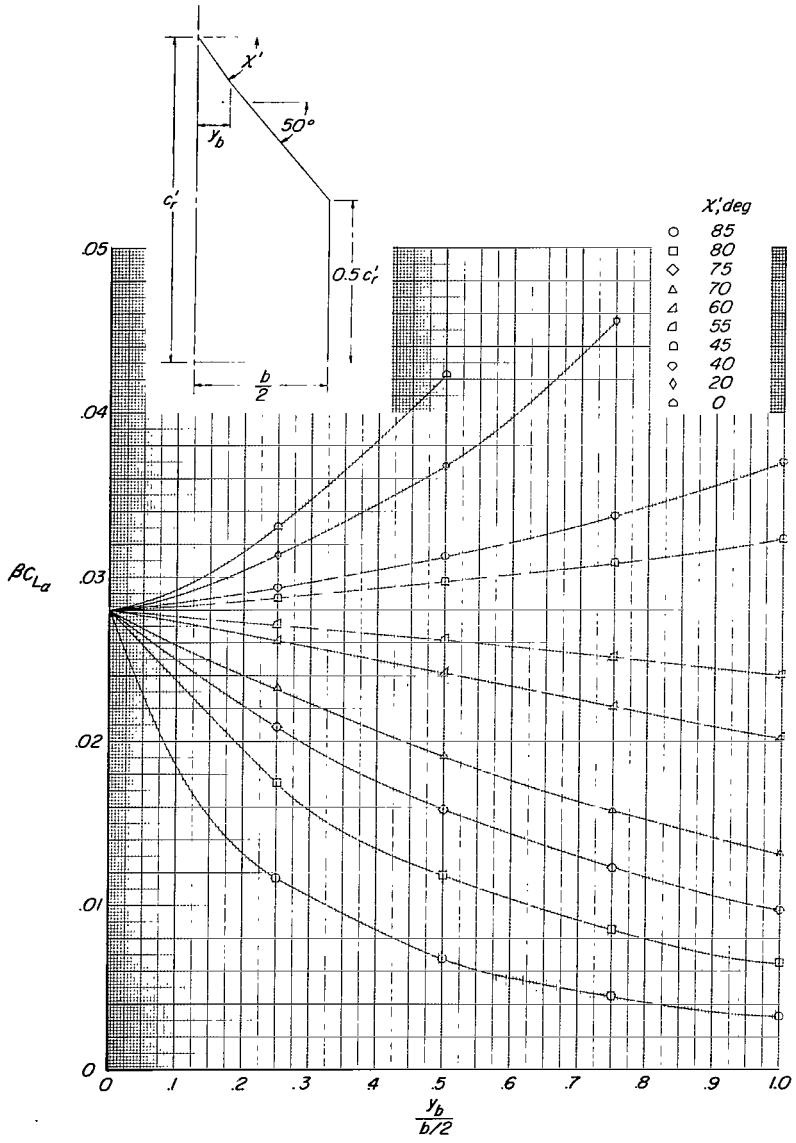

(c) $\Lambda' = 50^0$; $\lambda = 0.50$.

Figure 5.- Continued.

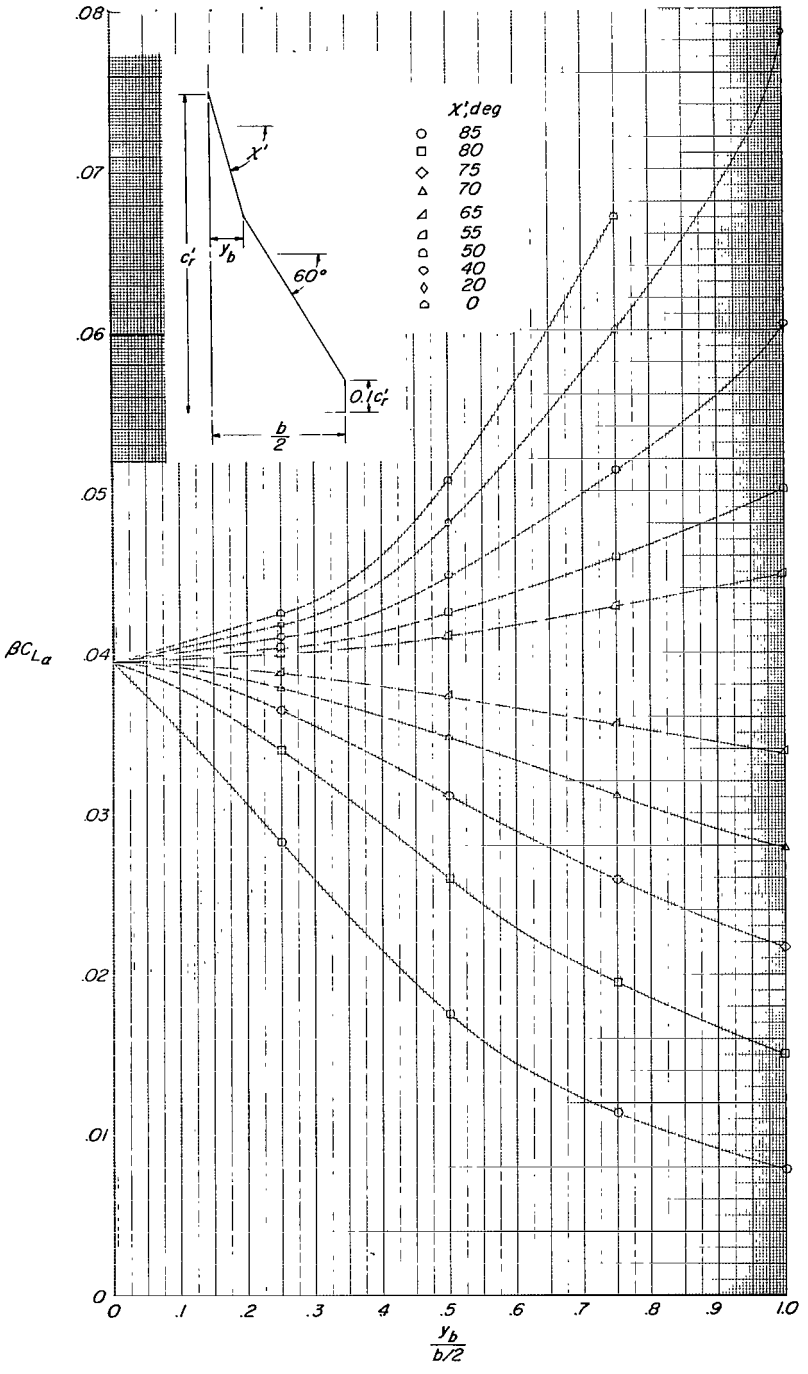

(d) $\Lambda' = 60^0$; $\lambda = 0.10$.

Figure 5.- Continued.

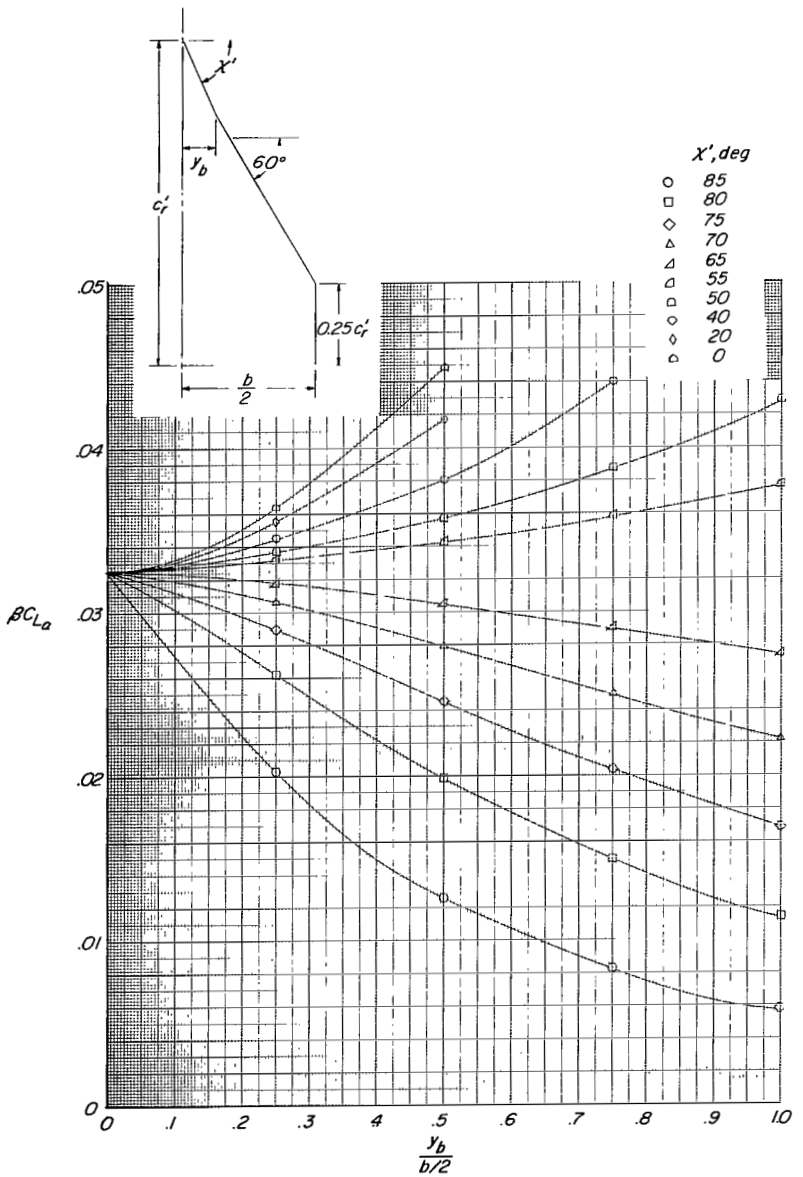

(e) $\Lambda' = 60^0$; $\lambda = 0.25$.

Figure 5.- Continued.

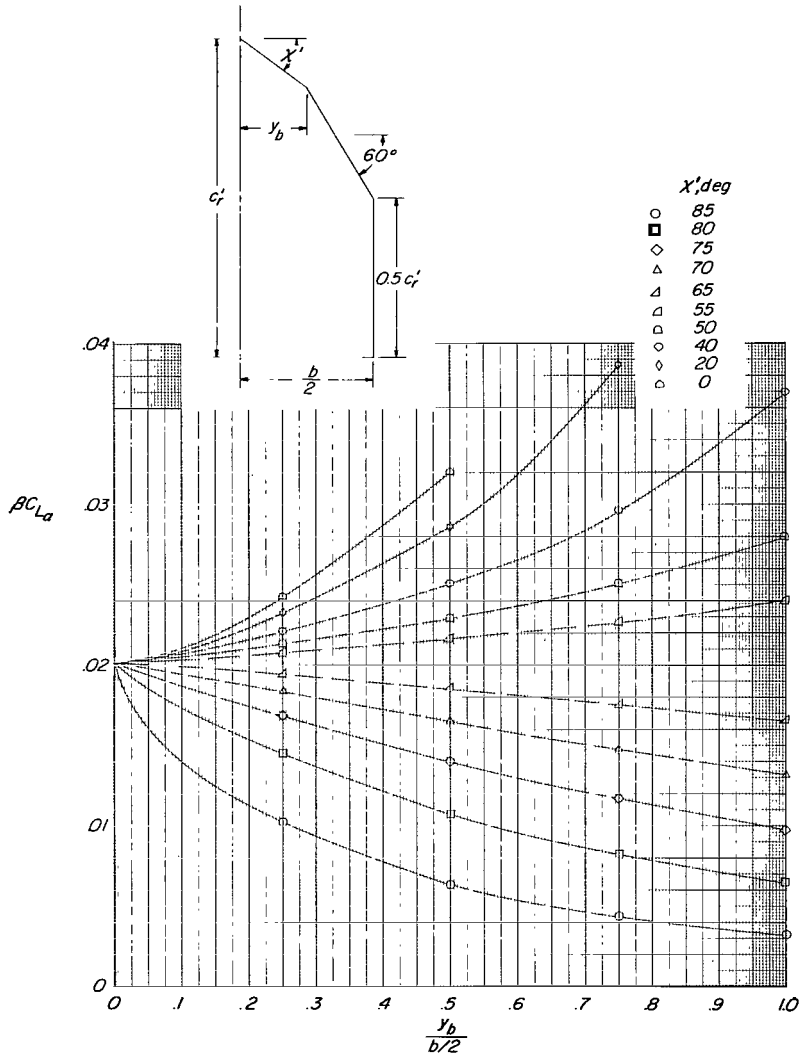

(f) $\Lambda' = 60^0$; $\lambda = 0.50$.

Figure 5.- Continued.

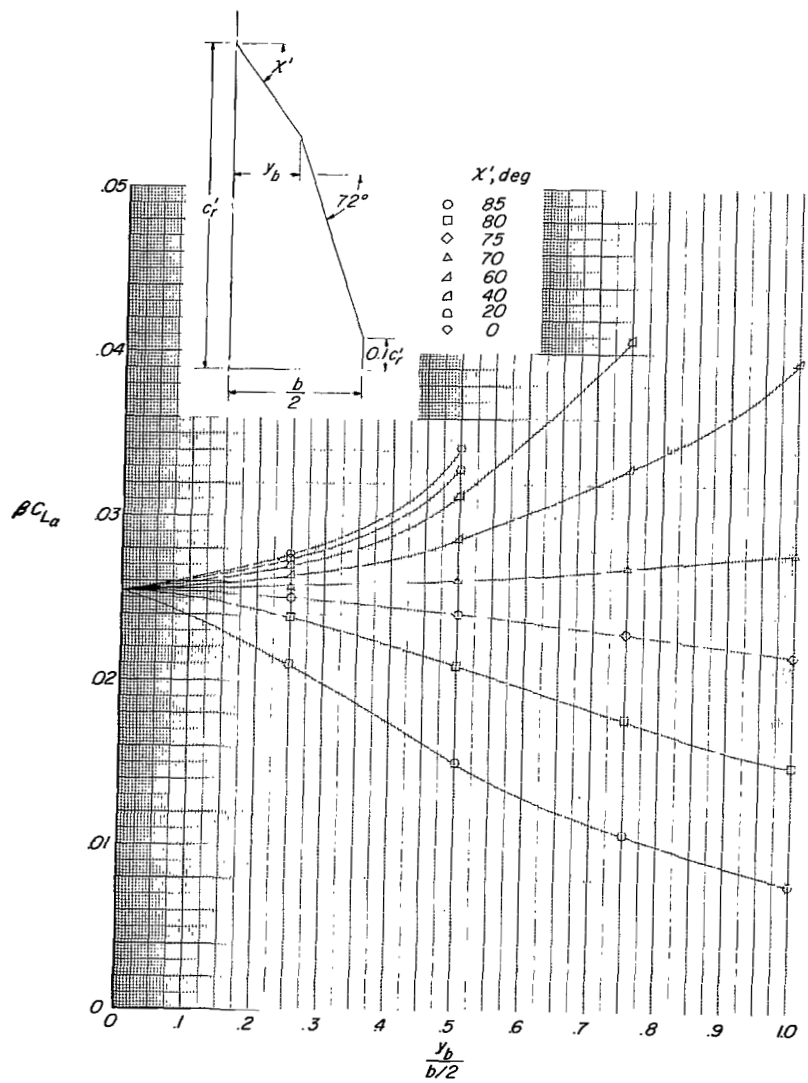

(g) $\Lambda' = 72^0$; $\lambda = 0.10$.

Figure 5.- Continued.

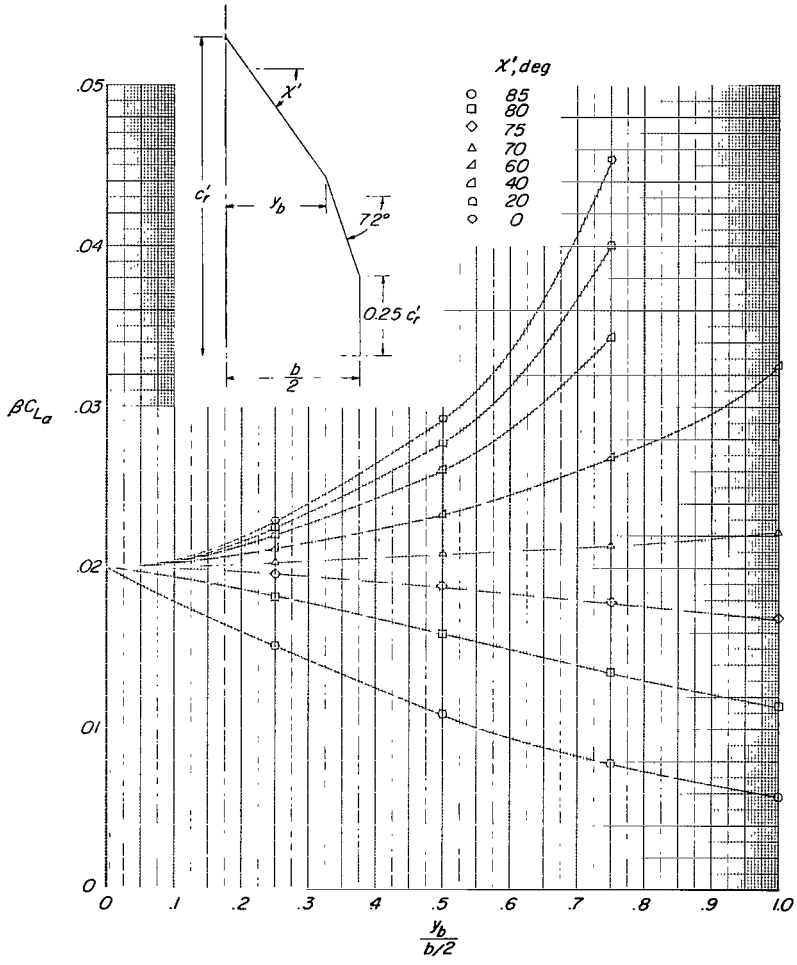

(h) $\Lambda' = 72^0$; $\lambda = 0.25$.

Figure 5.- Continued.

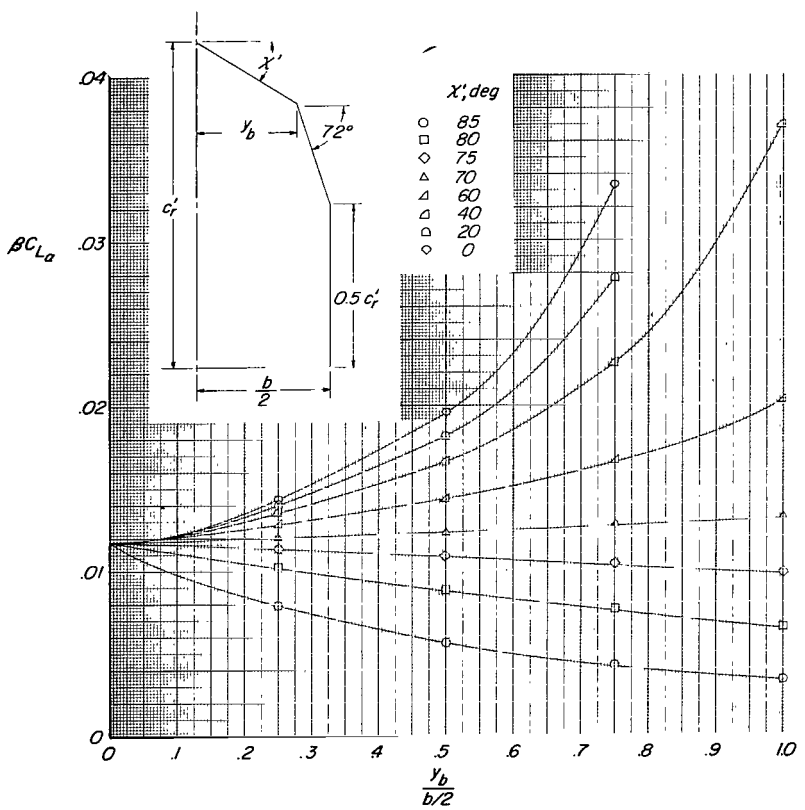

(i) $\Lambda' = 72^0$; $\lambda = 0.50$.

Figure 5.- Concluded.

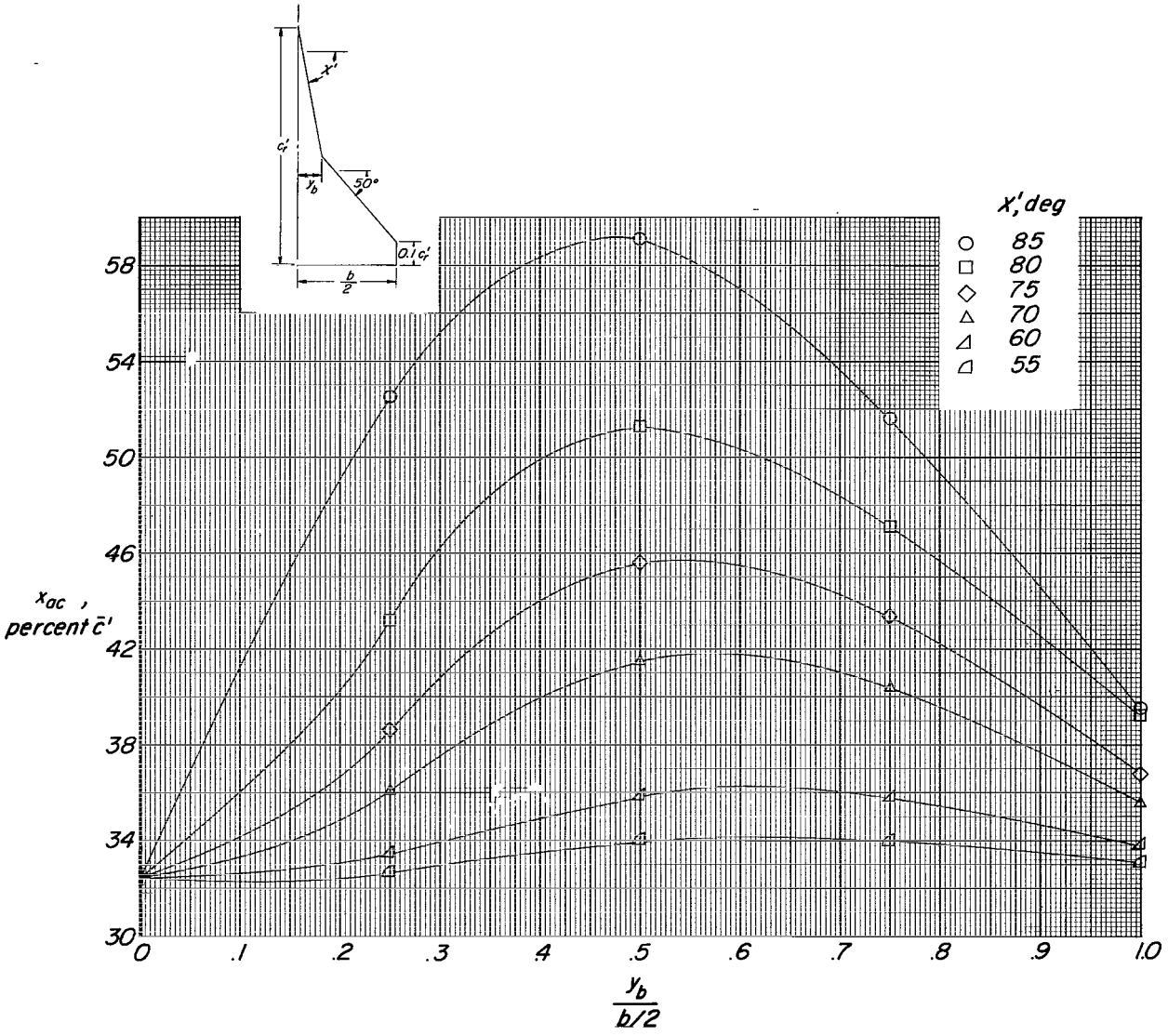

(a) $\Lambda' = 50^0$; $\lambda = 0.10$.

Figure 6.- Aerodynamic center for cropped double-delta planforms.

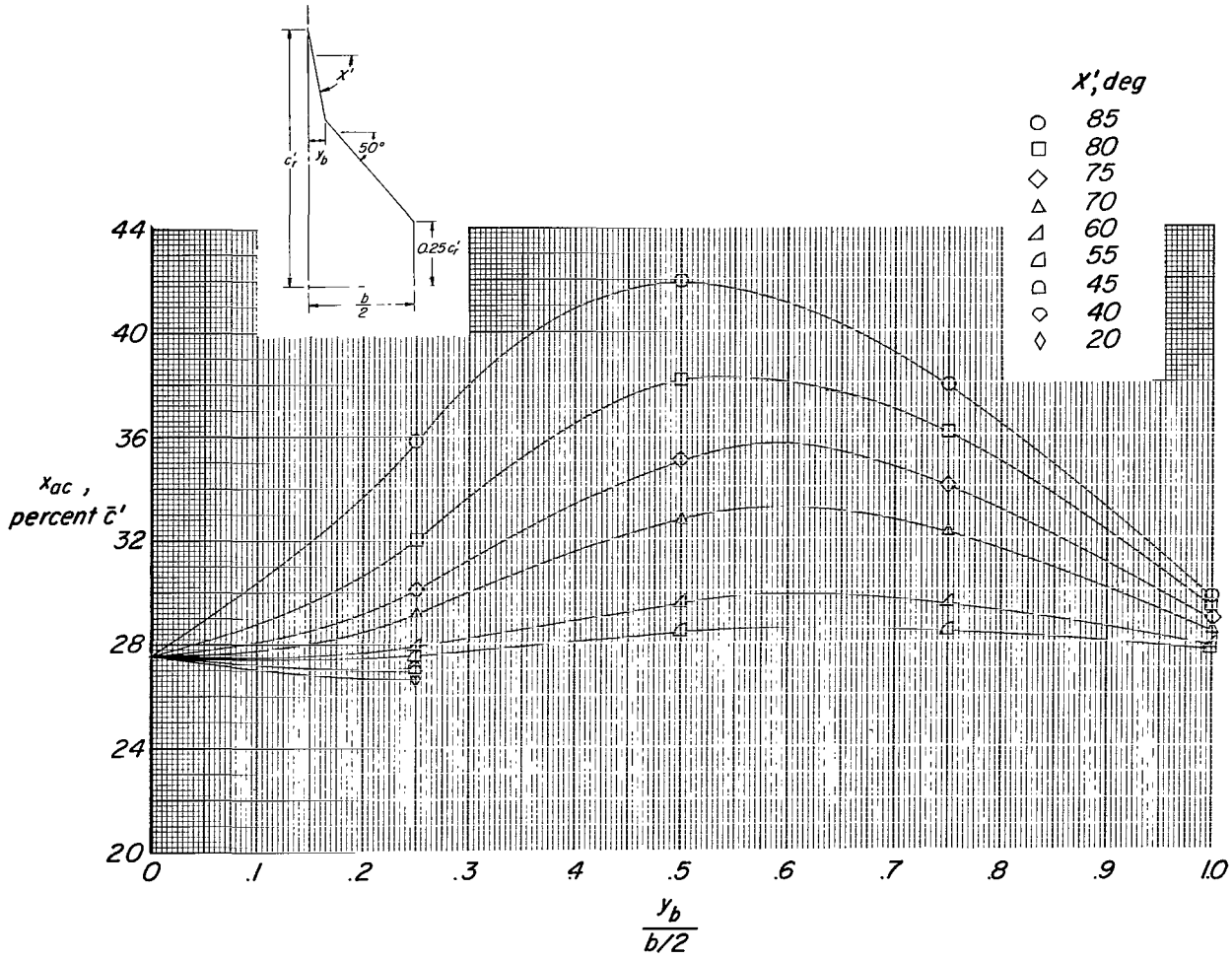

(b) $\Lambda' = 50^0$; $\lambda = 0.25$.

Figure 6.- Continued.

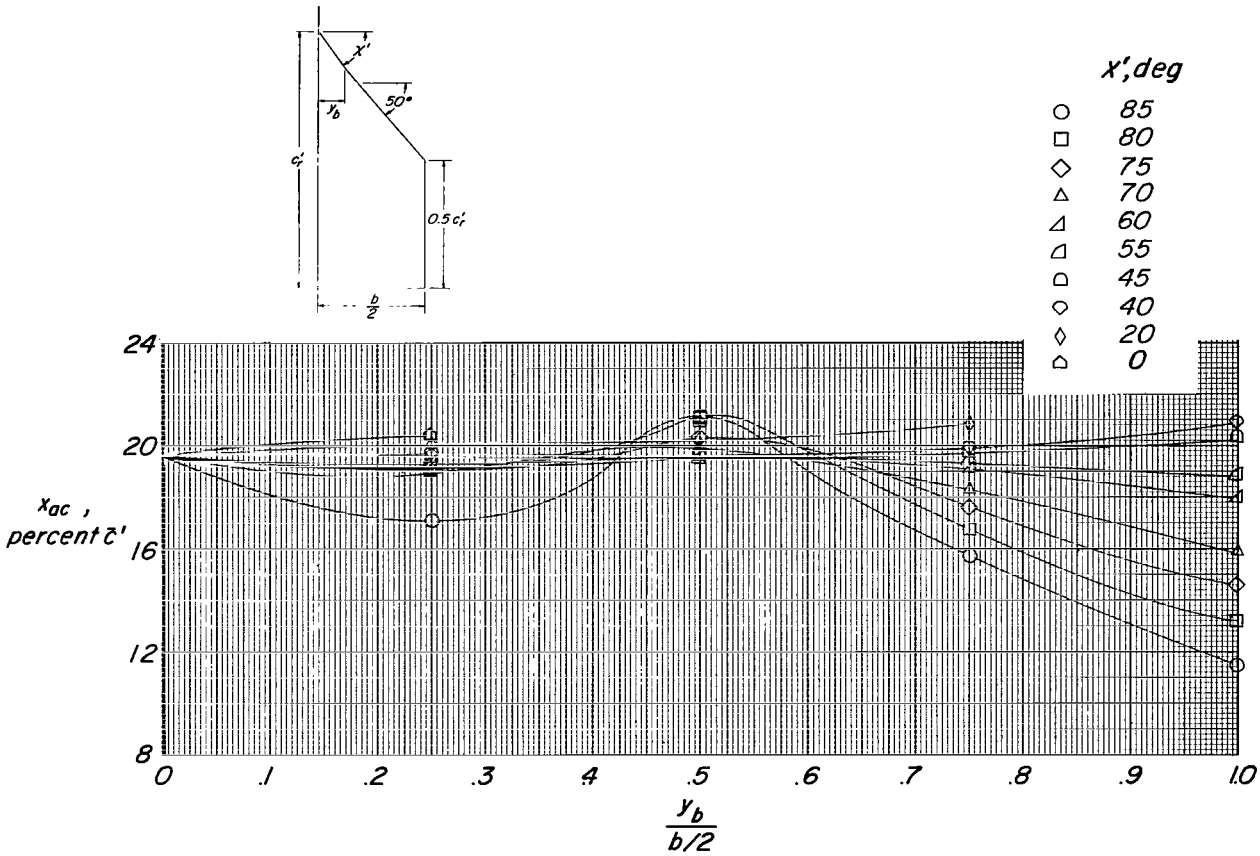

(c) $\Lambda' = 50^0$; $\lambda = 0.50$.

Figure 6.- Continued.

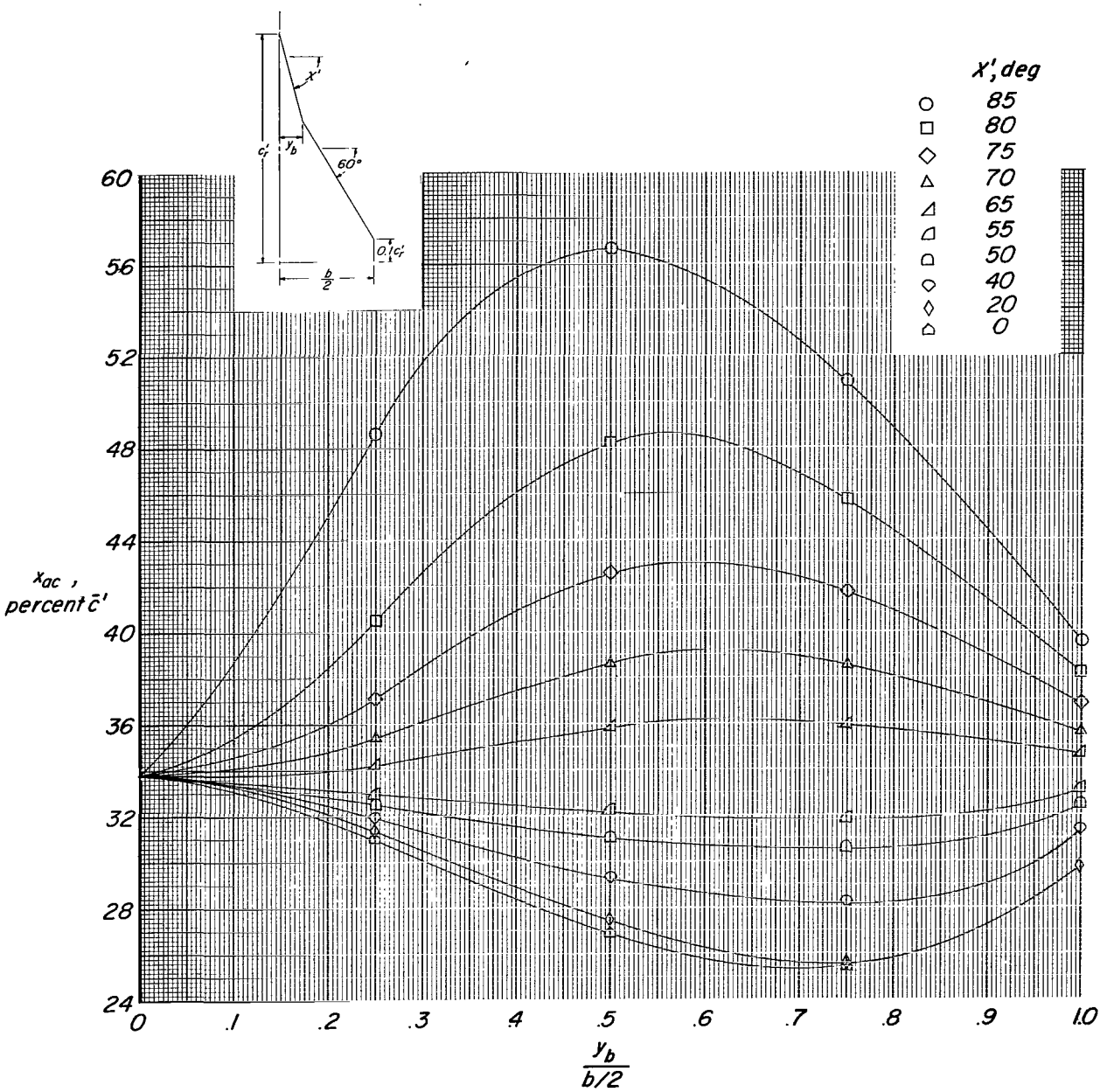

(d) $\Lambda' = 60^0$; $\lambda = 0.10$.

Figure 6.- Continued.

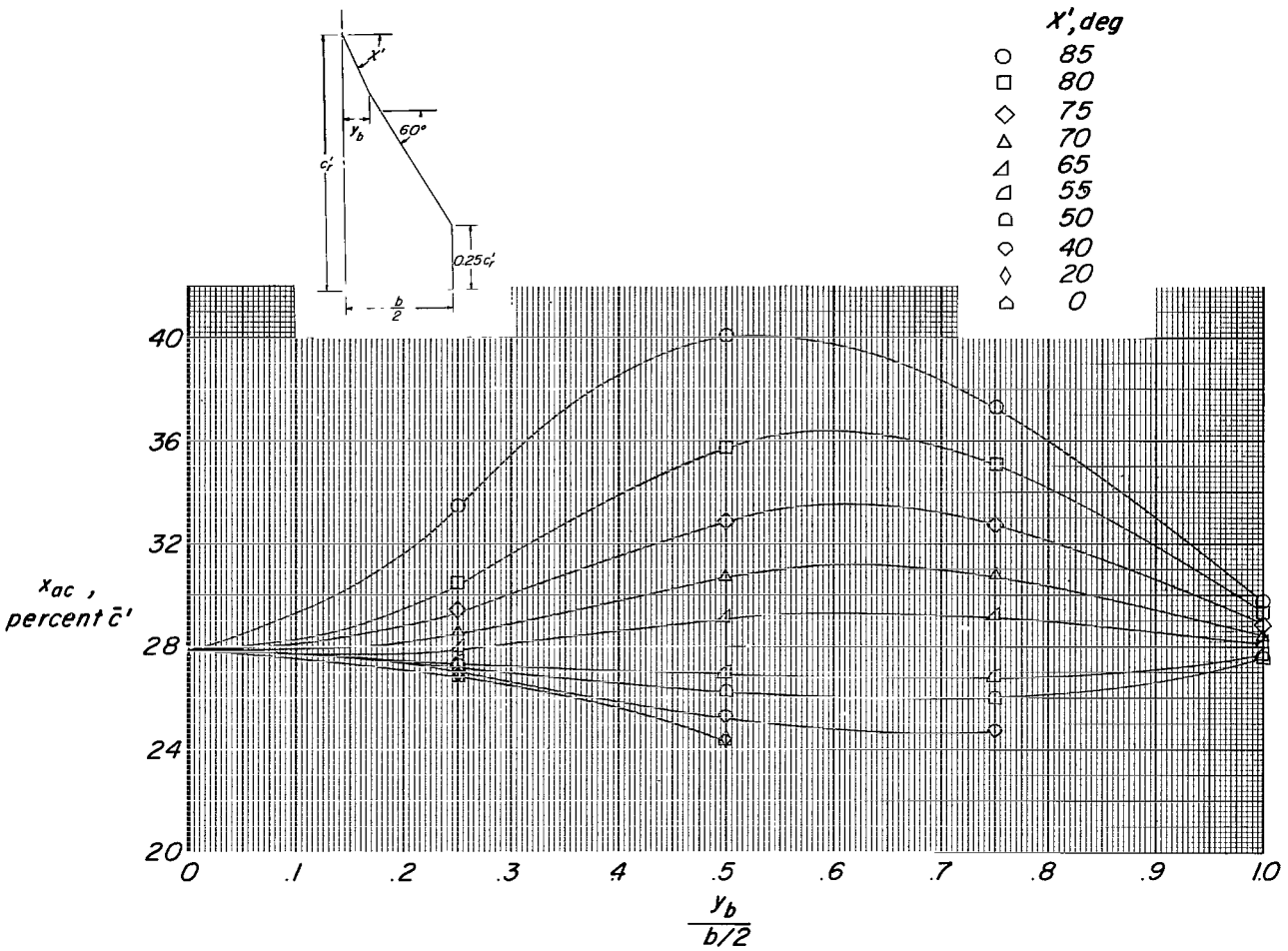

(e) $\Lambda' = 60^0$; $\lambda = 0.25$.

Figure 6.- Continued.

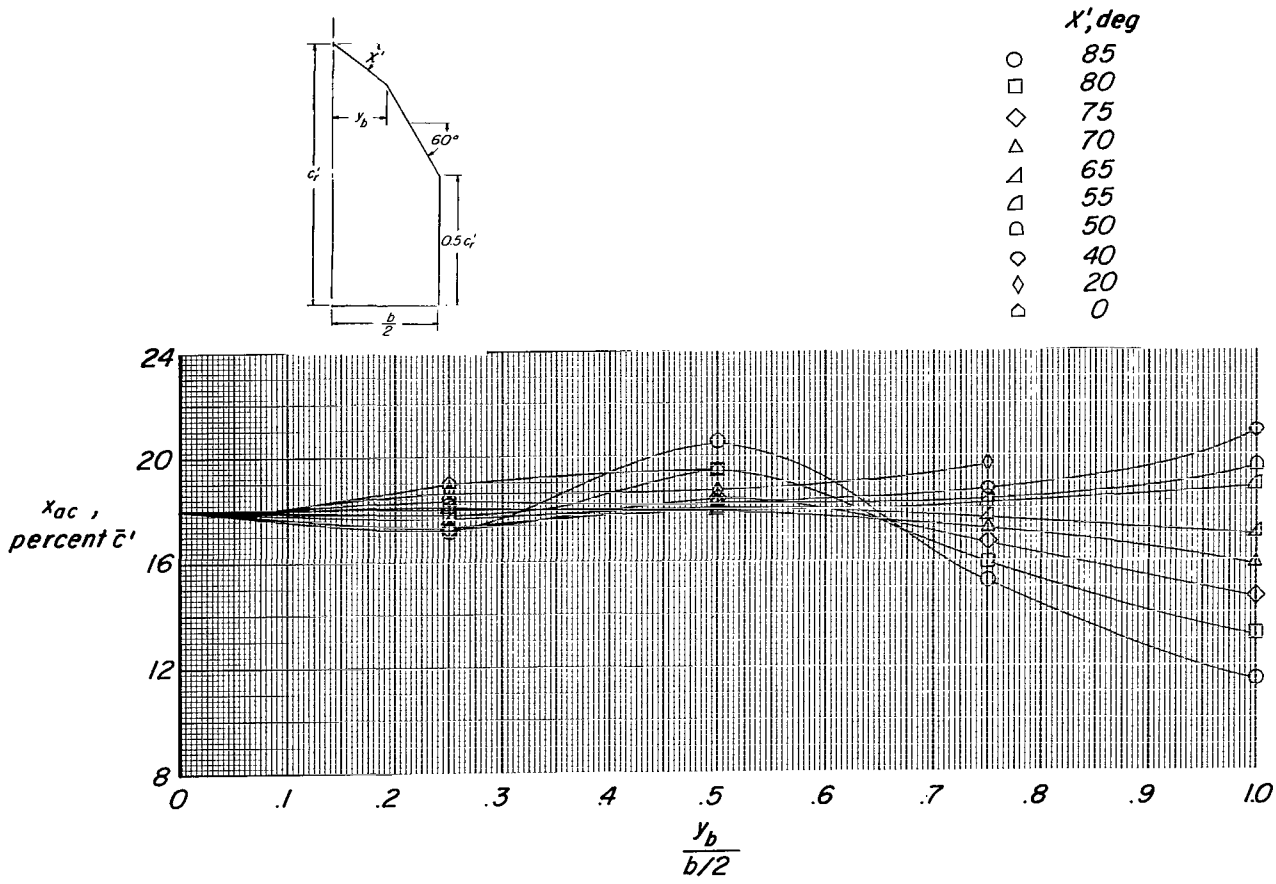

(f) $\Lambda' = 60^0$; $\lambda = 0.50$.

Figure 6.- Continued.

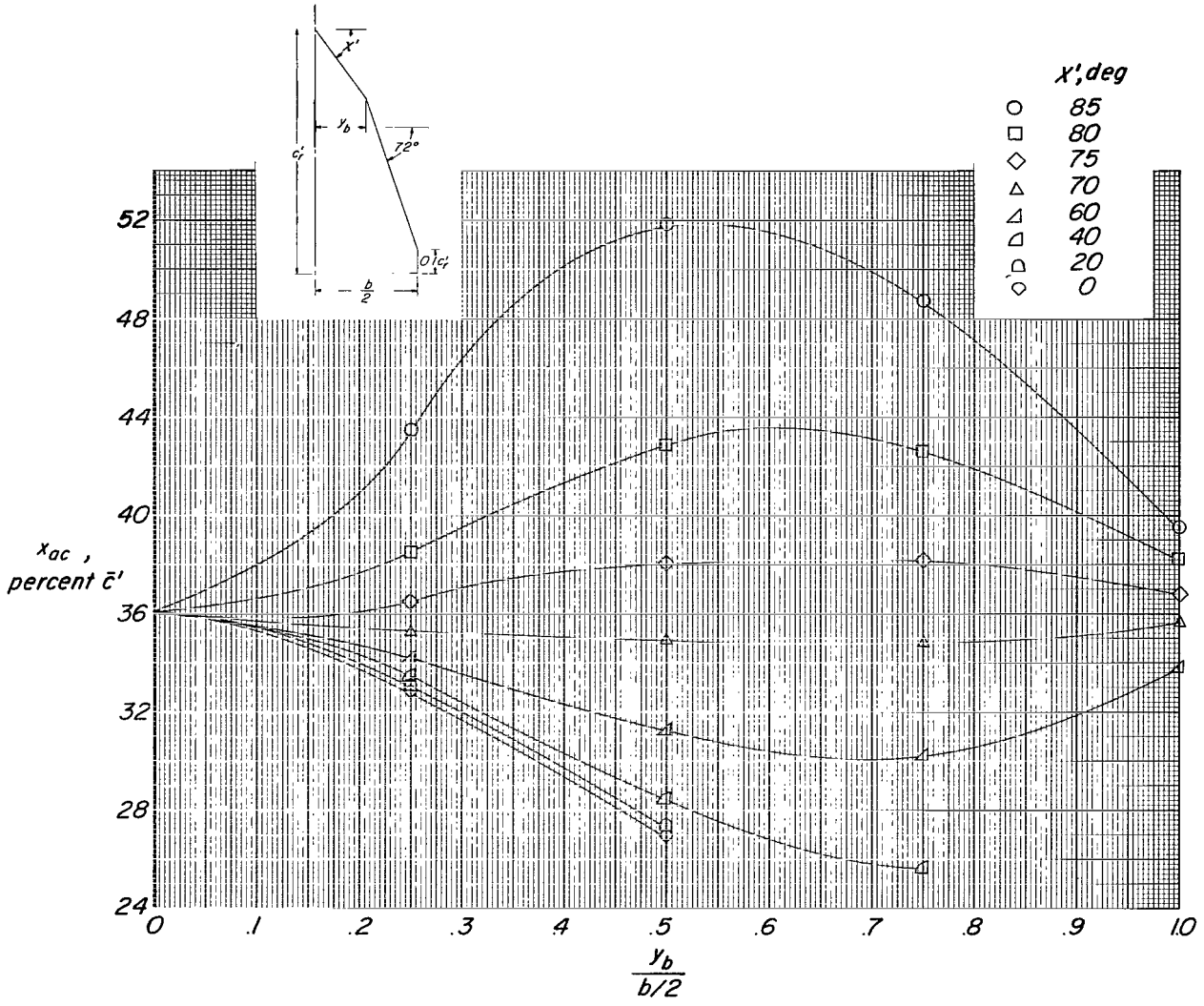

(g) $\Lambda' = 72^0$; $\lambda = 0.10$.

Figure 6.- Continued.

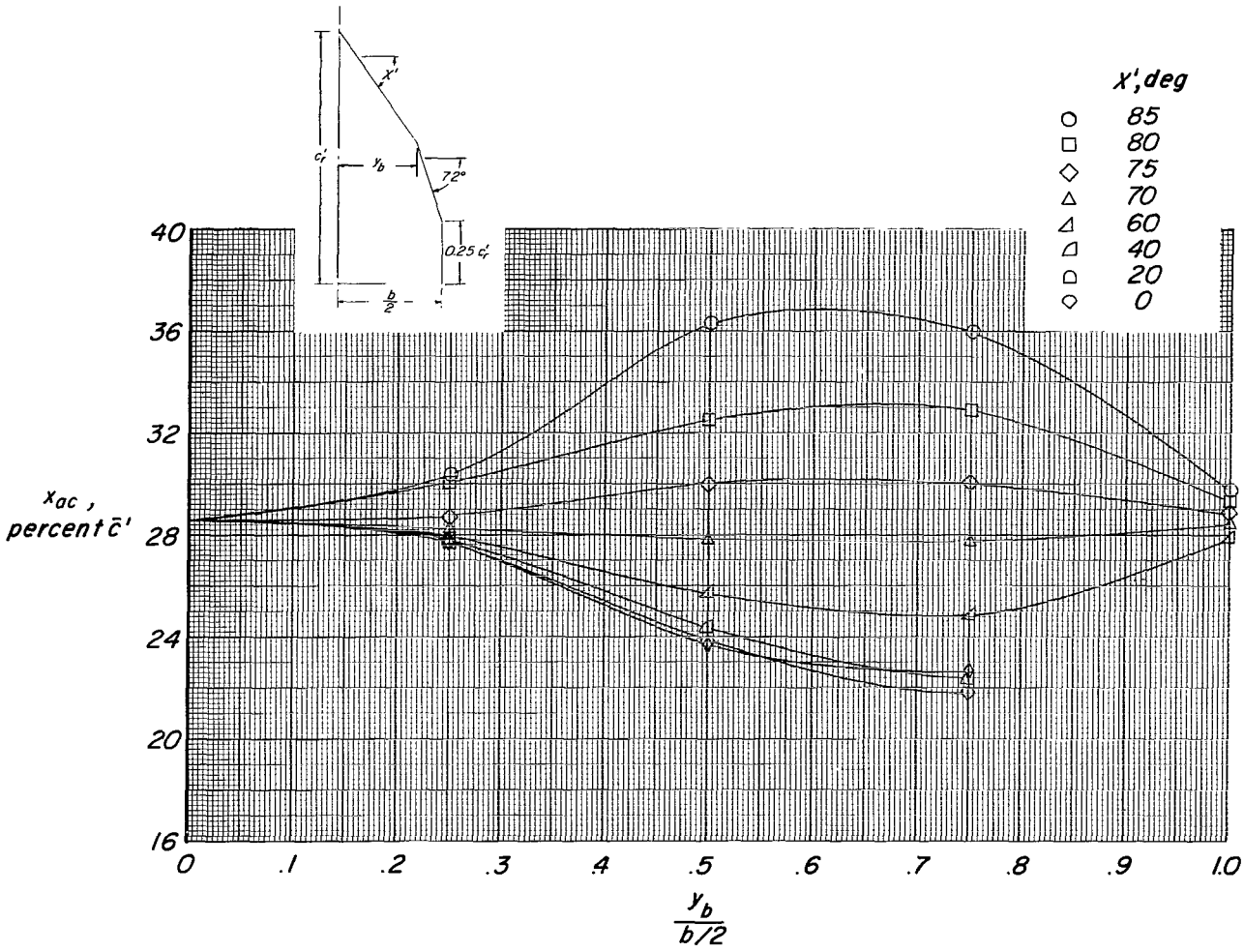

(h) $\Lambda' = 72^{0}$; $\lambda = 0.25$.

Figure 6.- Continued.

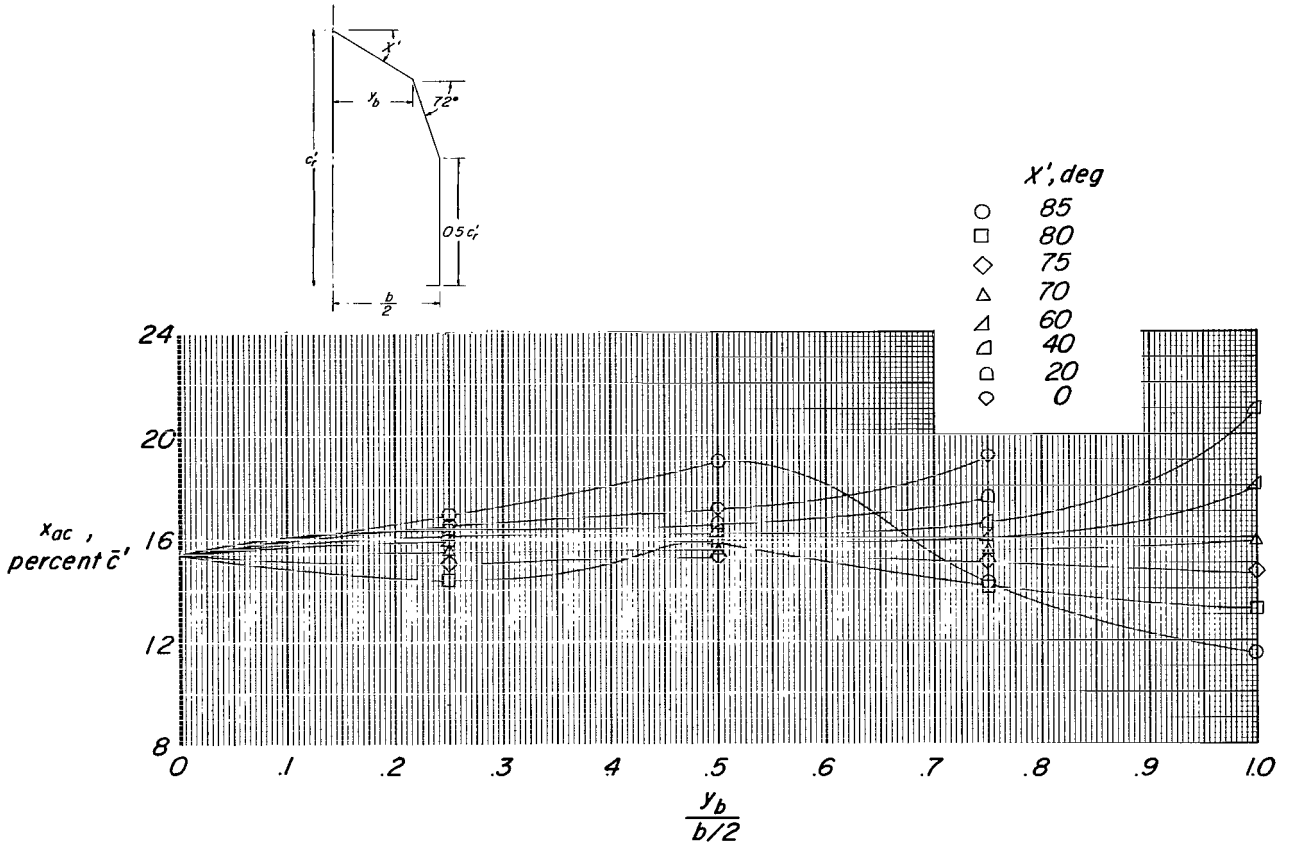

(i) $\Lambda' = 72^0$; $\lambda = 0.50$.

Figure 6.- Concluded.

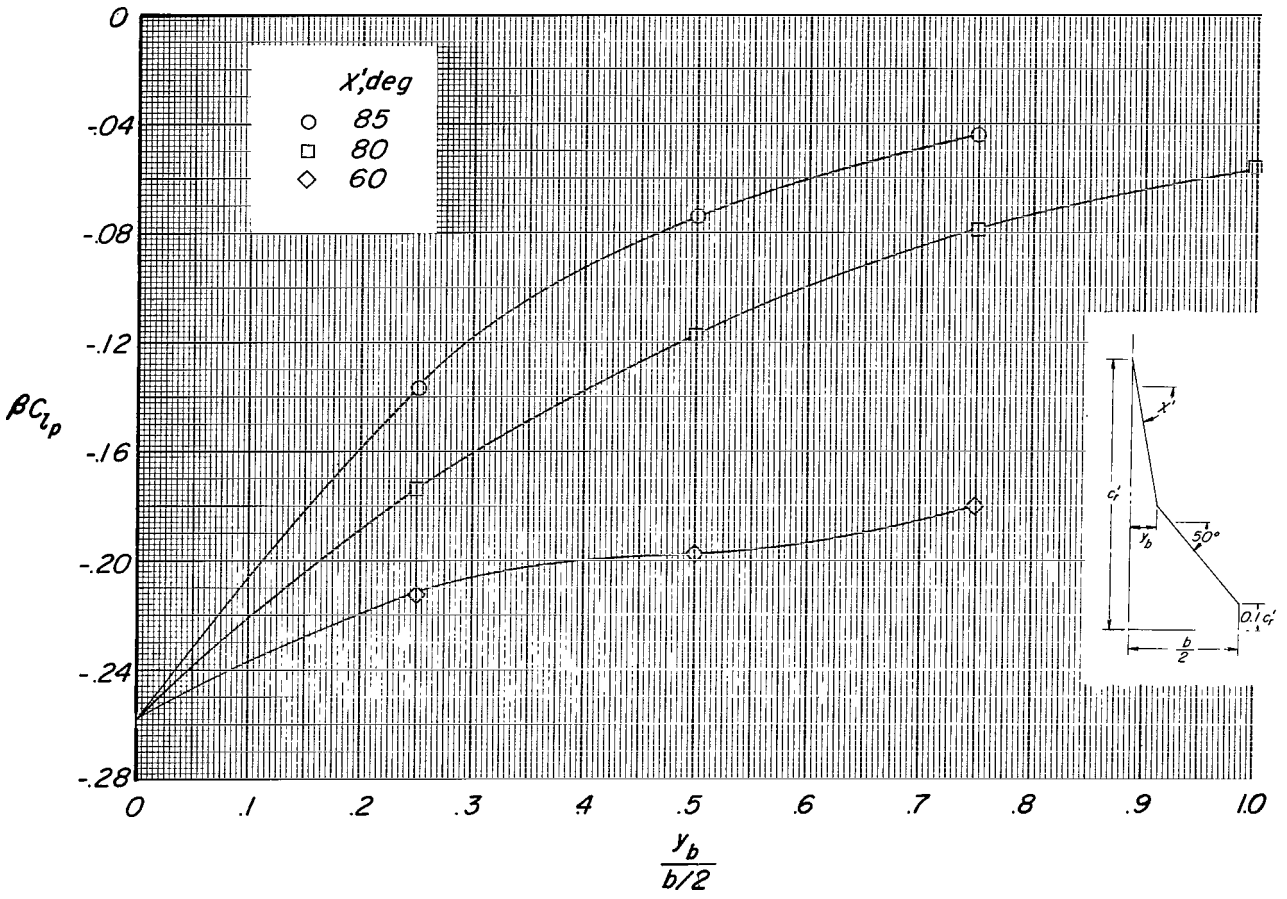

(a) $\Lambda' = 50^0$; $\lambda = 0.10$.

Figure 7.- Damping-in-roll rotary derivative for cropped double-delta planforms.

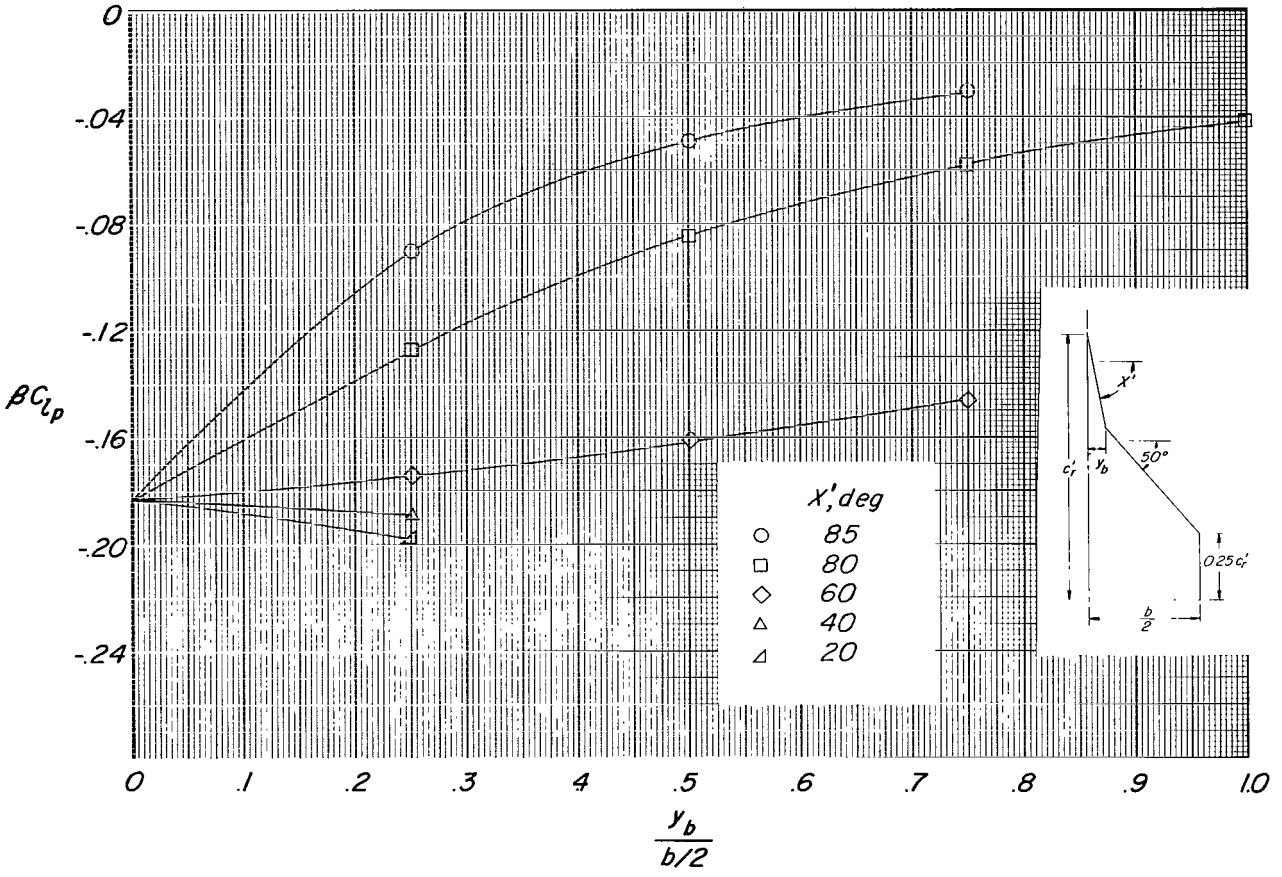

(b) $\Lambda' = 50^0$; $\lambda = 0.25$.

Figure 7.- Continued.

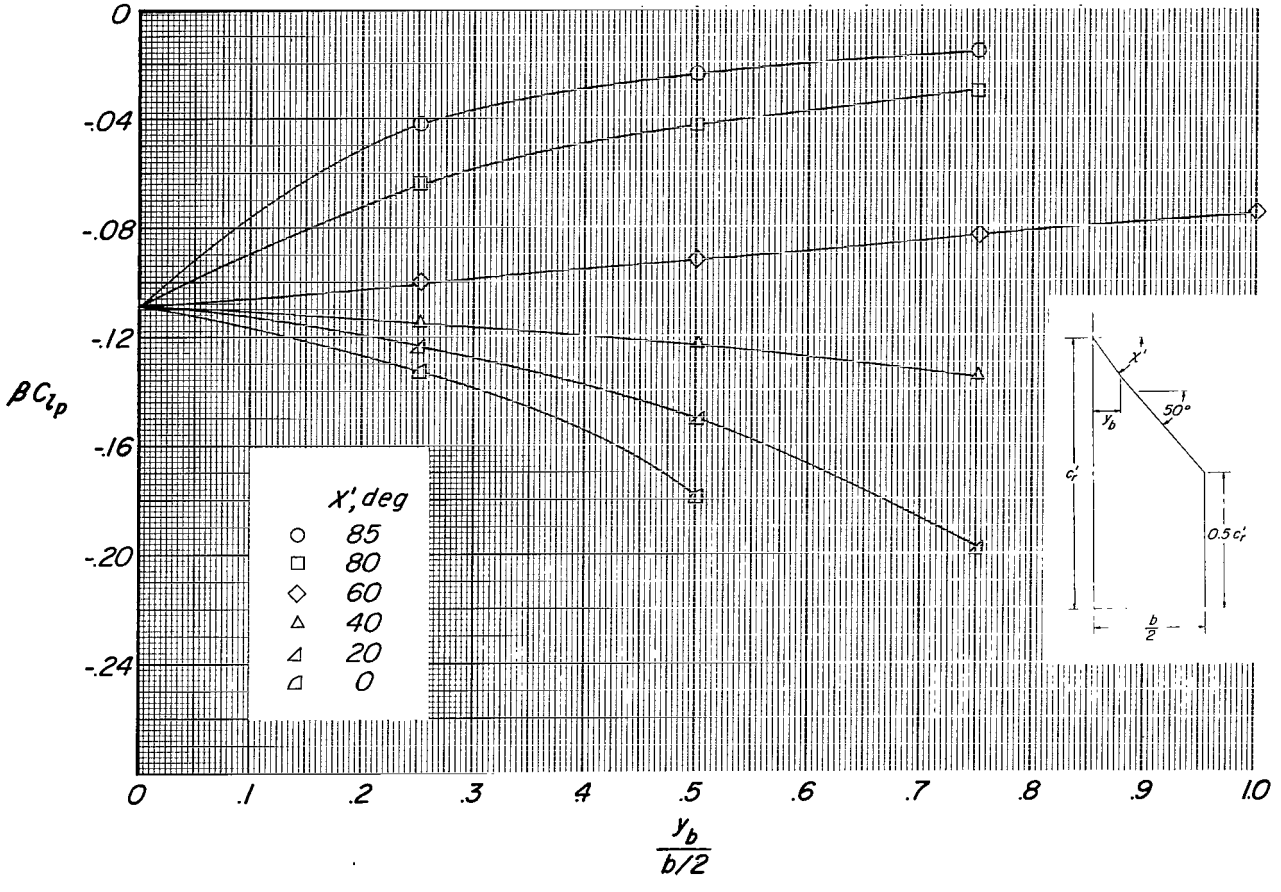

(c) $\Lambda' = 50^{0}$; $\lambda = 0.50$.

Figure 7.- Continued.

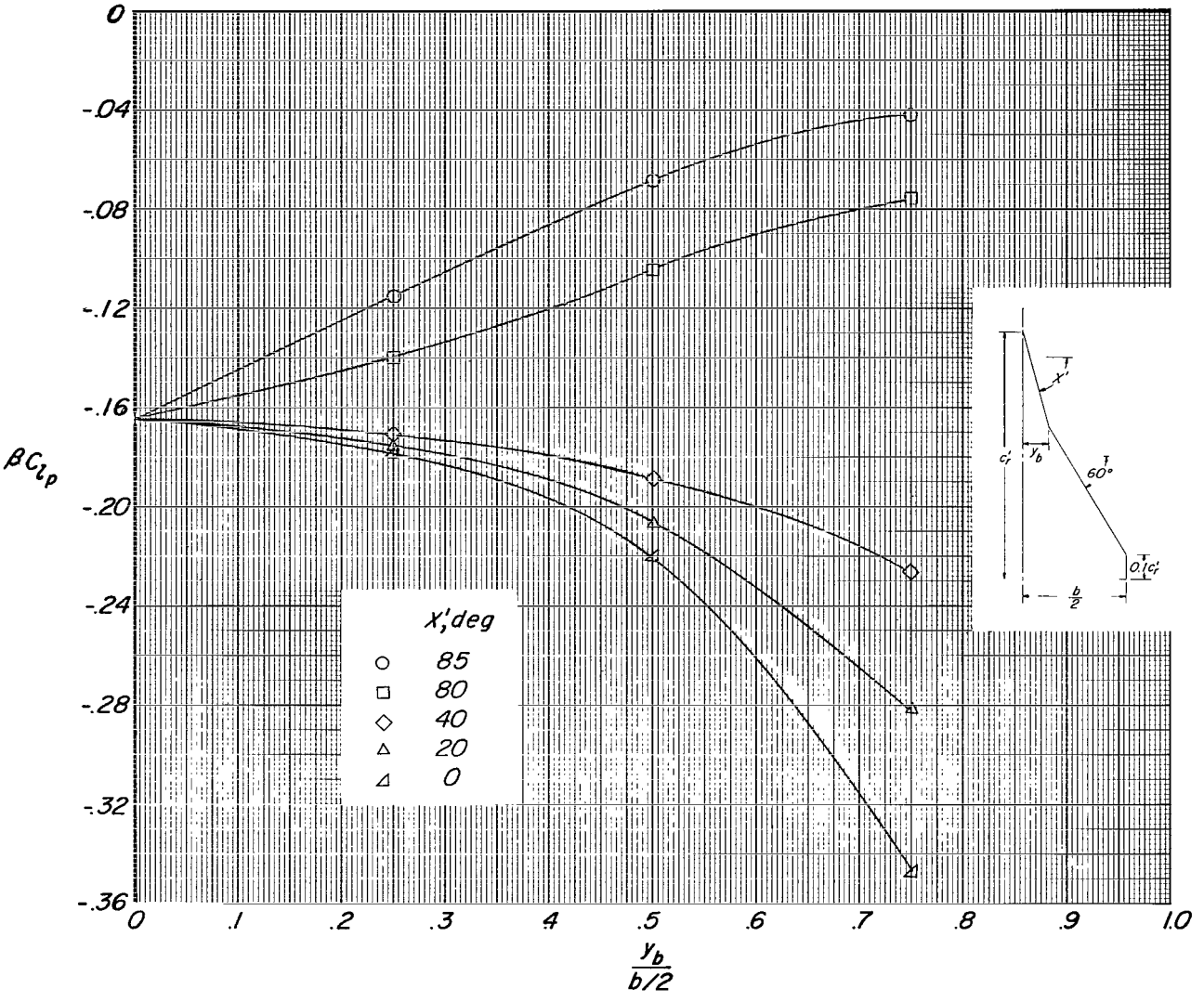

(d) $\Lambda' = 60^0$; $\lambda = 0.10$.

Figure 7.- Continued.

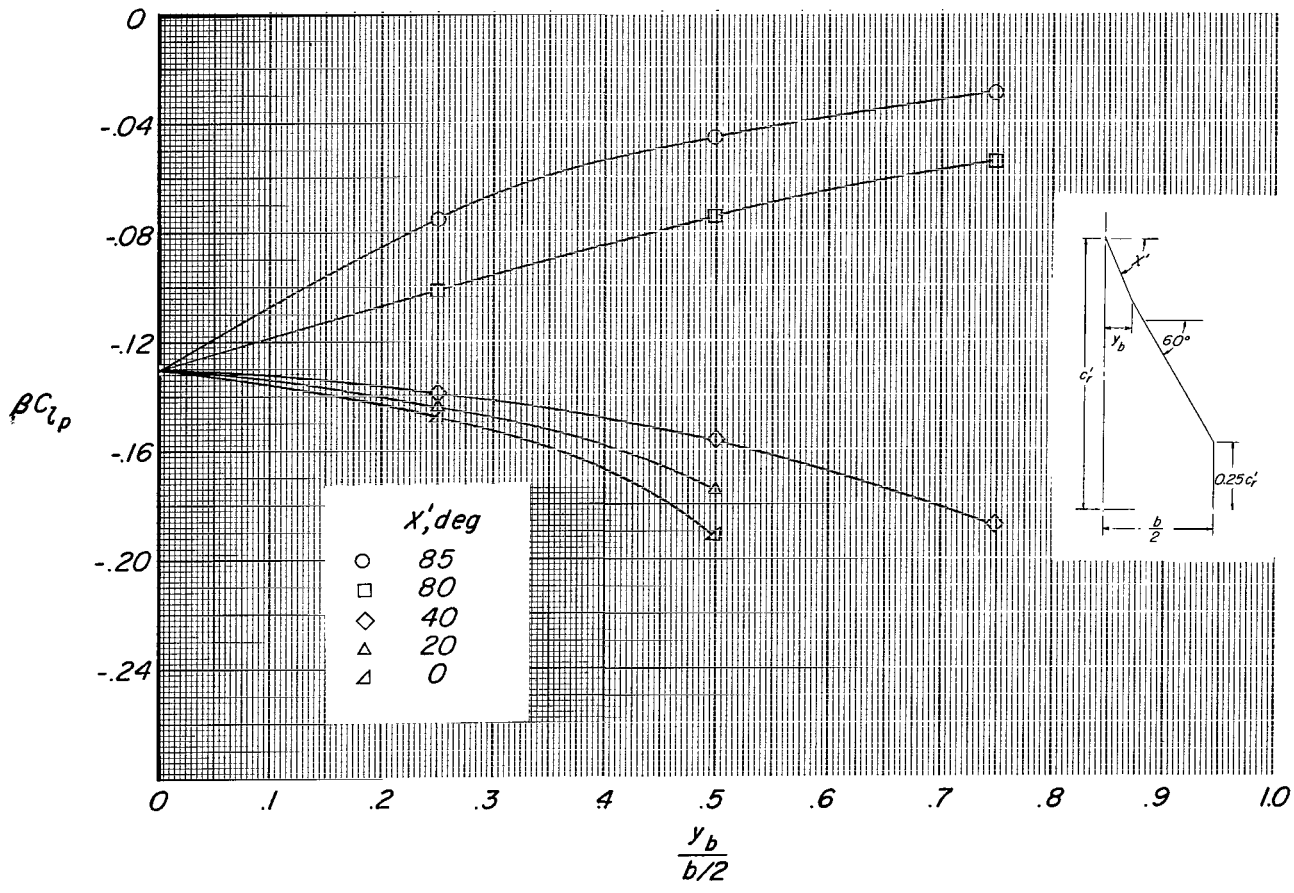

(e) $\Lambda' = 60^0$; $\lambda = 0.25$.

Figure 7.- Continued.

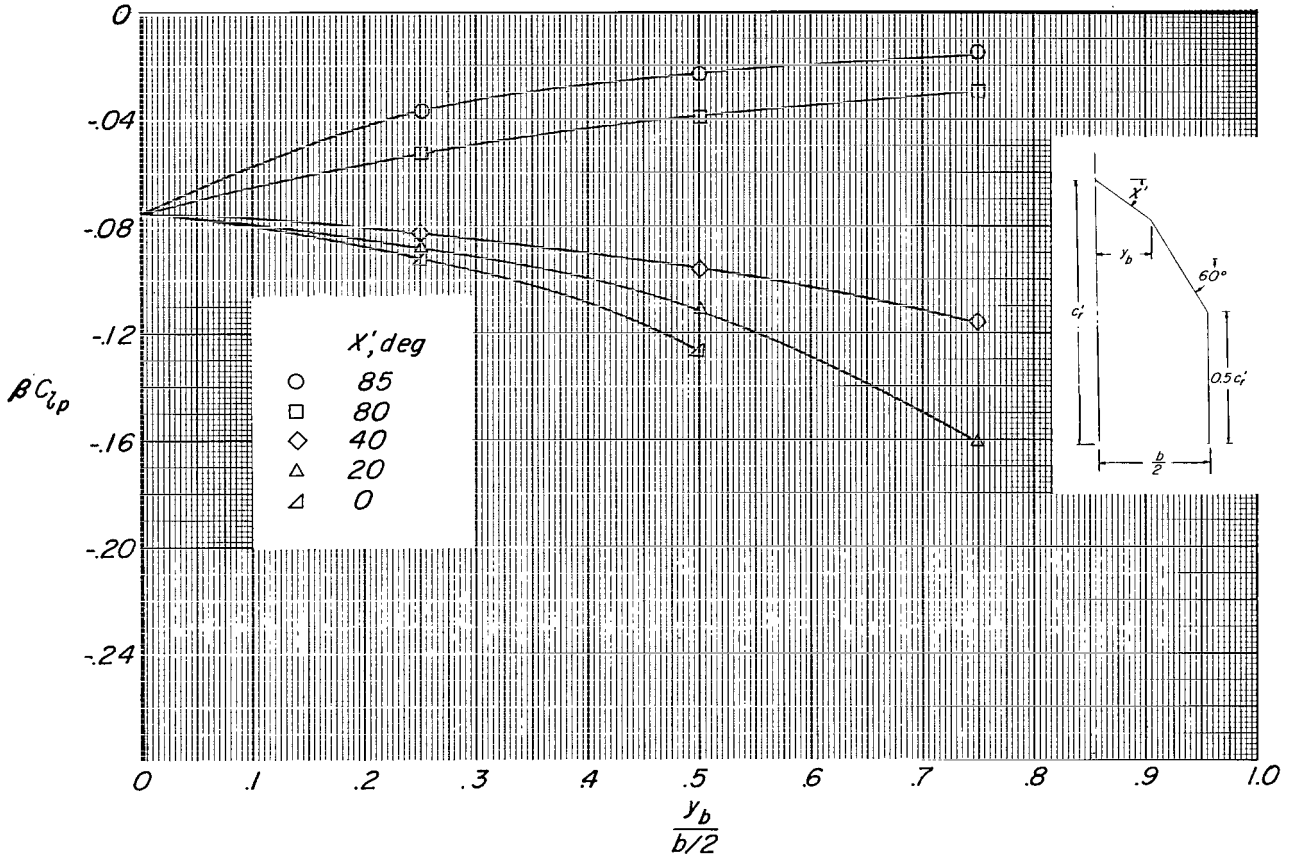

(f) $\Lambda' = 60^{\circ}$; $\lambda = 0.50$.

Figure 7.- Continued.

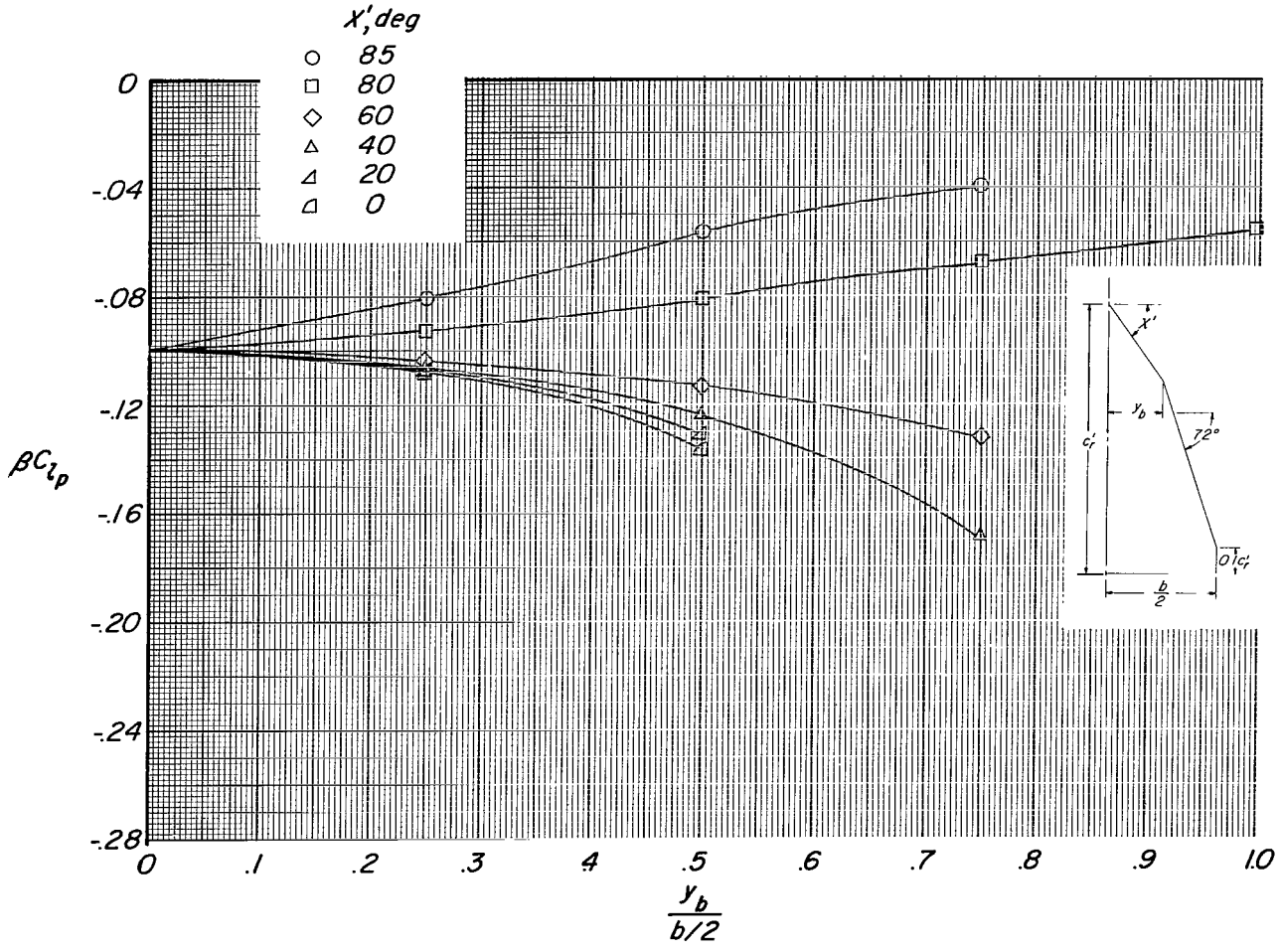

(g) $\Lambda' = 72^0$; $\lambda = 0.10$.

Figure 7.- Continued.

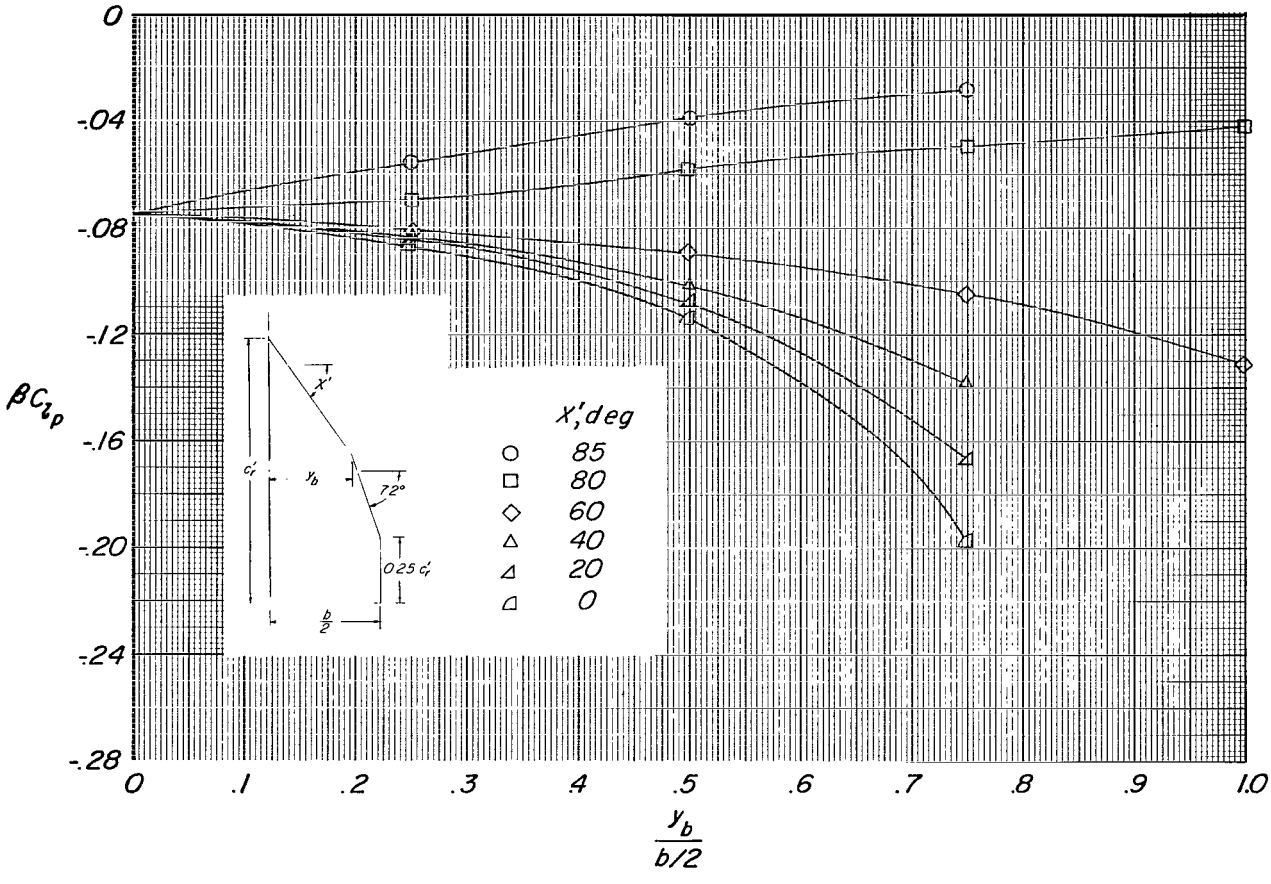

(h) $\Lambda' = 72^0$; $\lambda = 0.25$.

Figure 7.- Continued.

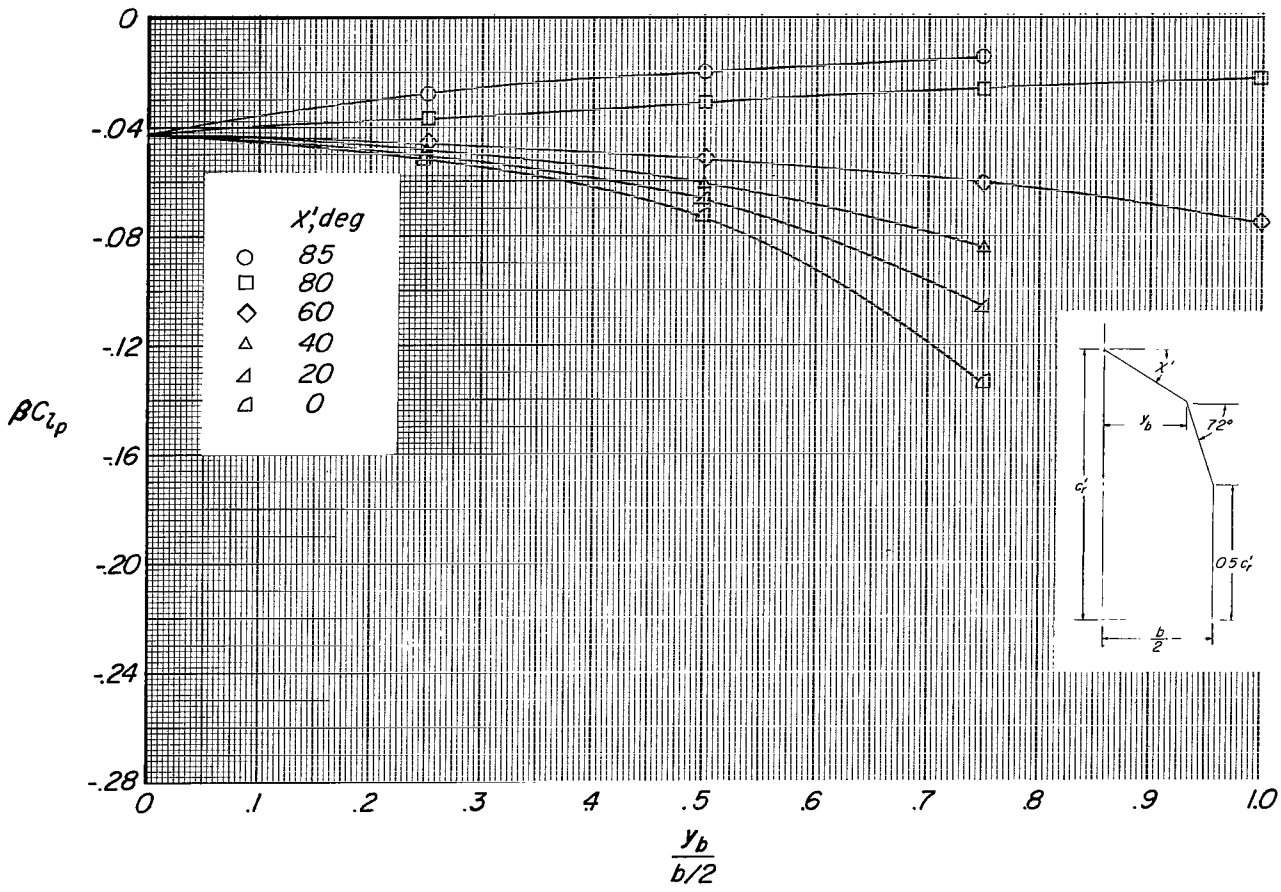

(i) $\Lambda' = 72^0$; $\lambda = 0.50$.

Figure 7.- Concluded.

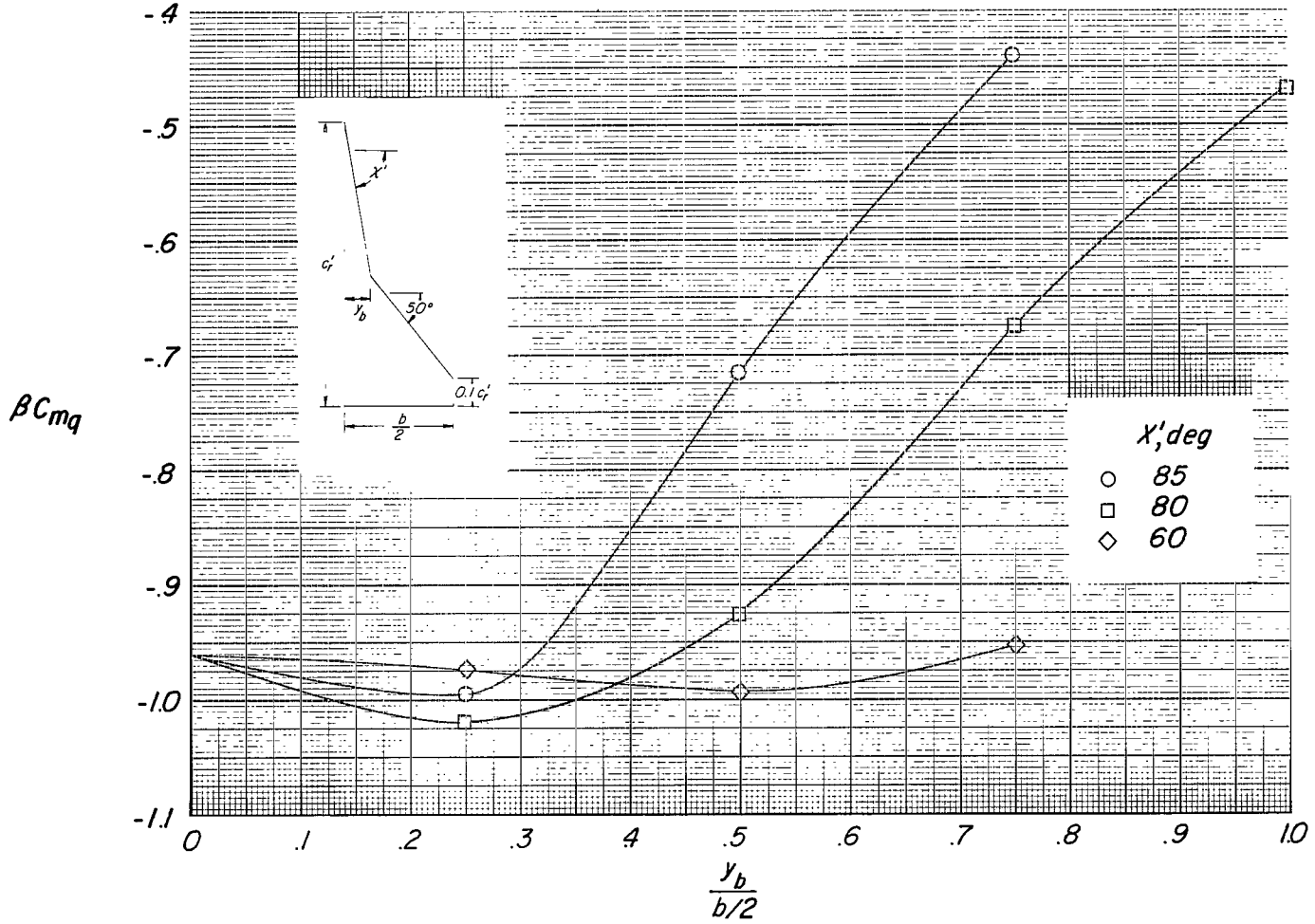

(a) $\Lambda' = 50^{\circ}$; $\lambda = 0.10$.

Figure 8.- Damping-in-pitch rotary derivative for cropped double-delta planforms.

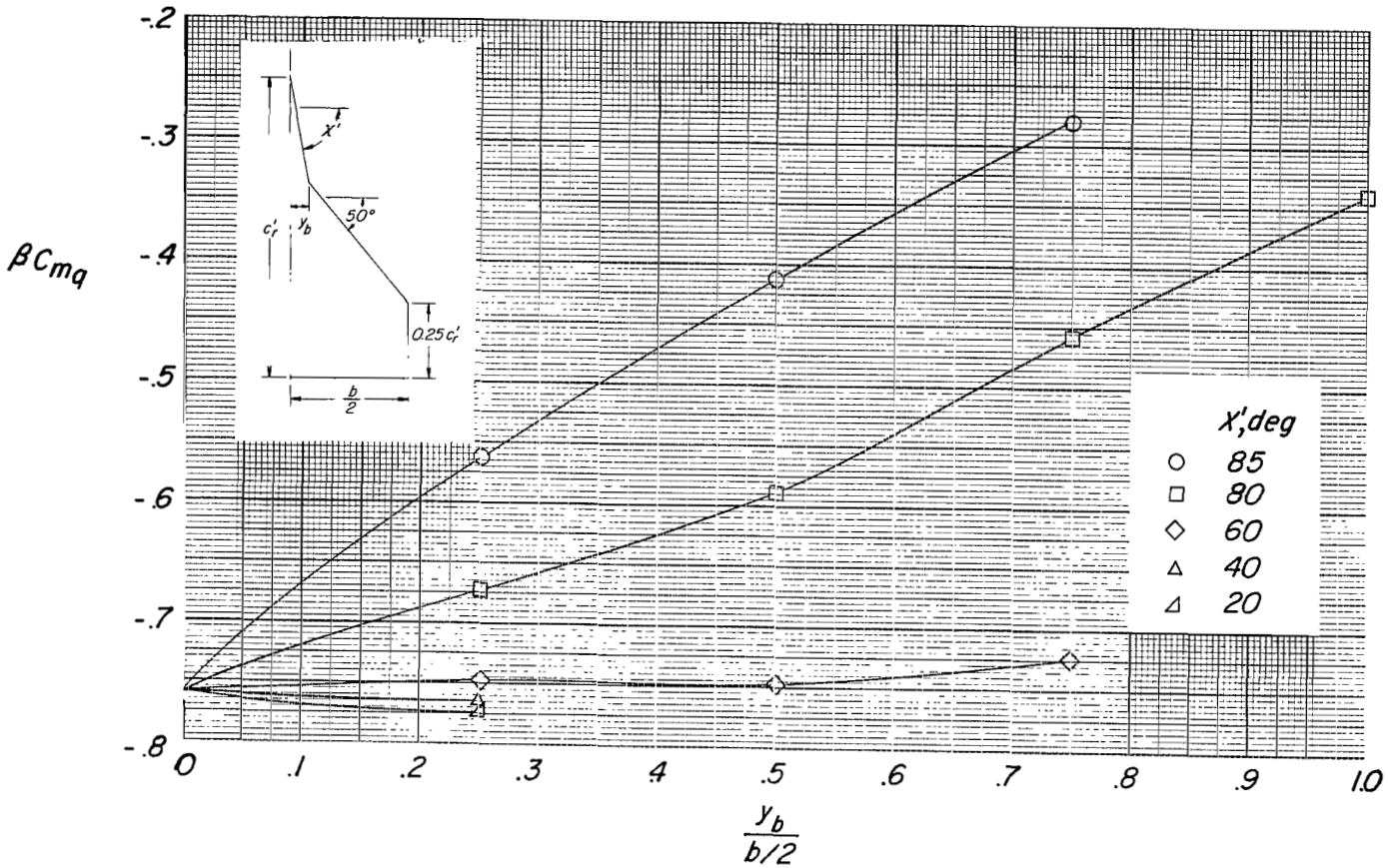

(b) $\Lambda' = 50^0$; $\lambda = 0.25$.

Figure 8.- Continued.

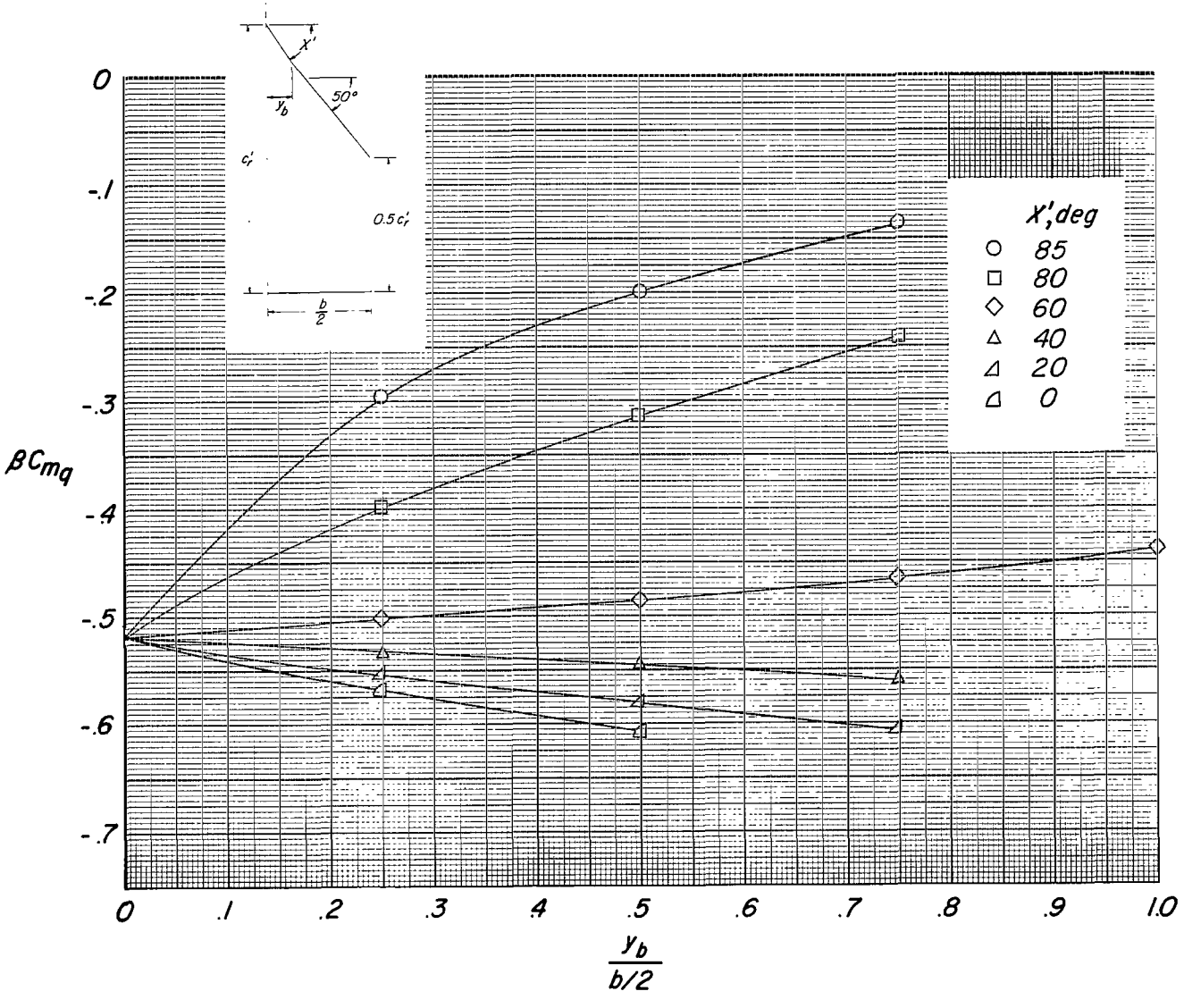

(c) $\Lambda' = 50^0$; $\lambda = 0.50$.

Figure 8.- Continued.

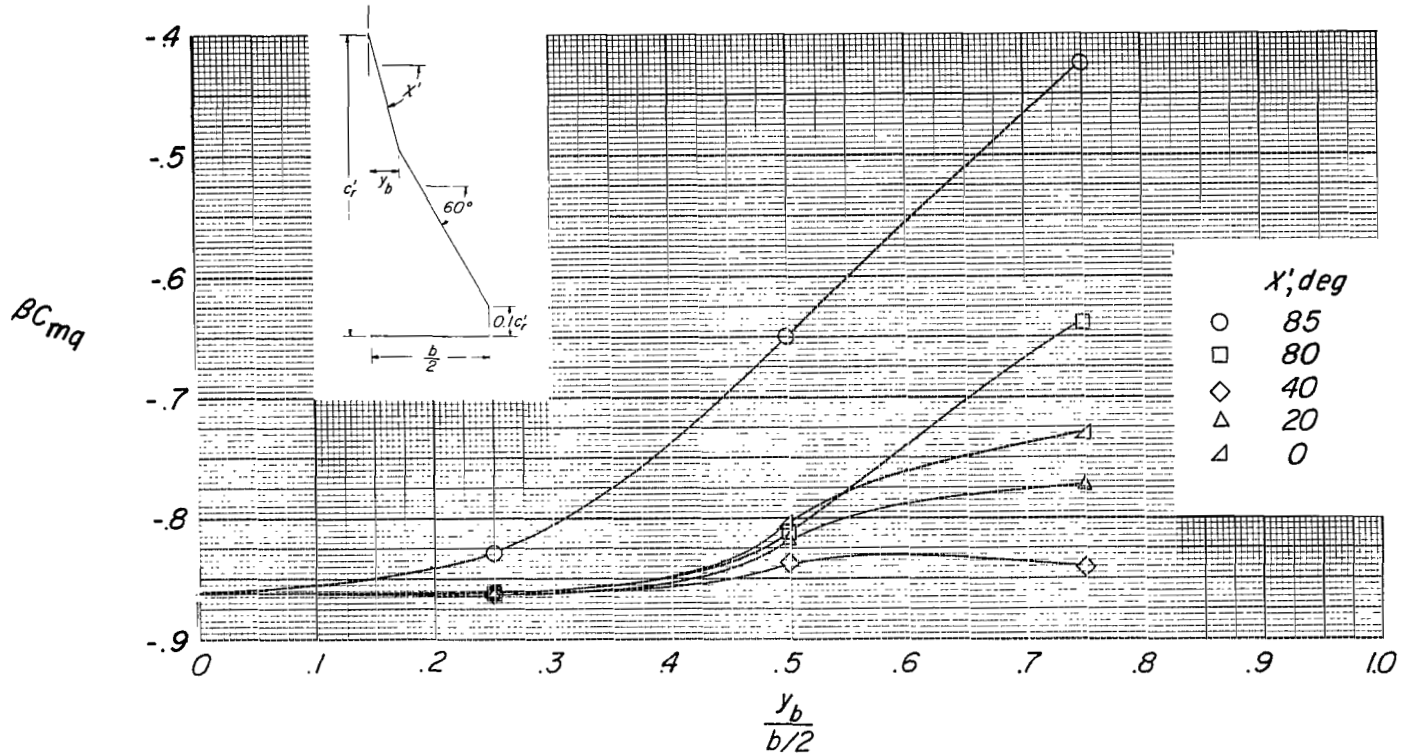

(d) $\Lambda' = 60^0$; $\lambda = 0.10$.

Figure 8.- Continued.

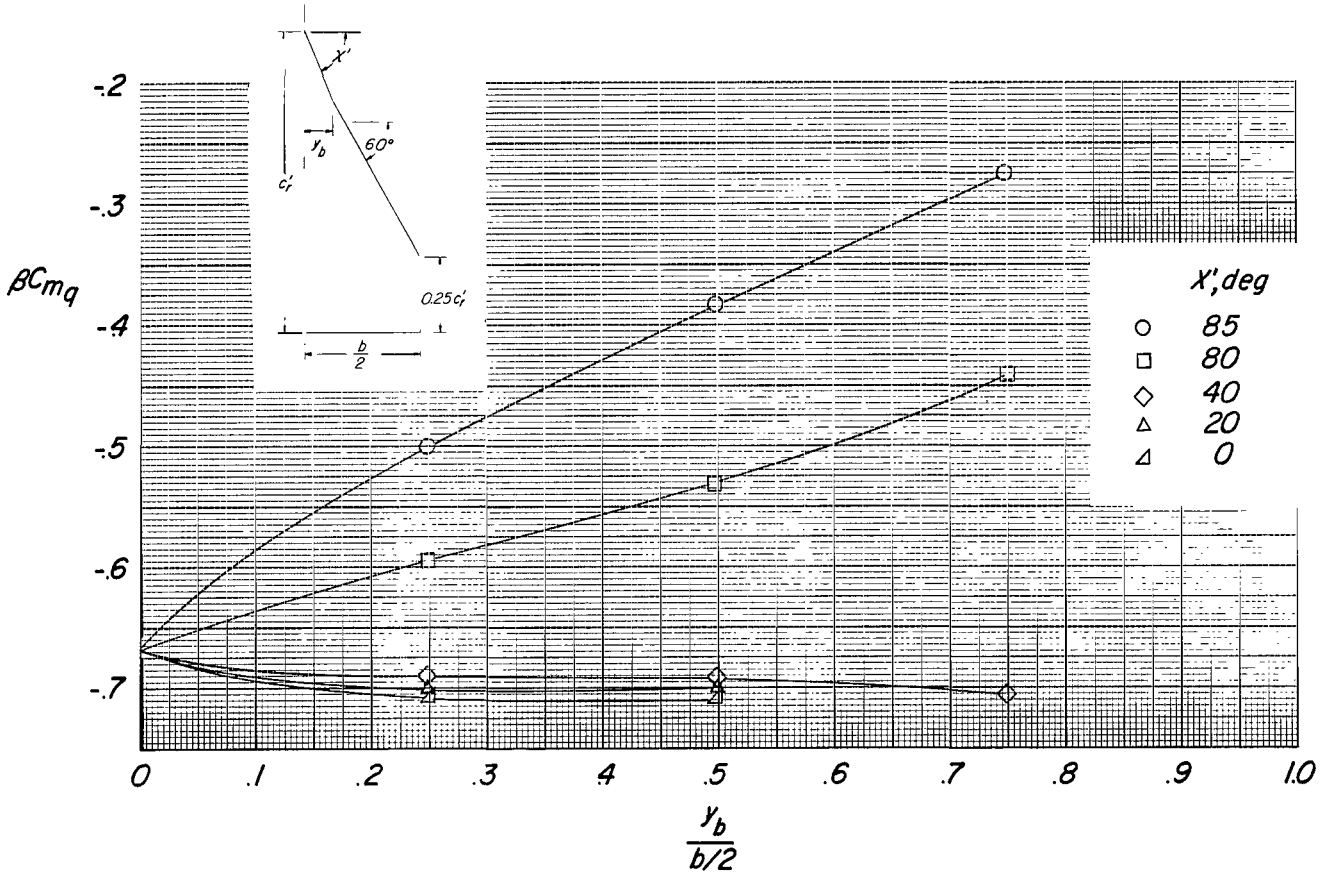

(e) $\Lambda' = 60^0$; $\lambda = 0.25$.

Figure 8.- Continued.

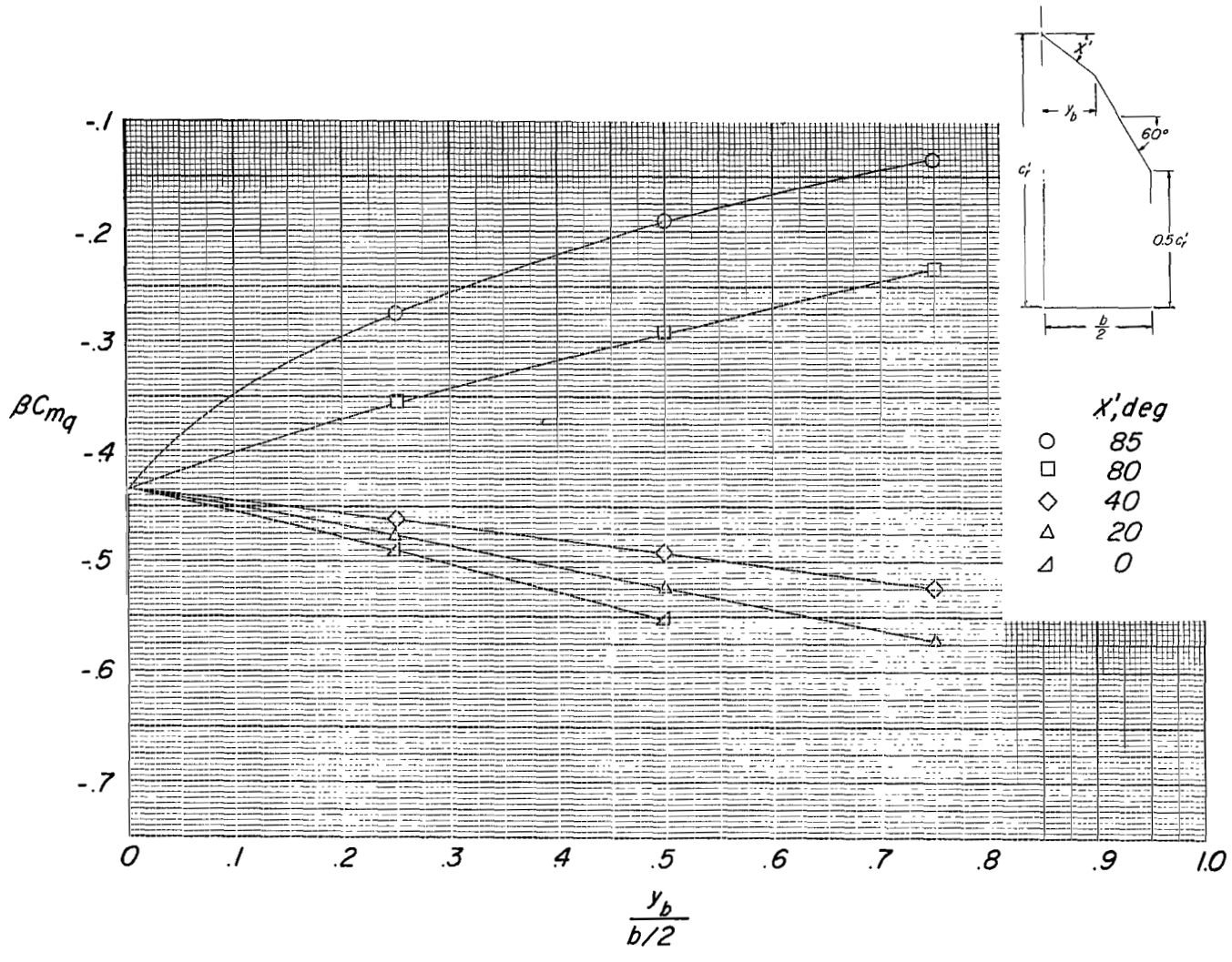

(f) $\Lambda' = 60^0$; $\lambda = 0.50$.

Figure 8.- Continued.

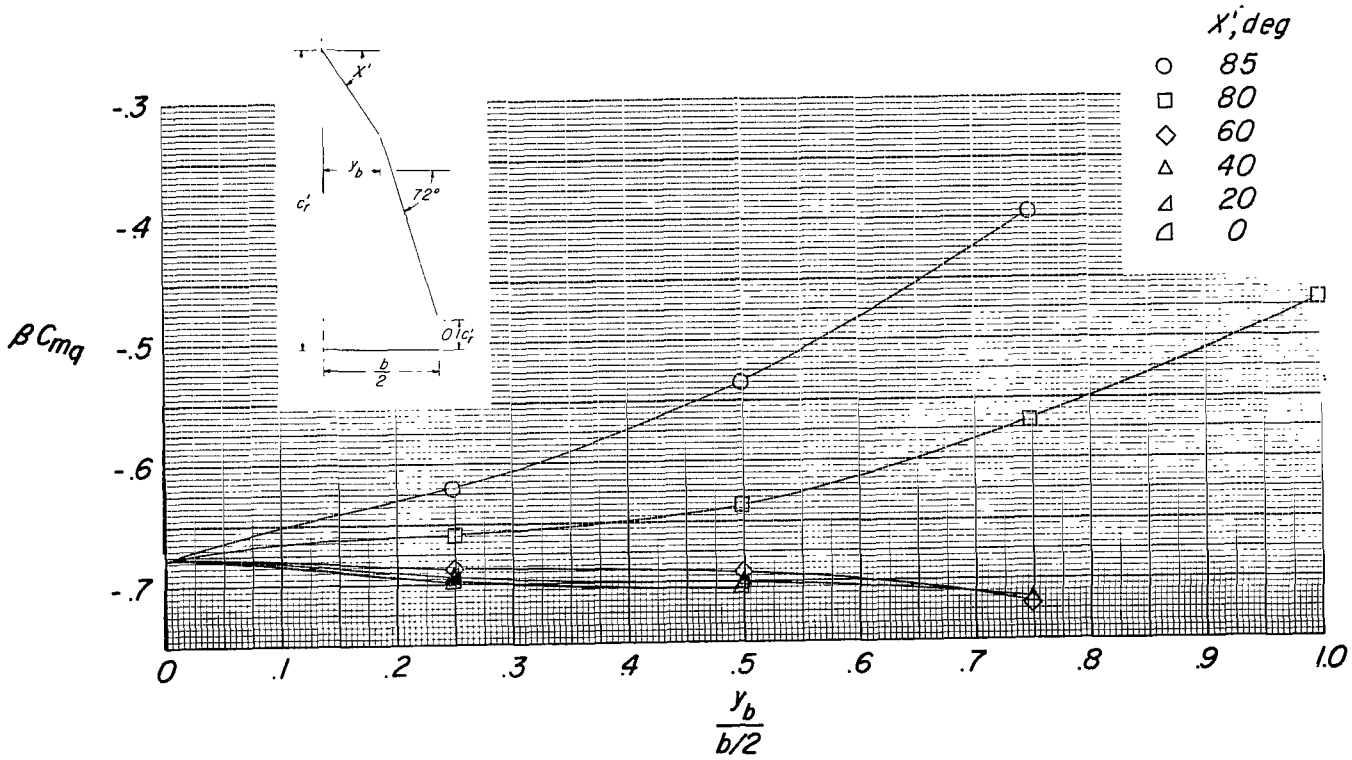

(g) $\Lambda' = 72^{0}$; $\lambda = 0.10$.

Figure 8.- Continued.

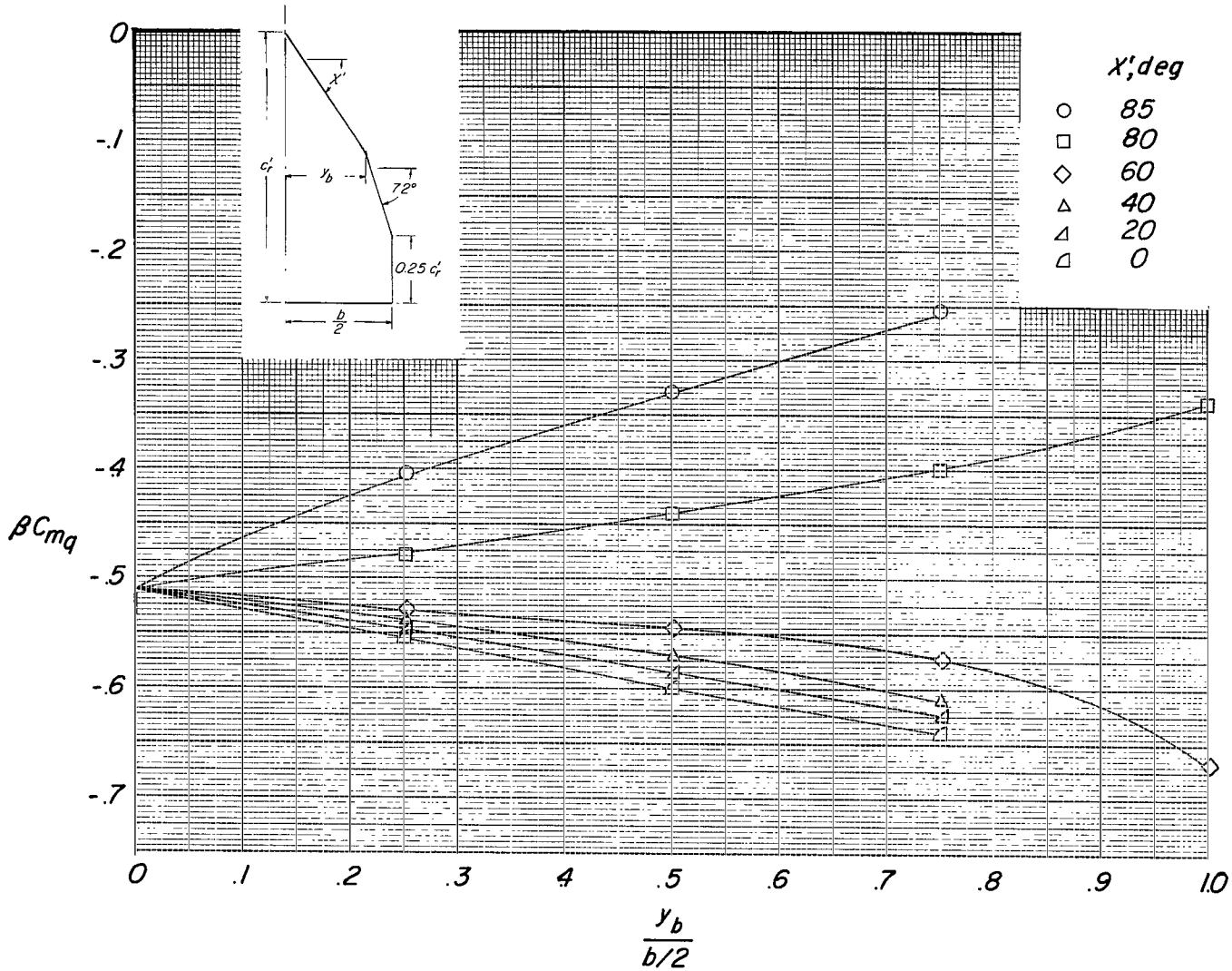

(h) $\Lambda' = 72^0$; $\lambda = 0.25$.

Figure 8.- Continued.

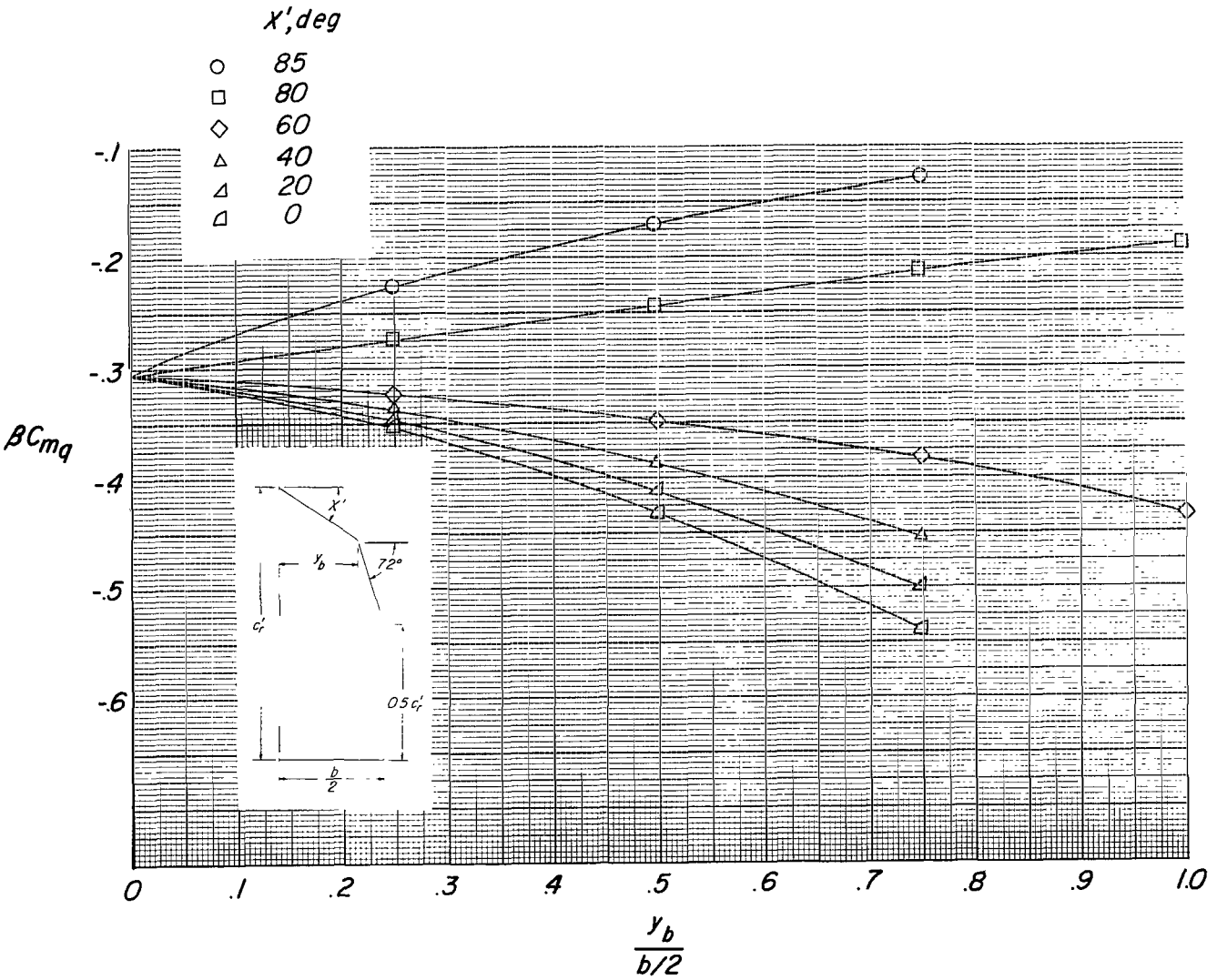

(i) $\Lambda' = 72^0$; $\lambda = 0.50$.

Figure 8.- Concluded.

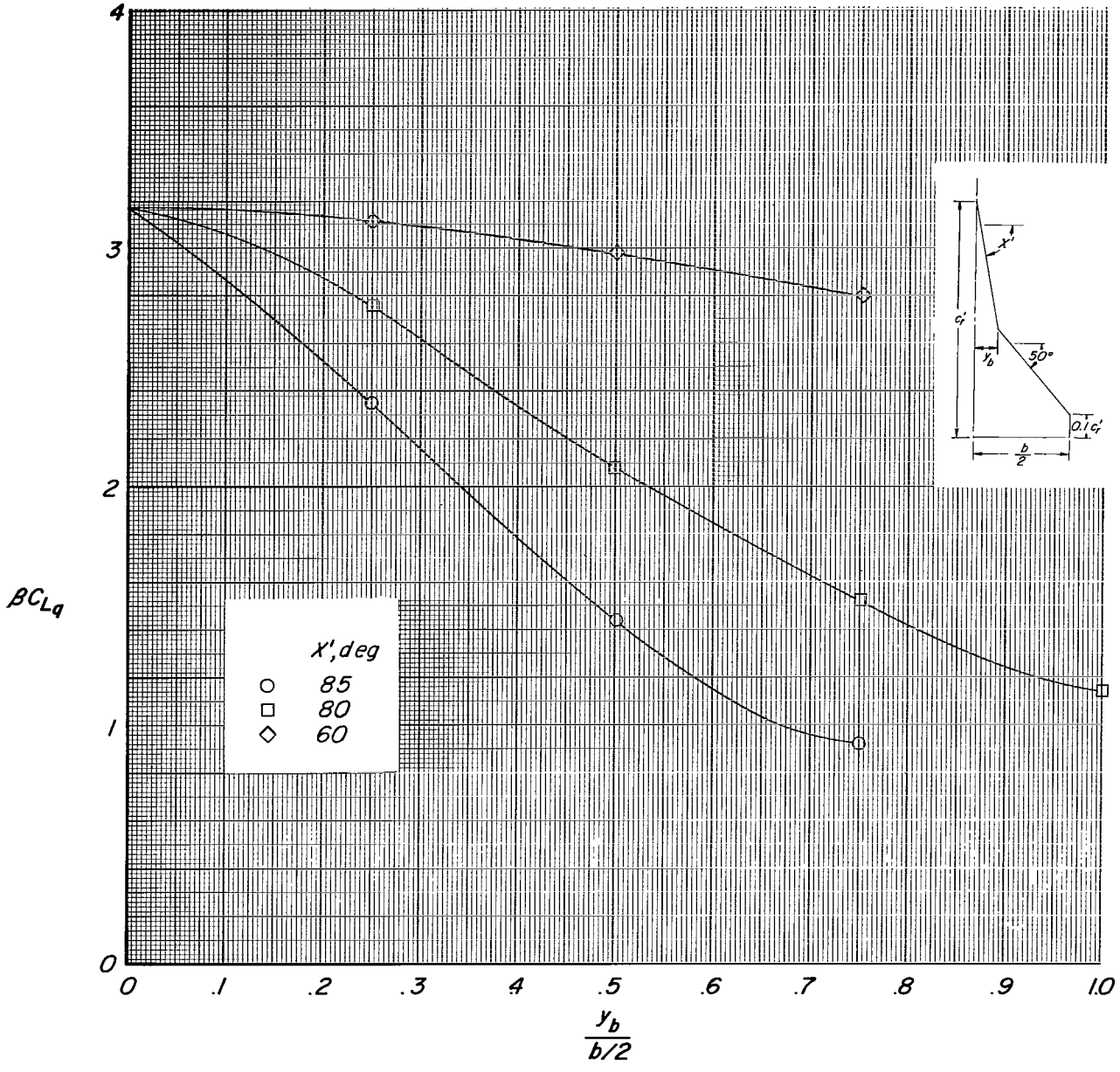

(a) $\Lambda' = 50^{0}$; $\lambda = 0.10$.

Figure 9.- Rotary derivatives of lift coefficient due to pitch rate for cropped double-delta planforms.

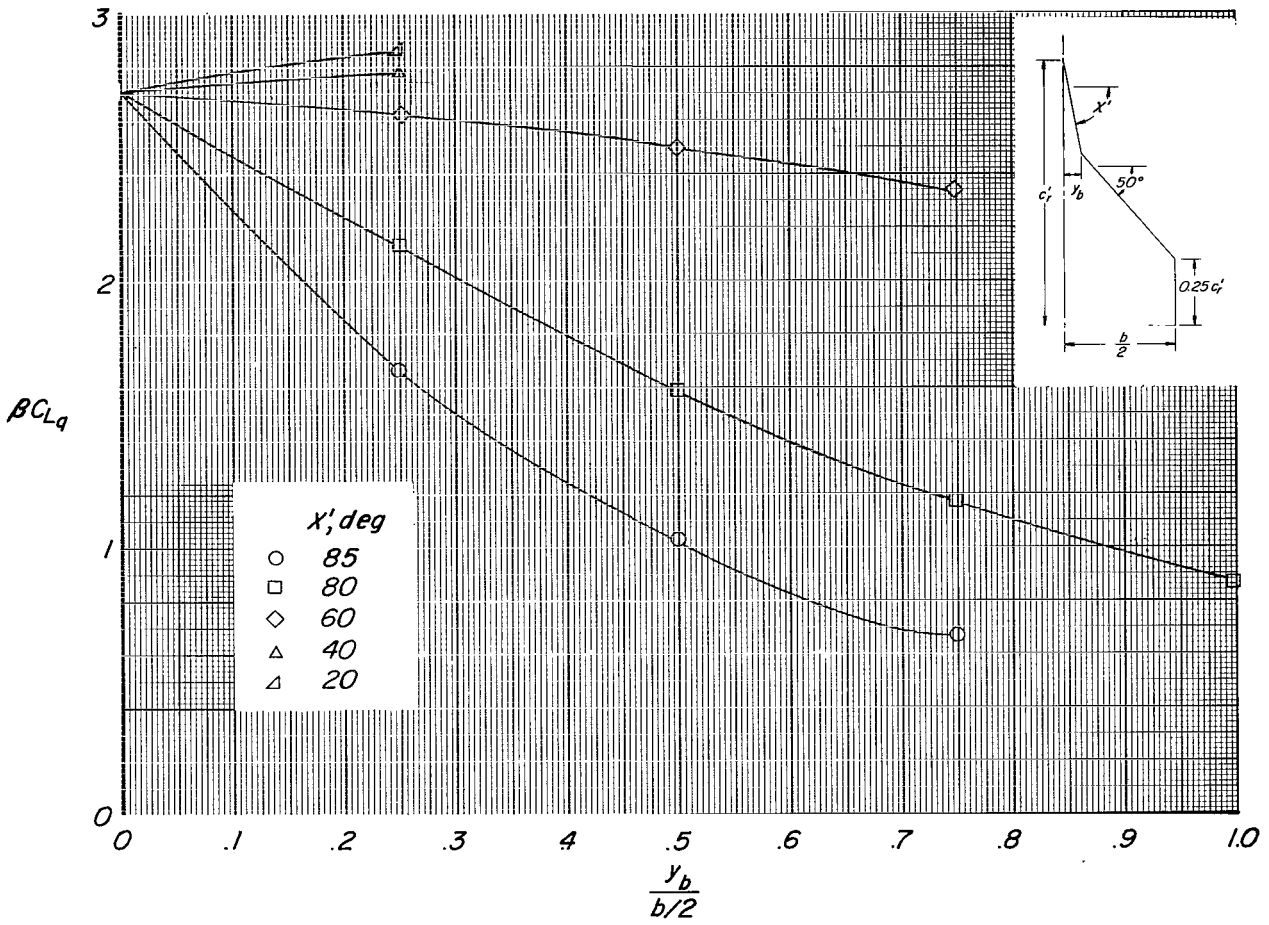

(b) $\Lambda' = 50^0$; $\lambda = 0.25$.

Figure 9.- Continued.

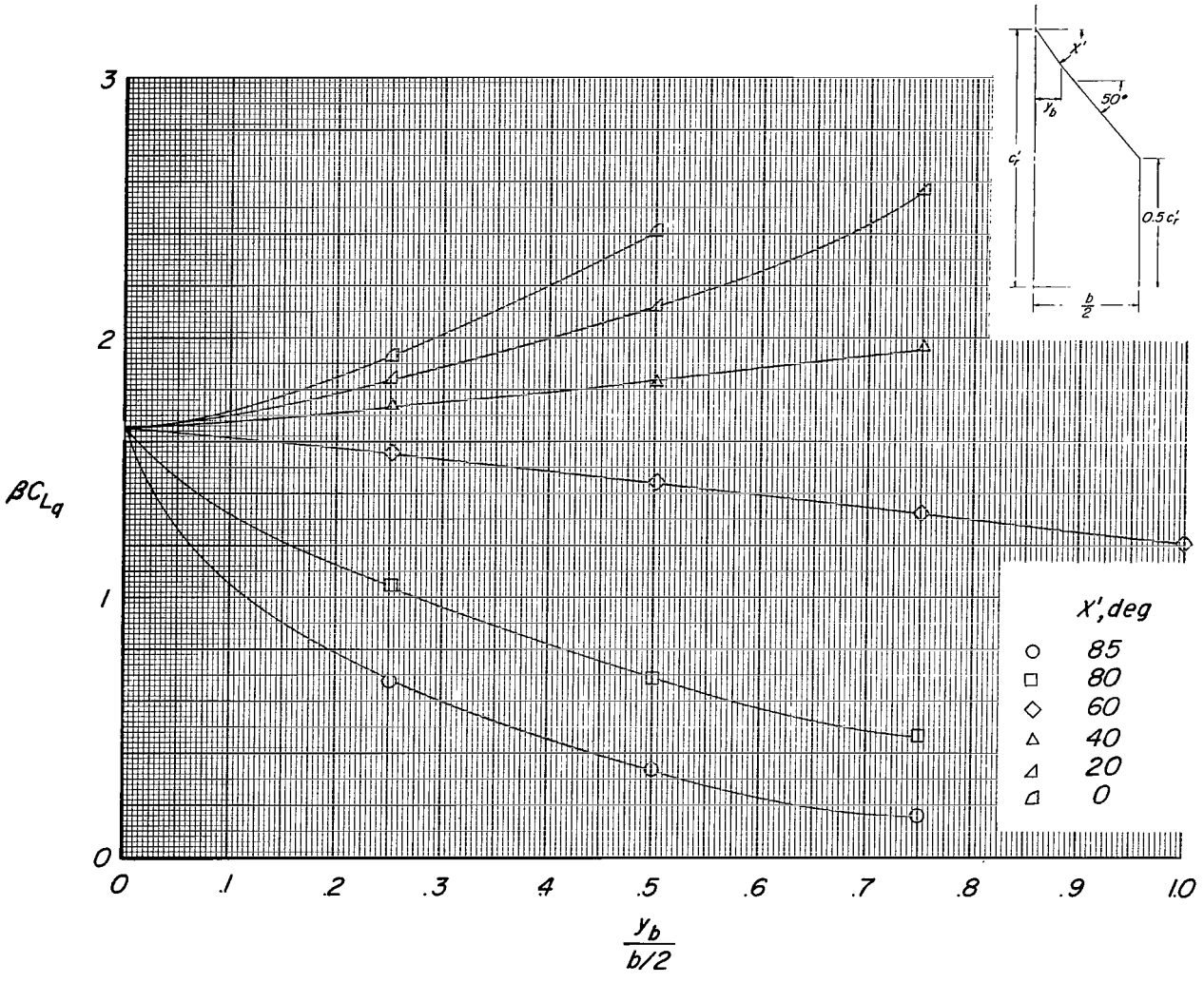

(c) $\Lambda' = 50^0$; $\lambda = 0.50$.

Figure 9.- Continued.

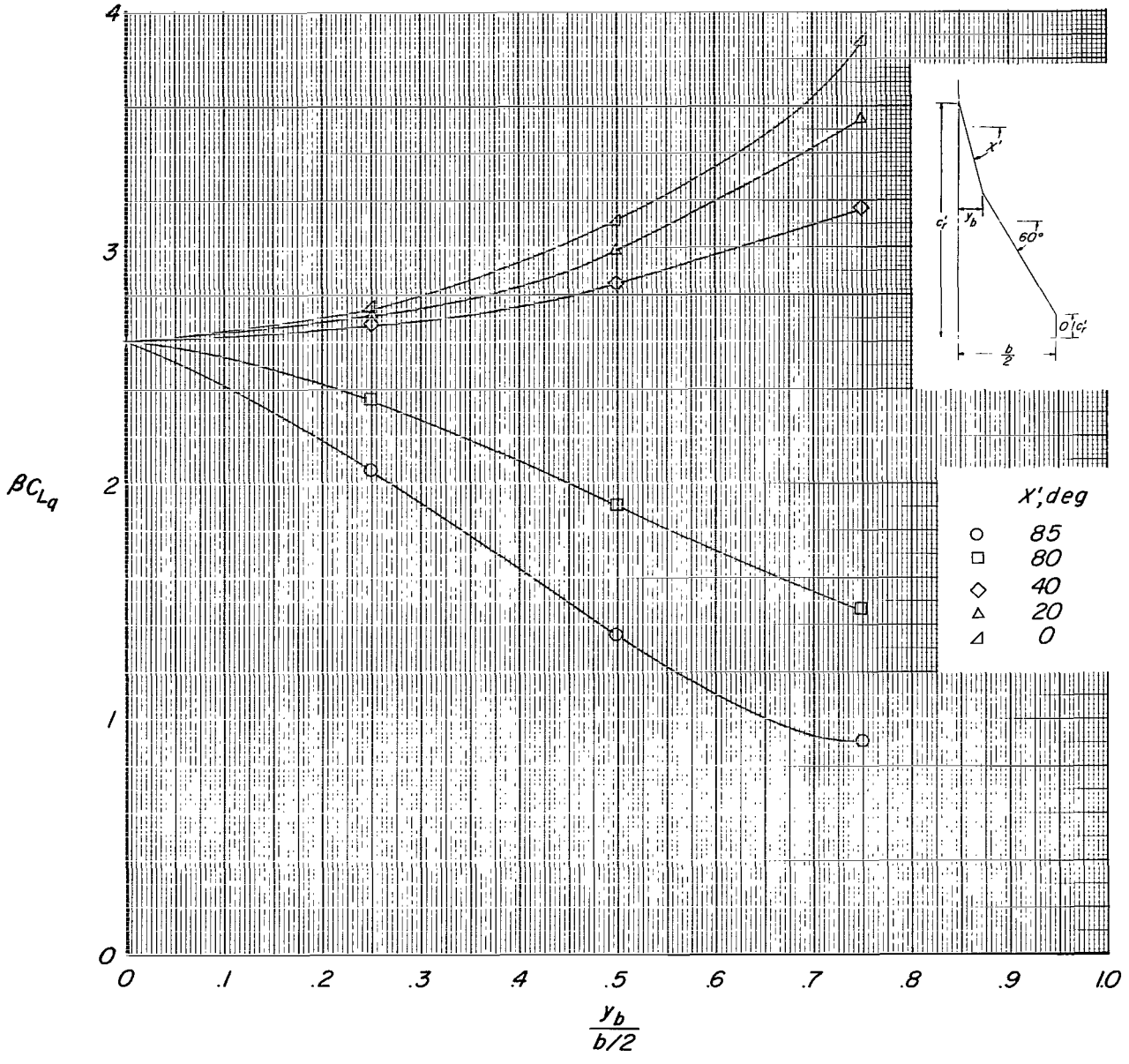

(d) $\Lambda' = 60^0$; $\lambda = 0.10$.

Figure 9.- Continued.

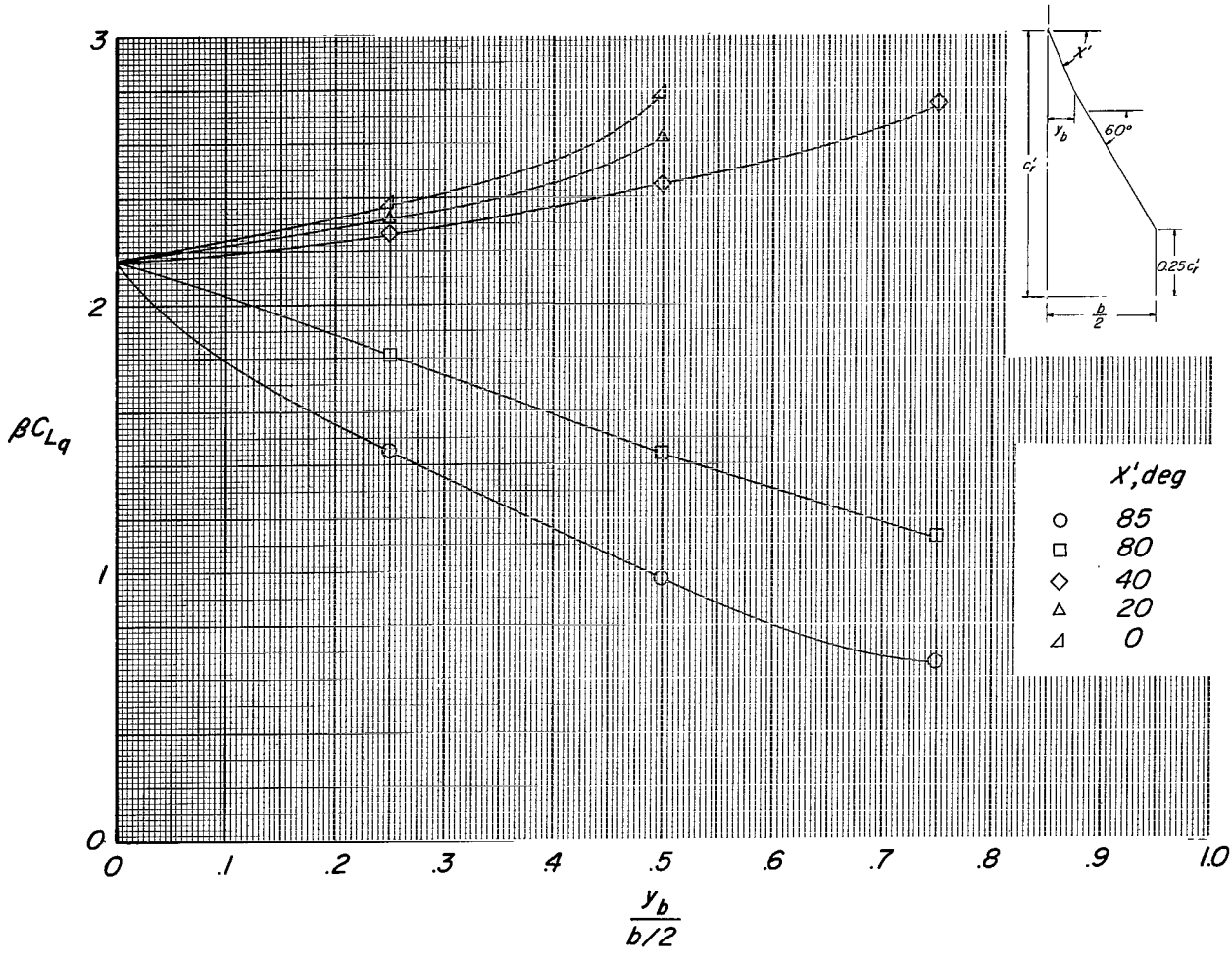

(e) $\Lambda' = 60^0$; $\lambda = 0.25$.

Figure 9.- Continued.

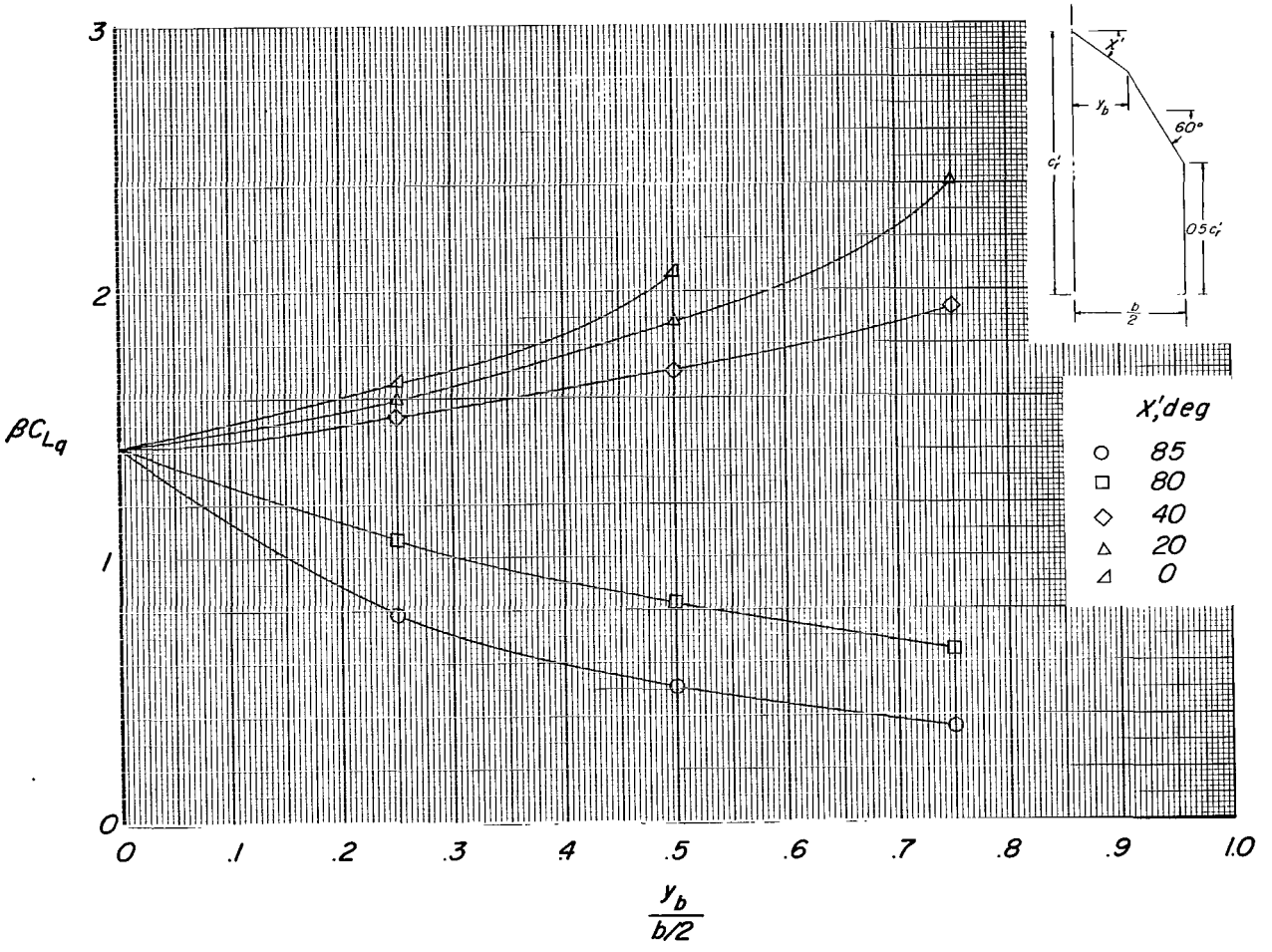

(f) $\Lambda' = 60^0$; $\lambda = 0.50$.

Figure 9.- Continued.

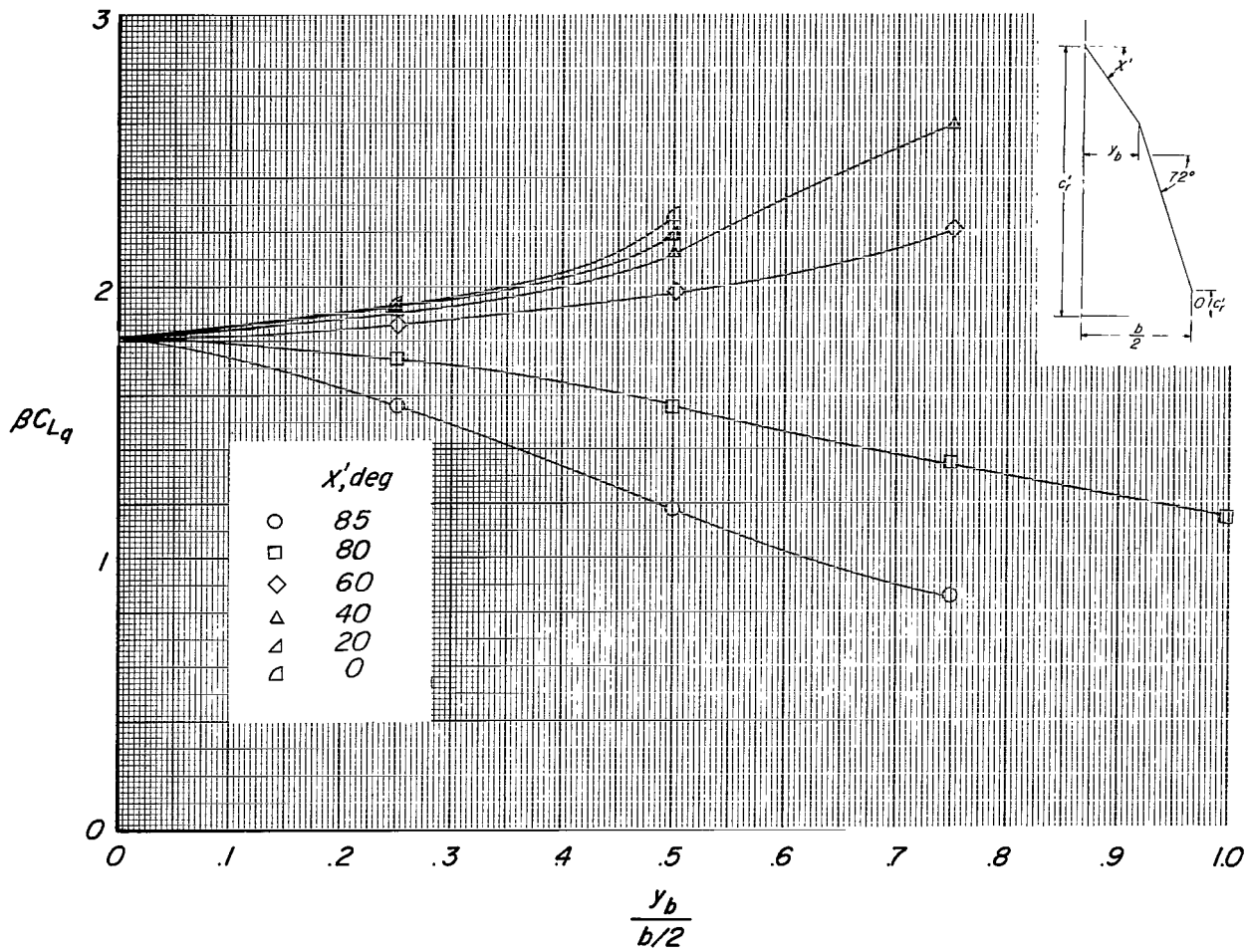

(g) $\Lambda' = 72^0$; $\lambda = 0.10$.

Figure 9.- Continued.

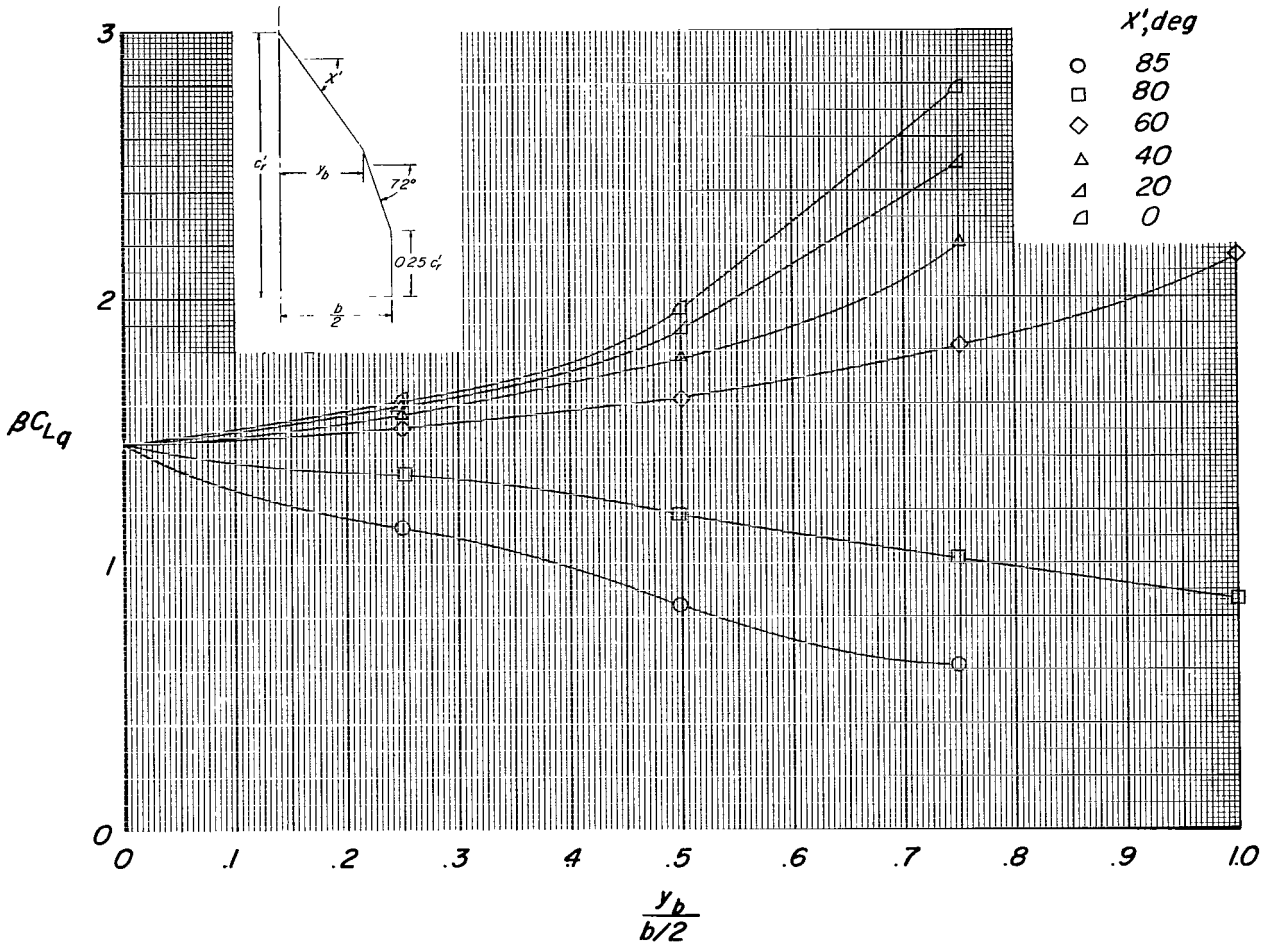

(h) $\Lambda' = 72^{\circ}$; $\lambda = 0.25$.

Figure 9.- Continued.

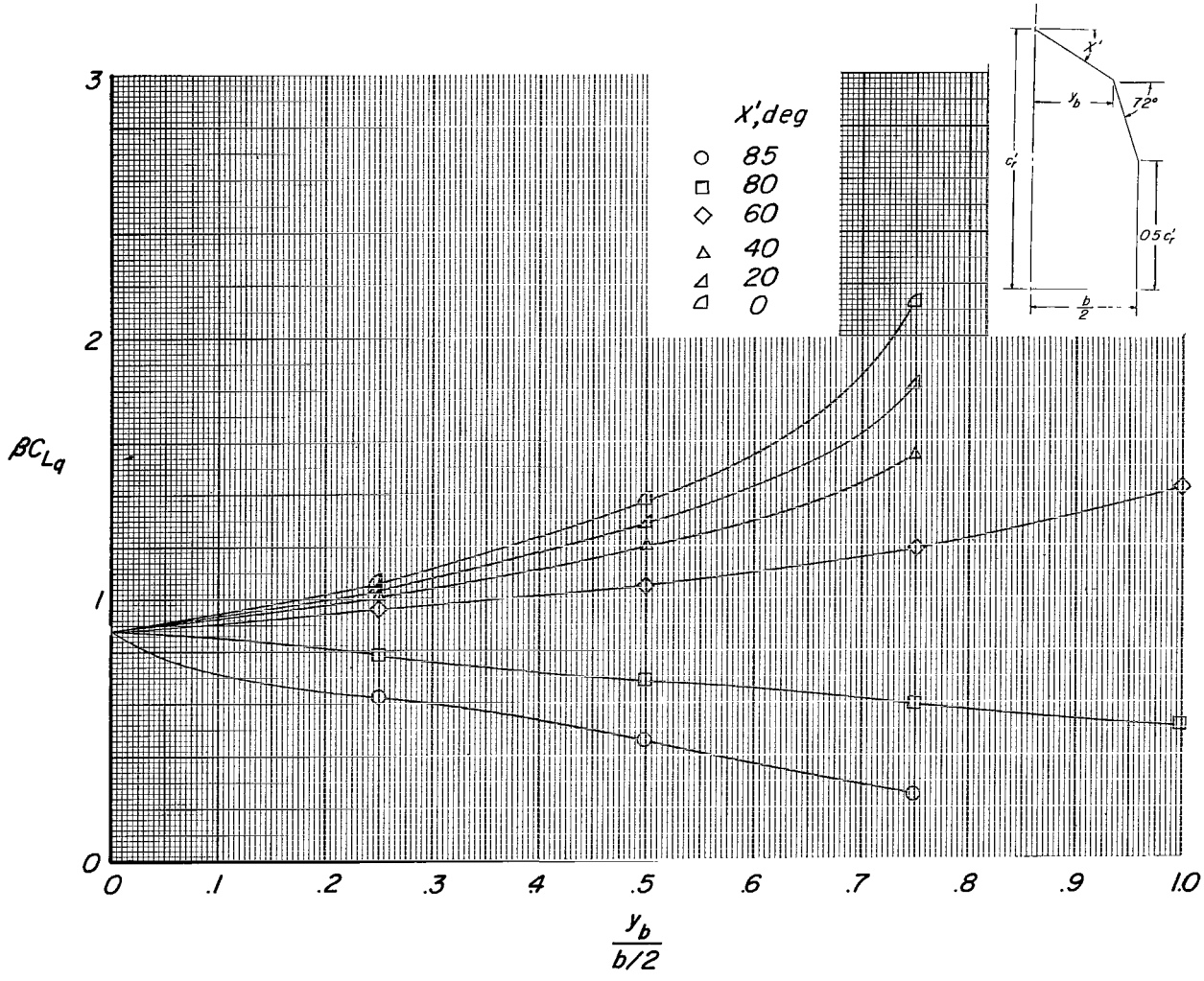

(i) $\Lambda' = 72^0$; $\lambda = 0.50$.

Figure 9.- Concluded.

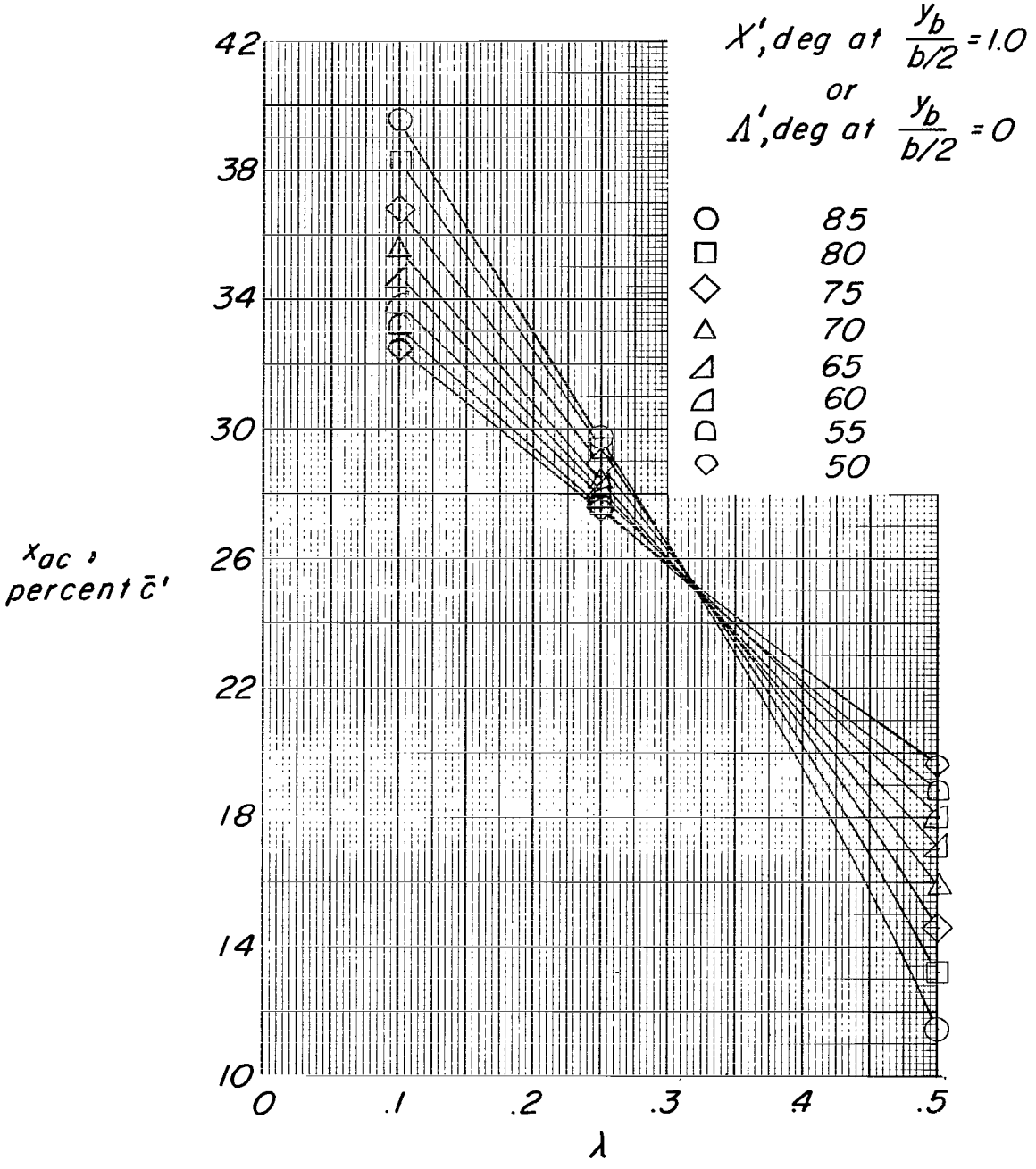

Figure 10.- Aerodynamic center for cropped delta planforms.

"The aeronautical and space activities of the United States shall be conducted so as to contribute . . . to the expansion of human knowledge of phenomena in the atmosphere and space. The Administration shall provide for the widest practicable and appropriate dissemination of information concerning its activities and the results thereof."

—NATIONAL AERONAUTICS AND SPACE ACT OF 1958

NASA SCIENTIFIC AND TECHNICAL PUBLICATIONS

TECHNICAL REPORTS: Scientific and technical information considered important, complete, and a lasting contribution to existing knowledge.

TECHNICAL NOTES: Information less broad in scope but nevertheless of importance as a contribution to existing knowledge.

TECHNICAL MEMORANDUMS: Information receiving limited distribution because of preliminary data, security classification, or other reasons.

CONTRACTOR REPORTS: Scientific and technical information generated under a NASA contract or grant and considered an important contribution to existing knowledge.

TECHNICAL TRANSLATIONS: Information published in a foreign language considered to merit NASA distribution in English.

SPECIAL PUBLICATIONS: Information derived from or of value to NASA activities. Publications include conference proceedings, monographs, data compilations, handbooks, sourcebooks, and special bibliographies.

TECHNOLOGY UTILIZATION PUBLICATIONS: Information on technology used by NASA that may be of particular interest in commercial and other non-aerospace applications. Publications include Tech Briefs, Technology Utilization Reports and Notes, and Technology Surveys.

Details on the availability of these publications may be obtained from:

SCIENTIFIC AND TECHNICAL INFORMATION DIVISION

NATIONAL AERONAUTICS AND SPACE ADMINISTRATION

Washington, D.C. 20546